

When do spectral gradient updates help in deep learning?

Damek Davis*

Dmitriy Drusvyatskiy†

Abstract

Spectral gradient methods, such as the recently popularized Muon optimizer, are a promising alternative to standard Euclidean gradient descent for training deep neural networks and transformers, but it is still unclear in which regimes they are expected to perform better. We propose a simple layerwise condition that predicts when a spectral update yields a larger decrease in the loss than a Euclidean gradient step. This condition compares, for each parameter block, the squared nuclear-to-Frobenius ratio of the gradient to the stable rank of the incoming activations. To understand when this condition may be satisfied, we first prove that post-activation matrices have low stable rank at Gaussian initialization in random feature regression, feedforward networks, and transformer blocks. In spiked random feature models we then show that, after a short burn-in, the Euclidean gradient’s nuclear-to-Frobenius ratio grows with the data dimension while the stable rank of the activations remains bounded, so the predicted advantage of spectral updates scales with dimension. We validate these predictions in synthetic regression experiments and in NanoGPT-scale language model training, where we find that intermediate activations have low-stable-rank throughout training and the corresponding gradients maintain large nuclear-to-Frobenius ratios. Together, these results identify conditions for spectral gradient methods, such as Muon, to be effective in training deep networks and transformers.

1 Introduction

Modern deep neural networks are almost always trained with first-order methods, most prominently stochastic gradient descent (SGD) and its adaptive variants such as **Adam** [29], **RMSprop** [53], and **AdaGrad** [15]. These algorithms can be viewed as Euclidean gradient descent equipped with inexpensive preconditioners, typically diagonal rescalings or structured approximations such as Kronecker-factored schemes (**K-FAC** [39], **Shampoo** [17]). Despite differences in their per-iteration cost, they share a common design principle: one follows the Euclidean gradient that is adjusted by a preconditioner derived from past gradients or curvature information. A complementary line of work takes a different viewpoint and modifies the *geometry* of the update itself by operating on the spectrum of layerwise gradient matrices. The spectral gradient descent method (**SpecGD** [8]) replaces the raw gradient with its polar factor, thus moving in a direction with the same singular vectors but unit spectral norm and step length given by the nuclear norm. The recently proposed optimizer **MUON** [26] implements a momentum-based variant of this spectral update, and has been observed to match or surpass variants of **Adam** [29] in large-language-model pretraining. Motivated by these empirical findings, we ask the following question.

*Department of Statistics and Data Science, The Wharton School, University of Pennsylvania; www.damekdavis.com. Research of Davis supported by NSF DMS award 2047637.

†Halıcıoğlu Data Science Institute (HDSI), University of California San Diego, La Jolla, CA, sites.google.com/view/dmitriy-drusvyatskiy. Research of Drusvyatskiy was supported by NSF DMS-2306322, NSF DMS-2023166, and AFOSR FA9550-24-1-0092 awards.

In what regimes should one expect spectral updates to outperform standard Euclidean gradient methods for training deep neural networks and transformers?

The explanation we propose is based on a simple but prevalent structural property of the post-activation matrices. We show experimentally and theoretically that the *post-activation matrices in intermediate layers of deep neural networks have stable rank bounded by a small numerical constant that is independent of the ambient dimension*. This low stable rank reflects a strong degeneracy of the learned representations and, in particular, implies an ill-conditioned optimization landscape when viewed through the Euclidean lens. Spectral updates, such as **SpecGD**, which align with the singular vector directions and depend only on spectral and nuclear norms, are naturally adapted to this regime. We make this precise in a sequence of toy and semi-realistic settings, where the advantage of spectral over Euclidean updates can be quantified directly in terms of the stable rank of post-activation matrices. Our goal is not to analyze **MUON** in all of its practical details, but rather to understand why its underlying spectral update rule is well suited to the low-stable-rank structure that arises when training modern neural networks.

At a technical level, our results are organized around a one-step comparison of Euclidean and spectral updates acting on a single matrix block. Let W be any matrix parameter that multiplies an incoming activation matrix A (for example, a layer weight acting on the post-activations from the previous layer), and let $G = \nabla_W \mathcal{L}(W)$ denote the corresponding block of the gradient. A simple argument (carried out in Section 1.2 and extended in Section 1.2.1) shows that the guaranteed decrease in the loss after one Euclidean gradient step and one spectral step can be bounded as

$$\Delta_{\text{GD}} \asymp \frac{\|G\|_F^2}{\|A\|_{\text{op}}^2} \quad \text{and} \quad \Delta_{\text{Spec}} \asymp \frac{\|G\|_*^2}{\|A\|_F^2},$$

so that spectral descent is favored whenever

$$\frac{\|G\|_*^2}{\|G\|_F^2} \geq \frac{\|A\|_F^2}{\|A\|_{\text{op}}^2}, \quad (1.1)$$

see also (1.5). The right-hand side is precisely the stable rank $\text{st}(A) := \|A\|_F^2/\|A\|_{\text{op}}^2$ of the incoming features, while the left-hand side measures how spread out the singular values of the gradient are; we will refer to this ratio as the *nuclear rank* of G and denote it by

$$\text{nr}(G) := \frac{\|G\|_*^2}{\|G\|_F^2}.$$

In terms of these quantities, the ratio of the one-step descent guarantees is

$$\frac{\Delta_{\text{Spec}}}{\Delta_{\text{GD}}} \asymp \frac{\text{nr}(G)}{\text{st}(A)}.$$

In particular, when $\text{st}(A)$ is $O(1)$ and $\text{nr}(G)$ grows with the dimension—as we prove in random-feature models after a single GD step and observe empirically in realistic networks—the predicted speedup of spectral over Euclidean updates is itself dimension-dependent (and in our examples linear in d), matching the large early-time advantage we see for spectral methods in practice.

In a multilayer network, the parameters naturally decompose into matrix blocks W_ℓ with gradients G_ℓ that interact with post-activations $A_{\ell-1}$. The same one-step comparison then yields a *layerwise* condition

$$\text{nr}(G_\ell) \geq \text{st}(A_{\ell-1}),$$

which characterizes when a blockwise spectral update on W_ℓ is favored over a Euclidean one. For standard MLPs, $A_{\ell-1}$ is simply the usual post-activation of the previous layer, so the inequality compares a gradient-based quantity $\text{nr}(G_\ell)$ to the stable rank of the propagated data seen by that layer. In Section 1.2.1 we show that the same blockwise condition continues to hold for a broad class of layered architectures, including transformers. In that setting, the relevant $A_{\ell-1}$ is the normalized or MLP activation feeding each projection (for example the RMS-normalized hidden states entering W_Q, W_K, W_V , or the MLP post-activations entering W_2). The upshot is a simple rule of thumb: spectral updates are most advantageous on those blocks whose incoming features are low-stable-rank and whose gradients have large nuclear rank $\text{nr}(G_\ell)$.¹

Beyond this one-step picture, we also show that the nuclear-rank advantage of spectral updates is not a purely transient phenomenon. In spiked random-feature regression models, the gradient nuclear rank becomes large after a short burn-in period and then remains high along a macroscopic window of gradient-descent iterations. More precisely, in both realizable and teacher–student variants we prove that there is a window of $\Theta(d)$ iterations on which $\text{nr}(\nabla \mathcal{L}(W_t)) = \Omega(d)$ and, for any fixed $\varepsilon > 0$, a longer window of $\Theta(d \log d)$ iterations on which $\text{nr}(\nabla \mathcal{L}(W_t)) \geq d^{1-\varepsilon}$ (Theorem 3.6 and Corollary 3.12). In the same models, Euclidean gradient descent needs $\Theta(d \log(d/\delta))$ steps to reach relative error $\delta \in (0, 1)$, so for any fixed target accuracy this $\Theta(d \log d)$ window represents a constant fraction of the training time. Thus, if we were to restart a spectral method such as **SpecGD** or **MUON** from any point in this window, its one-step improvement over Euclidean gradient descent would itself be dimension-dependent.

These blockwise conditions show that spectral updates are most advantageous precisely when incoming activations are low-stable-rank and gradients have large nuclear rank. In the remainder of the paper we first show that such low-stable-rank activations arise under mild assumptions in feedforward networks and transformer blocks, and then verify the same structure, together with large gradient nuclear ranks, in simplified models and NanoGPT-scale training runs.²

1.1 Post activation matrices have low-stable rank.

In order to state our theoretical guarantees, consider a feedforward neural network parametrized by weight matrices W_1, \dots, W_L . Define now the post-activation matrices

$$A_0 = X \quad \text{and} \quad A_\ell = \sigma(W_\ell A_{\ell-1}) \quad \forall \ell = 1 \dots, L. \quad (1.2)$$

Here $X \in \mathbf{R}^{d \times n}$ is a matrix containing the original feature vectors as its columns and A_ℓ are the data matrices encountered by any layer-wise training algorithm. The function $\sigma: \mathbf{R} \rightarrow \mathbf{R}$ is applied elementwise, with common examples being ReLU $\sigma(t) = \max\{0, t\}$ and its various smooth approximations. Our thesis is that under mild assumptions on the initial data X , the propagated data matrices $\{A_\ell\}_\ell^L$ tend to all have stable rank $\text{st}(A_\ell) := \|A_\ell\|_F^2 / \|A_\ell\|_{\text{op}}^2$ that is bounded by a numerical constant independent of the intermediate layer weights. Indeed, we will prove the following statements are true with high probability over the initial data X (e.g. i.i.d. Gaussian entries) and for all usual activation functions (e.g. absolute value, ReLU, square ReLU).

1. **(Second-layer)** For any fixed weights W_1 , the stable rank $\text{st}(A_1)$ of the first layer post-activation matrix is bounded by a small numerical constant independent of W_1 (Theorem 2.6).

¹Similar gradient nuclear ranks also appear implicitly or explicitly in convergence analyses of spectral optimizers such as MUON and Scion [44, 49]; our focus here is to relate this ratio to the *stable rank of the propagated data* and to show that the resulting inequality is naturally activated in realistic networks.

²The reader may find code to reproduce our experiments at <https://github.com/damek/specgd/>.

2. **(Any layer with random weights)** For any fixed data X and weights $W_1, \dots, W_{\ell-1}$ and random W_ℓ with iid Gaussian entries, the stable rank of the ℓ 'th layer post-activation matrix $\text{st}(A_\ell)$ is bounded by a numerical constant (Theorem 2.7).
3. **(Any layer with quadratic activations)** If the activation function is the quadratic $\sigma(t) = t^2$, then for any fixed weights W_1, \dots, W_ℓ , the stable rank $\text{st}(A_\ell)$ is bounded by a numerical constant that depends only on the depth ℓ (Theorem 2.8).

Even though these guarantees apply under idealized assumptions, the conclusions appear to hold experimentally for more sophisticated models. To illustrate, we run two experiments. First, we run a synthetic experiment training a three layer neural network for learning the sparse function $f(x) = x_1 x_2 x_3$; Figure 1 depicts the stable rank of the post-activation matrices along a run of Gradient Descent (GD) and a variant of the Spectral Gradient Descent method (SpecGD [8], which only applies spectral updates to layers 2, 3; see Section 1.2.1 for a justification.). As claimed the stable rank of the post-activation matrices is small, relative to the input dimension.

Going beyond synthetic data, Figure 2 plots the stable rank of the MLP post-activations in a MUON run when training modded-NanoGPT [28] (which popularized MUON for language models). As is clear from the figure, the MLP post-activations in every block indeed have low stable rank.

In transformer architectures, the blockwise condition (1.8) involves not only MLP post-activations but also several RMS-normalized hidden states feeding the attention and MLP projections. For later reference, we state the corresponding initialization guarantee separately.

4. **(Transformer blocks at initialization).** For decoder-only transformer architectures with RMS-normalized attention/MLP blocks, we show that, at Gaussian initialization, the hidden representations entering the attention and MLP projections (RMS-normalized hidden states and MLP post-activations) have stable rank bounded by a depth-dependent numerical constant that depends only on the empirical token frequencies and is independent of width and sequence length. A detailed statement is given in Section 2.2, see in particular Corollary 2.15.

Taken together, these observations and guarantees indicate that the data matrices seen by typical weight blocks in both multilayer perceptrons and transformer architectures are highly degenerate in stable rank. In the generic feedforward setting above we treat the input matrix $A_0 = X$ as arbitrary and our theoretical bounds start at the first nontrivial post-activations A_ℓ for $\ell \geq 1$, whereas for transformers we will later show that even the embedding activations entering the first block have low stable rank under a mild condition on the empirical token frequencies (Section 2.2). In the next subsection, we examine how this degeneracy affects the behavior of Euclidean and spectral updates in a simple but representative model.

1.2 Impact of post-activation degeneracy on training algorithms

Low-stable-rank post-activations have a pronounced impact on the behavior of first-order training algorithms. We first make this precise in the random-feature regression model:

$$\min_{W \in \mathbb{R}^{m \times k}} \mathcal{L}(W) := \frac{1}{2n} \|WA - Y\|_F^2.$$

We will think about W as the ℓ 'th layer weight matrix to be trained and A is the post-activation matrix of the propagated data from the previous layers. The random feature model is a standard and analytically tractable simplification of neural networks; see for example [11, 13, 45–47].

Now being a quadratic, the function \mathcal{L} may be rewritten as a Taylor-expansion:

$$\mathcal{L}(W + U) = \mathcal{L}(W) + \langle \nabla \mathcal{L}(W), U \rangle + \frac{1}{2n} \|UA\|_F^2. \quad (1.3)$$

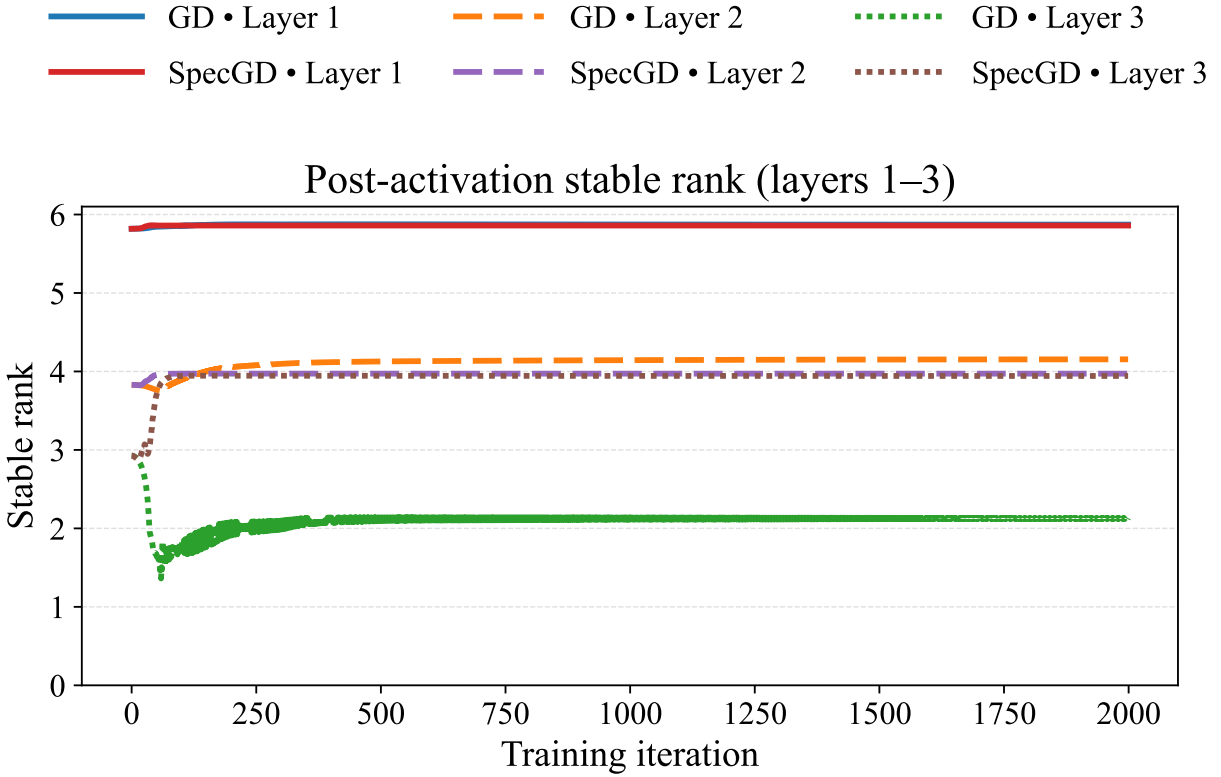


Figure 1: We generate $n = 512$ random gaussian vectors of dimension $d = 128$ and use target y which is the product of the first 3 coordinates. We then train a 4 layer feedforward neural network, with activation function $\sigma(t) = \max\{0, t\}^2$, mapping from input space \mathbb{R}^d to \mathbb{R} as follows: $\mathbb{R}^d \rightarrow \mathbb{R}^{4d} \rightarrow \mathbb{R}^{4d} \rightarrow \mathbb{R}^{4d} \rightarrow \mathbb{R}$. We start at the standard pytorch random initialization and run full batch algorithms: Gradient Descent and a Spectral descent method (only on layers 2 and 3, while layer 1 and 4 simply take Euclidean gradient steps; see Section 1.2.1 for a justification of this choice) and observe the stable ranks of the activation matrices. We note that the maximum possible stable rank of such matrices is 256.

The usual starting point for first-order algorithms is based on the majorization principle: one upper-bounds the pure quadratic term $\|UA\|_F^2$ in (1.3) by a function that depends only on U and not on the data A . The update direction of the algorithm is then obtained by minimizing this simple (data-independent) upper model over U . Euclidean gradient descent (**GD**) and spectral gradient descent (**SpecGD**) proposed in [8] utilize the following two approximations, respectively:³

$$\frac{1}{n}\|UA\|_F^2 \leq \underbrace{\frac{1}{n}\|A\|_{\text{op}}^2}_{=:L_F} \cdot \|U\|_F^2 \quad \text{and} \quad \frac{1}{n}\|UA\|_F^2 \leq \underbrace{\frac{1}{n}\|A\|_F^2}_{=:L_{\text{op}}} \cdot \|U\|_{\text{op}}^2. \quad (1.4)$$

Thus **GD** and **SpecGD** impose the (Euclidean) Frobenius norm and the (non-Euclidean) operator norm on the domain, respectively. Combining (1.3) with each of the inequalities (1.4) and minimizing in U yields the explicit updates for **GD** and **SpecGD**, respectively:

$$W_{\text{GD}} := W - \frac{1}{L_F} \nabla \mathcal{L}(W) \quad \text{and} \quad W_{\text{SD}} = W - \frac{\|\nabla \mathcal{L}(W)\|_*}{L_{\text{op}}} \text{polar}(\nabla \mathcal{L}(W)).$$

³Note that both of these inequalities are tight for some matrix U .

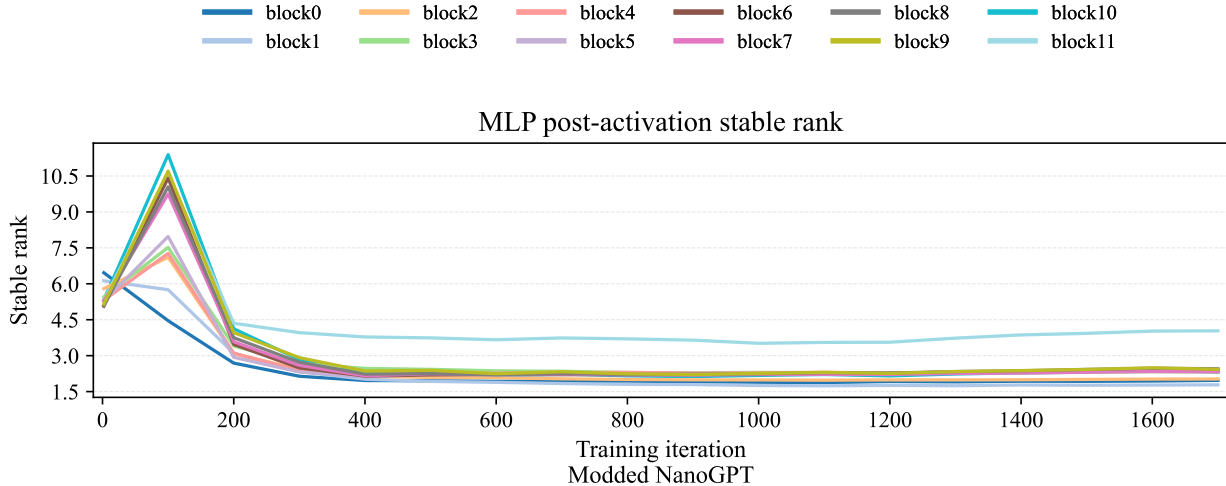


Figure 2: Stable rank of MLP post activations while running a particular snapshot (specifically [25]) of the modded-NanoGPT repo [28]. We also include the July 18th snapshot of the architecture at the time of training in Section 19. We note that the maximal rank of any activation matrix in this plot is 3072. Thus, the the stable rank of the post-activations are far below their maximal value.

Here, the polar of the matrix is the product of the left and right orthogonal factors appearing in its singular value decomposition. MUON is a variant of SpecGD, where the polar is approximated by the Newton-Schulz algorithm, and one further incorporates momentum. Now the guaranteed function decrease achieved by GD and SpecGD is fully determined by the dual norm of the gradient:

$$\mathcal{L}(W) - \mathcal{L}(W_{\text{GD}}) \geq \frac{1}{2L_F} \|\nabla \mathcal{L}(W)\|_F^2 \quad \text{and} \quad \mathcal{L}(W) - \mathcal{L}(W_{\text{SD}}) \geq \frac{1}{2L_{\text{op}}} \|\nabla \mathcal{L}(W)\|_*^2.$$

Comparing the two bounds, we see that SpecGD promises more descent than GD whenever

$$\text{nr}(\nabla \mathcal{L}(W)) \geq \text{st}(A), \quad (1.5)$$

When the stable rank of the post-activation $\text{st}(A)$ is constant (independent of dimension), one expects that (1.5) will hold, since the ratio on the left-side can scale with the dimension.

Using the exact expansion (1.3), we can in fact obtain a two-sided comparison of the function values after one step. For the Euclidean step with stepsize $1/L_F$, we have

$$\mathcal{L}(W_{\text{GD}}) = \mathcal{L}\left(W - \frac{1}{L_F} \nabla \mathcal{L}(W)\right) = \mathcal{L}(W) - \frac{1}{L_F} \|\nabla \mathcal{L}(W)\|_F^2 + \frac{1}{2n} \|U_{\text{GD}} A\|_F^2 \geq \mathcal{L}(W) - \frac{1}{L_F} \|\nabla \mathcal{L}(W)\|_F^2,$$

where U_{GD} is the search direction and we drop the quadratic term because it is nonnegative. On the other hand, the descent estimate for the spectral step shows that $\mathcal{L}(W_{\text{SD}}) \leq \mathcal{L}(W) - \frac{1}{2L_{\text{op}}} \|\nabla \mathcal{L}(W)\|_*^2$. Therefore, whenever

$$\text{nr}(\nabla \mathcal{L}(W)) \geq 2 \text{st}(A),$$

the upper bound on $\mathcal{L}(W_{\text{SD}})$ lies below the lower bound on $\mathcal{L}(W_{\text{GD}})$, and thus $\mathcal{L}(W_{\text{SD}}) \leq \mathcal{L}(W_{\text{GD}})$. An analogous interval argument applies in the settings we consider later, but we omit it.

As a numerical illustration (Figure 3), we compare the performance of GD and SpecGD on random feature regression corresponding to training second layer weights, namely $A_1 = \sigma(W_1 X)$, where $W_1 \in \mathbb{R}^{100 \times 50}$ and $X \in \mathbb{R}^{100 \times 50}$ have iid standard Gaussian entries and $\sigma(t) = \max\{0, t\}$ is the ReLU

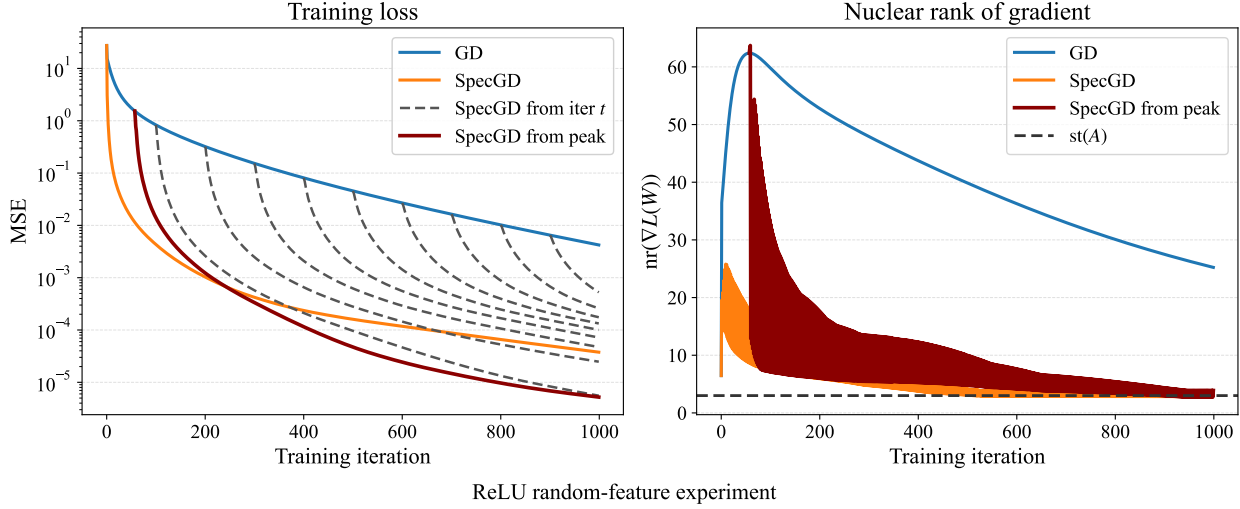


Figure 3: Comparison of gradient descent (GD) and spectral gradient descent (SpecGD) on the random feature model $\min_W \mathcal{L}(W) = \frac{1}{2n} \|WA - Y\|_F^2$ with $W \in \mathbb{R}^{100 \times 100}$. The ground truth matrix $W_{\sharp} \in \mathbb{R}^{100 \times 100}$ is drawn with iid standard Gaussian entries. The data matrix is generated by $A = \sigma(W_1 X)$, where $W_1 \in \mathbb{R}^{100 \times 50}$ and $X \in \mathbb{R}^{100 \times 400}$ have iid standard Gaussian entries and $\sigma(t) = \max\{0, t\}$ is the ReLU activation function applied coordinatewise. The target matrix $Y = W_{\sharp} A$ is generated from a ground truth matrix $W_{\sharp} \in \mathbb{R}^{100 \times 100}$ that has iid standard Gaussian entries. Both methods are initialized at the all-zeros matrix. Left: supoptimality gap in function value along the GD (solid blue) and SpecGD (solid gold) iterations. The dashed curves plot the suboptimality gap if we were to initialize SpecGD at the current GD step, plotted every 100 iterations. The superior performance of SpecGD is clear from the figure. Right: nuclear rank $\text{nr}(\nabla \mathcal{L}(W))$ of the gradient along the GD and SpecGD iterations initialized at the all-zeros matrix; the black dashed line signifies the level $\text{st}(A)$, above which SpecGD is superior to GD. The nuclear rank $\text{nr}(\nabla \mathcal{L}(W))$ can be large (with (1.5) holding) along the trajectories.

activation function applied coordinatewise. It is clear from the figure that (i) equation (1.5) holds along both GD and SpecGD trajectories and (ii) SpecGD significantly outperforms GD as expected.

The argument we presented above is particularly clean for least squares, but it can be generalized much further. As a first example, we stay within the random feature model and consider a smooth loss f on WA for which the gradient ∇f is L -Lipschitz. Note that we can think of W as a fixed layer within a network, keeping the rest of the weights frozen, and A would be the previous layers post-activations. Now, define $\mathcal{L}(W) := f(WA)$ and note that

$$\mathcal{L}(W + U) \leq \mathcal{L}(W) + \langle \nabla \mathcal{L}(W), U \rangle + \frac{L}{2} \|UA\|_F^2 \quad (1.6)$$

Then, as before, we may bound $\|UA\|_F^2$ by $\|A\|_{\text{op}}^2 \|U\|_F^2$ or $\|A\|_F^2 \|U\|_{\text{op}}$, and minimize the two constructed bounds in the variable U . This gives us GD and SpecGD, respectively:

$$W_{\text{GD}} := W - \frac{1}{L_F \cdot L} \nabla \mathcal{L}(W) \quad \text{and} \quad W_{\text{SD}} = W - \frac{\|\nabla \mathcal{L}(W)\|_*}{L_{\text{op}} \cdot L} \text{polar}(\nabla \mathcal{L}(W)),$$

Plugging in the update in (1.6), we find

$$\mathcal{L}(W) - \mathcal{L}(W_{\text{GD}}) \geq \frac{1}{2L_F \cdot L} \|\nabla \mathcal{L}(W)\|_F^2 \quad \text{and} \quad \mathcal{L}(W) - \mathcal{L}(W_{\text{SD}}) \geq \frac{1}{2L_{\text{op}} \cdot L} \|\nabla \mathcal{L}(W)\|_*^2.$$

Thus, descent promised by **SpecGD** is again greater than that promised by **GD** whenever (1.5) holds.

Although the random feature model is idealized, the derived conclusions appear to hold more generally. For example, in Figure 18 we build on the sparse regression setting of Figure 1, plotting the performance of **GD** and **SpecGD**, along with the the nuclear rank $\text{nr}(\nabla \mathcal{L}(W))$. **SpecGD** exhibits significantly better performance than **GD**, especially early on in training when the nuclear ranks of the gradients are large. Further, building on Figure 2, we plot in Figure 5 the ratio $\text{nr}(\nabla \mathcal{L}(W))$ for the MLP layers when training the NanoGPT model. We observe that this ratio can indeed be large along the trajectory, thereby suggesting a significant advantage of **MUON/SpecGD** over **GD**.

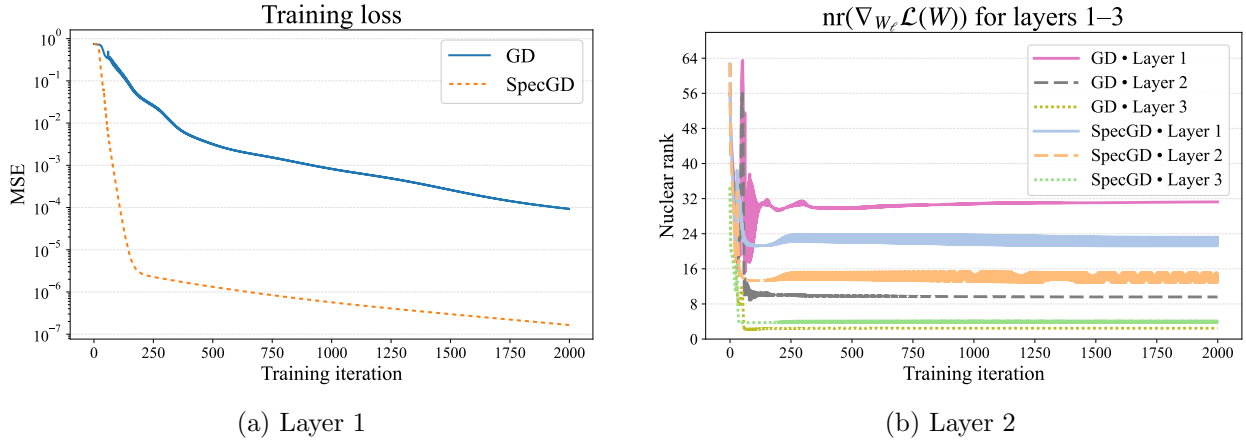


Figure 4: The training loss and gradient nuclear rank associated to the sparse regression problem in Figure 1. We see that the training loss for **SpecGD** decreases significantly faster than for **GD** during the initial phase of training, when the nuclear rank of the gradient is large. The maximum possible nuclear rank at layer 1 is 128, while for layers 2 and 3, it is 256.

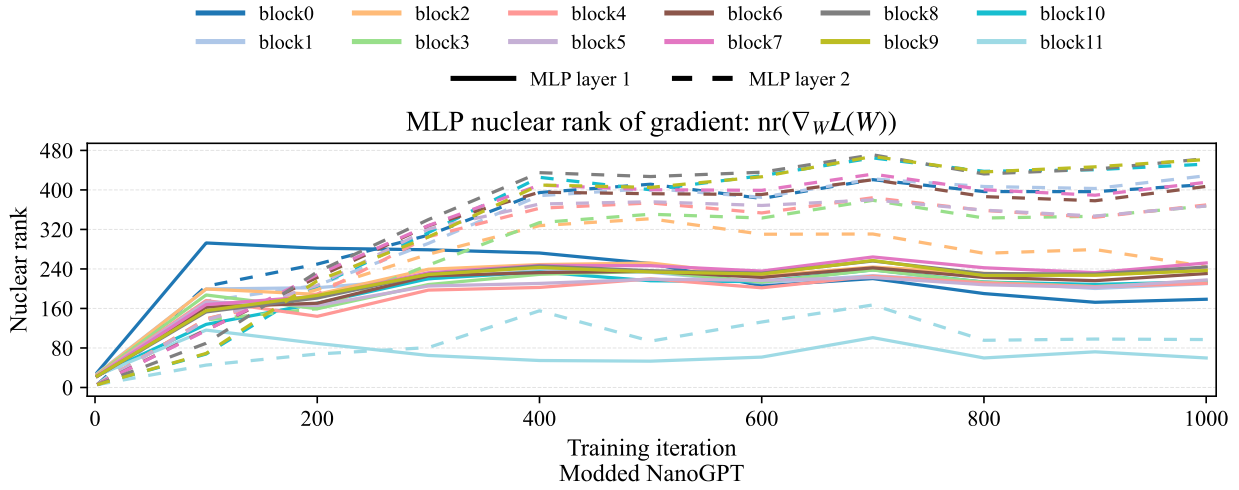


Figure 5: Modded NanoGPT MLP gradient nuclear ranks.

1.2.1 Multiple layers and transformer blocks

The discussion so far has treated a single matrix block W acting on a post-activation matrix A , and has shown that whenever the incoming features have low stable rank and the gradient has large nuclear rank, a spectral update on W enjoys a strictly better one-step guarantee than its Euclidean counterpart. In practice, however, we train *all* layers of a deep architecture simultaneously, and the parameters interact through a highly coupled nonlinearity. To understand when spectral methods are still favored in this setting, we abstract the architecture into a general layered model and study the full Hessian of the composite loss.

In Section 4 we formalize this viewpoint. We fix preactivation matrices $X_\ell(W) = W_\ell A_{\ell-1}(W)$ at each layer and let the activations $A_\ell(W)$ be obtained from $(X_1(W), \dots, X_\ell(W))$ through a twice differentiable map Φ_ℓ . The outer loss f is defined on the collection of preactivations (X_1, \dots, X_L) , and the training objective is $\mathcal{L}(W) := f(X_1(W), \dots, X_L(W))$. In this setting we show that the Hessian of \mathcal{L} is controlled by a feature-based term plus a smaller parameter-dependent term:

$$\langle \Delta W, \nabla^2 \mathcal{L}(W) \Delta W \rangle \leq C_F(W) \sum_{\ell=1}^L \|\Delta W_\ell A_{\ell-1}(W)\|_F^2 + C_{\text{op}}(W) \sum_{\ell=1}^L \|\Delta W_\ell\|_{\text{op}}^2,$$

for all perturbations $\Delta W = (\Delta W_1, \dots, \Delta W_L)$ and some finite constants $C_F(W)$ and $C_{\text{op}}(W)$ depending smoothly on the current iterate. For the standard $1/n$ -averaged losses we consider (squared loss, cross-entropy), $C_F(W)$ scales like $O(1/n)$, so the feature-based curvature constants inherit the usual $1/n$ dependence on the batch size. Both $C_F(W)$ and $C_{\text{op}}(W)$ are otherwise dimension-free in the sense that they depend only on the network architecture, depth, and current weight operator norms, and not on width or sequence length.⁴

Applying Taylor's theorem with remainder, we may therefore write,

$$\mathcal{L}(W + \Delta W) = \mathcal{L}(W) + \sum_{\ell=1}^L \langle G_\ell(W), \Delta W_\ell \rangle + \frac{1}{2} \langle \Delta W, \nabla^2 \mathcal{L}(W) \Delta W \rangle + R(\Delta W), \quad (1.7)$$

where $G_\ell(W) := \nabla_{W_\ell} \mathcal{L}(W)$ and $R(\Delta W) = o(\|\Delta W\|_F)$ collects higher order terms. Combining the Hessian bound with the basic norm inequalities

$$\|\Delta W_\ell A_{\ell-1}\|_F \leq \|A_{\ell-1}\|_{\text{op}} \|\Delta W_\ell\|_F, \quad \|\Delta W_\ell A_{\ell-1}\|_F \leq \|A_{\ell-1}\|_F \|\Delta W_\ell\|_{\text{op}},$$

we obtain feature-based blockwise curvature coefficients

$$L_\ell^F(W) := C_F(W) \|A_{\ell-1}(W)\|_{\text{op}}^2, \quad L_\ell^{\text{op}}(W) := C_F(W) \|A_{\ell-1}(W)\|_F^2.$$

Their ratio is exactly the stable rank of the incoming features:

$$\frac{L_\ell^{\text{op}}(W)}{L_\ell^F(W)} = \frac{\|A_{\ell-1}(W)\|_F^2}{\|A_{\ell-1}(W)\|_{\text{op}}^2} = \text{st}(A_{\ell-1}(W)).$$

These feature-based constants suggest natural blockwise step sizes. In the layered analysis of Section 4 (see in particular Section 4.4), we proceed as follows. For each block ℓ we fix two descent directions:

$$\text{GD direction: } -G_\ell(W), \quad \text{spectral direction: } -\text{polar}(G_\ell(W)),$$

⁴For simplicity, we state our Hessian bounds with a single feature term $\sum_\ell \|\Delta W_\ell A_{\ell-1}\|_F^2$ and a single parameter term $\sum_\ell \|\Delta W_\ell\|_{\text{op}}^2$. All of our arguments, most importantly the layerwise criterion comparing $\text{nr}(G_\ell)$ to $\text{st}(A_{\ell-1})$, continue to hold if one instead uses blockwise curvature weights $C_{\ell,F}(W)$ in front of $\|\Delta W_\ell A_{\ell-1}\|_F^2$ and $C_{\ell,\text{op}}(W)$ in front of $\|\Delta W_\ell\|_{\text{op}}^2$. This refinement only rescales the natural step sizes $L_\ell^F, L_\ell^{\text{op}}$ for each block and does not affect the nuclear-versus-stable-rank comparison.

and then choose scalar step sizes along these directions that minimize the quadratic upper bound in the Taylor model (1.7) under the mixed Hessian bound. This produces two full updates: a Euclidean update W^{GD} and a mixed spectral update W^{Spec} which applies spectral steps on blocks in $\mathcal{S} \subseteq [L]$ and Euclidean steps on the remaining blocks.

At the level of the quadratic model, their one-step guarantees take the form

$$\begin{aligned}\mathcal{L}(W^{\text{GD}}) &\leq \mathcal{L}(W) - \frac{1}{2} \sum_{\ell=1}^L \Delta_{\text{GD},\ell}(W) + R(\Delta W^{\text{GD}}), \\ \mathcal{L}(W^{\text{Spec}}) &\leq \mathcal{L}(W) - \frac{1}{2} \sum_{\ell \in \mathcal{S}} \Delta_{\text{Spec},\ell}(W) - \frac{1}{2} \sum_{\ell \notin \mathcal{S}} \Delta_{\text{GD},\ell}(W) + R(\Delta W^{\text{Spec}}),\end{aligned}$$

where each term $\Delta_{\text{GD},\ell}(W)$ is proportional to $\|G_\ell(W)\|_F^2$ and each $\Delta_{\text{Spec},\ell}(W)$ is proportional to $\|G_\ell(W)\|_*^2$, with proportionality factors determined by the curvature constants $L_\ell^F(W)$, $L_\ell^{\text{op}}(W)$ and the dimension-free correction $C_{\text{op}}(W)$. The explicit expressions for these factors are given in Section 4.4.

Ignoring the common higher-order remainder R , the spectral update has at least as much predicted decrease as the Euclidean update whenever, for every $\ell \in \mathcal{S}$,

$$\Delta_{\text{Spec},\ell}(W) \geq \Delta_{\text{GD},\ell}(W).$$

Using the structure of the denominators coming from the mixed Hessian bound, Section 4.4 shows that a simple sufficient layerwise condition for this inequality to hold is the nuclear-rank versus stable-rank inequality

$$\text{nr}(G_\ell(W)) := \frac{\|G_\ell(W)\|_*^2}{\|G_\ell(W)\|_F^2} \geq \text{st}(A_{\ell-1}(W)). \quad (1.8)$$

Thus, already at the level of the layered quadratic model, we recover the same criterion as in the random-feature setting: spectral updates are favored on those blocks whose incoming activations $A_{\ell-1}(W)$ have low stable rank while their gradients $G_\ell(W)$ have high nuclear rank.

For fully connected networks this picture is particularly transparent. The matrices $A_{\ell-1}$ in the are precisely the layerwise post-activations introduced in (1.2). Section 2 shows that, under mild assumptions on the input data and initialization, the stable rank $\text{st}(A_{\ell-1})$ is bounded by a numerical constant for all internal layers, while the input $A_0 = X$ need not have any such structure. In this regime, the constants L_ℓ^{op} and L_ℓ^F differ only by a fixed factor for $2 \leq \ell \leq L-1$, but may be very different at the input and output layers. Our implementation of **SpecGD** therefore uses the spectral step with step size $\|G_\ell\|_*/L_\ell^{\text{op}}$ on all internal weight matrices, and keeps the first and last layers on standard Euclidean steps with step size $1/L_\ell^F$. In other words, we apply spectral updates exactly where the incoming post-activations are empirically low-stable-rank, and retain Euclidean updates where the features (raw inputs or task-specific heads) are not guaranteed to be degenerate.

Transformers require a slightly more detailed bookkeeping, because the matrices which appear multiplying a given weight are composites of several operations: normalization, attention, residual connections and MLPs. Nevertheless, the layered formalism and the seminorm $\sum_\ell \|\Delta W_\ell A_{\ell-1}\|_F^2$ apply unchanged once we view each transformer block as built from linear maps W_ℓ composed with smooth activation maps Φ_ℓ . For concreteness, we write formulas for a single decoder block acting on a sequence representation $X \in \mathbb{R}^{d_{\text{model}} \times T}$ (hidden dimension d_{model} , sequence length T), and we suppress masking, multiple-heads, and positional encodings (e.g. RoPE) from the notation. These simplifications do not affect the stable-rank or nuclear-rank quantities we study, and the arguments

extend essentially verbatim to standard multi-head causal attention with RoPE. The single-head attention sublayer can be written as

$$\begin{aligned} A^{\text{rms}} &= \text{RMSNorm}(X), \\ Q &= W_Q A^{\text{rms}}, \quad K = W_K A^{\text{rms}}, \quad V = W_V A^{\text{rms}}, \\ P &= \text{softmax}(d_{\text{model}}^{-1/2} K^\top Q), \\ H &= VP, \\ X^{\text{att}} &= X + W_O H, \end{aligned}$$

where W_Q, W_K, W_V, W_O are the attention weight matrices and d_{embed} is the embedding dimension. The MLP sublayer then takes the form

$$\begin{aligned} A_{\text{mlp}}^{\text{rms}} &= \text{RMSNorm}(X^{\text{att}}), \\ B &= \sigma(W_1 A_{\text{mlp}}^{\text{rms}}), \\ X^+ &= X^{\text{att}} + W_2 B, \end{aligned}$$

where σ is a pointwise nonlinearity (e.g. GELU) and W_1, W_2 are the MLP weights. At the end of the network, a language-modeling head applies an RMS normalization followed by a linear map

$$A_{\text{final}}^{\text{rms}} = \text{RMSNorm}(X^+), \quad Z = W_{\text{lm}} A_{\text{final}}^{\text{rms}},$$

producing logits Z over the vocabulary.

In this block-level description, each trainable matrix appears exactly in the affine form $X_\ell = W_\ell A_{\ell-1}$ required by our layered model. The corresponding incoming features $A_{\ell-1}$ are:

$$A_{\ell-1} \in \{A^{\text{rms}}, A_{\text{mlp}}^{\text{rms}}, B, H, A_{\text{final}}^{\text{rms}}\},$$

depending on whether W_ℓ is one of $W_Q, W_K, W_V, W_O, W_1, W_2, W_{\text{lm}}$. For simplicity we have written RMSNorm as parameter-free, but in practice each normalization can carry a learned weight vector $\gamma \in \mathbf{R}^{d_{\text{model}}}$ acting elementwise as $x \mapsto \gamma \circ \frac{x}{\|x\|_{\text{rms}}}$. In our notation these weights can be treated as additional diagonal blocks $W_{\text{rms}} := \text{Diag}(\gamma)$ acting on the parameter-free RMS-normalized activations \tilde{A}^{rms} , so that $A^{\text{rms}} = W_{\text{rms}} \tilde{A}^{\text{rms}}$ and the affine form $X_\ell = W_\ell A_{\ell-1}$ continues to hold. The corresponding updates are slightly different. Indeed, on diagonal blocks spectral updates reduce to a sign-type update in the gain. We discuss this in more detail in Appendix 4.5. Note that the modded-NanoGPT repo [25] does not train the RMSNorm parameter, and instead uses fixed weight $\gamma = \mathbf{1}$.

Our measurements in Figure 2 (MLP post-activations B) and in Figure 6 (RMS activations $A^{\text{rms}}, A_{\text{mlp}}^{\text{rms}}, A_{\text{final}}^{\text{rms}}$) show that the RMS-normalized activations $A^{\text{rms}}, A_{\text{mlp}}^{\text{rms}}, A_{\text{final}}^{\text{rms}}$ and the MLP post-activations B all have low stable rank throughout training. For the attention output features H we may further write

$$H = VP = W_V A^{\text{rms}} P,$$

so that for perturbations of the output projection W_O we have

$$\Delta W_O H = \Delta W_O W_V A^{\text{rms}} P.$$

Here the RMS-normalized activations A^{rms} sit *between* two linear operators, but submultiplicativity still isolates their contribution:

$$\|\Delta W_O H\|_F = \|\Delta W_O W_V A^{\text{rms}} P\|_F \leq \|\Delta W_O\|_{\text{op}} \|W_V\|_{\text{op}} \|A^{\text{rms}}\|_F \|P\|_{\text{op}}.$$

More generally, each seminorm term $\|\Delta W_\ell A_{\ell-1}\|_F$ associated with a transformer block can be written as a product of the form

$$\Delta W_\ell A_{\ell-1} = \Delta W_\ell M_{\ell,\text{left}} \tilde{A}_{\ell-1} M_{\ell,\text{right}},$$

where $\tilde{A}_{\ell-1}$ is one of the low-stable-rank matrices A^{rms} , $A_{\text{mlp}}^{\text{rms}}$, B , $A_{\text{final}}^{\text{rms}}$, and $M_{\ell,\text{left}}$, $M_{\ell,\text{right}}$ are fixed linear maps (products of attention projections, residual additions, or the attention kernel P). Using

$$\|\Delta W_\ell A_{\ell-1}\|_F = \|\Delta W_\ell M_{\ell,\text{left}} \tilde{A}_{\ell-1} M_{\ell,\text{right}}\|_F \leq \|\Delta W_\ell\|_{\text{op}} \|M_{\ell,\text{left}}\|_{\text{op}} \|M_{\ell,\text{right}}\|_{\text{op}} \|\tilde{A}_{\ell-1}\|_F,$$

we see that the curvature constants relevant for block ℓ scale with $\|\tilde{A}_{\ell-1}\|_F^2$, and the ratio $L_\ell^{\text{op}}/L_\ell^{\text{F}}$ is again governed by the stable rank of these RMS and MLP activations.

To make the connection between gradient nuclear ranks and the upstream feature matrices completely explicit, it is useful to summarize, for each parameter block, which activation matrix enters the condition (1.8). Table 1 records the correspondence we will use in our experiments.

Parameters W_ℓ	Activation in (1.8) (for W_ℓ)
W_Q	A^{rms}
W_K	A^{rms}
W_V	A^{rms}
W_O	A^{rms} (via $H = W_V A^{\text{rms}} P$)
W_1	$A_{\text{mlp}}^{\text{rms}}$
W_2	B
W_{lm}	$A_{\text{final}}^{\text{rms}}$
Embedding	X (moderate stable-rank guarantee)

Table 1: For each parameter block W_ℓ , the activation matrix whose stable rank appears on the right-hand side of (1.8). The corresponding left-hand side is always the gradient nuclear rank $\text{nr}(G_\ell)$ for that same block.

Figures 5, 6, 7, 8, and 9 illustrate how these quantities behave in a NanoGPT run. The plots in Figure 5 show that the gradient nuclear ranks for the MLP weights remain consistently large along training, while Figures 2 and 6 demonstrate that both the MLP post-activations B and the RMS-normalized activations A^{rms} , $A_{\text{mlp}}^{\text{rms}}$, $A_{\text{final}}^{\text{rms}}$ have stable rank bounded by a small numerical constant. Thus, for these blocks, the inequality (1.8) is strongly activated, and the simple GD-based model predicts a clear advantage for spectral-style updates. This is consistent with the convergence bounds presented in [44], where improvements over Euclidean methods are also driven by large nuclear-to-Frobenius ratios.

Figures 8 and 9 shows a similar behavior for the attention weights: the gradient nuclear ranks for W_Q , W_K , W_O are typically large and W_V is more modestly sized, while their reference activations in Table 1 are the low-stable-rank RMS features of Figure 6. In contrast, Figure 7 reveals a different picture for the input embedding weights and the language-model head. The embedding matrix multiplies a raw token-indicator matrix whose stable rank hovers around 26 (see section 2.2.1 for more on this), which is modestly low relative to the ambient dimension but noticeably larger than the stable ranks of the internal post-activations; the nuclear rank of the embedding gradient grows from roughly 100 to 400 over the course of training (Figure 10). Thus the ratio $\text{nr}(G_{\text{emb}})/\text{st}(X)$ is only moderately larger than one and much smaller than the corresponding ratios for the hidden MLP and attention blocks, so our condition (1.8) predicts a milder advantage for spectral updates on the embedding matrix. This matches our empirical experience with the NanoGPT: applying

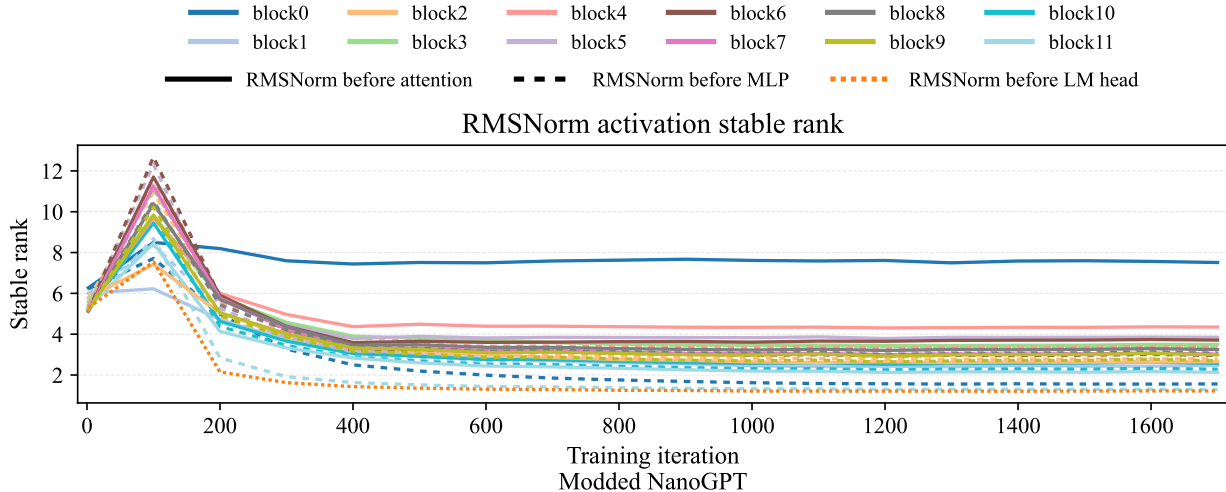


Figure 6: Stable rank of RMS-normalized activations A^{rms} , $A^{\text{rms}}_{\text{mlp}}$, $A^{\text{rms}}_{\text{final}}$.

MUON-style spectral updates to the input embedding in the Modded-NanoGPT run changes training and validation curves only slightly (not shown). From the viewpoint of [44], a more natural geometry for the embedding block is the $\ell_1 \rightarrow \ell_2$ operator norm, since the input tokens are one-hot vectors of ℓ_1 -norm one; in that setting the relevant Lipschitz constants are controlled by the maximum column norm of the embedding matrix rather than its spectral norm, and the stable-rank heuristic is replaced by an ℓ_1 -based argument. We do not pursue this alternative geometry here.

To sum up, All matrix-valued weights interior to the the transformer blocks—the attention projections and MLP matrices—see incoming features that are effectively low-stable-rank in the sense relevant for the Hessian bound, and their gradient nuclear ranks are typically large. For these blocks the inequality (1.8) is strongly activated, and spectral updates have a clear structural advantage over Euclidean ones. The input embedding weight matrix, by contrast, multiplies raw token indicators and lies only marginally in this regime, while the language-model head sits in an intermediate regime where the same inequality holds but with a much smaller margin. The resulting picture is consistent with current practice: the modded-NanoGPT repository applies spectral updates (implemented via MUON) to all 2D weight blocks inside the transformer, while keeping both the token embedding and the language-model head on AdamW-style updates. Moreover, Section 2.2 and Corollary 2.15 show that, at initialization, the transformer activations that feed these blocks have stable rank bounded by numerical constants independent of width and sequence length, uniformly for the MLP post-activations, and growing at most quadratically with the layer index for the remaining RMS-normalized and hidden states. In view of the momentum-based implementation of MUON and the different effective geometry of AdamW, our comparison should be read as a geometric heuristic instead of a precise hyperparameter recommendation: the nuclear-rank versus stable-rank condition explains why spectral geometry is well matched to the internal layers of MLPs and transformers, even though our one-step comparison is carried out for Euclidean gradient descent instead of AdamW.

1.2.2 When are spectral updates less helpful?

Given the discussion thus far the reader might conclude that spectral updates are always preferred to Euclidean ones. This is not the case. The random-feature model already provides a simple

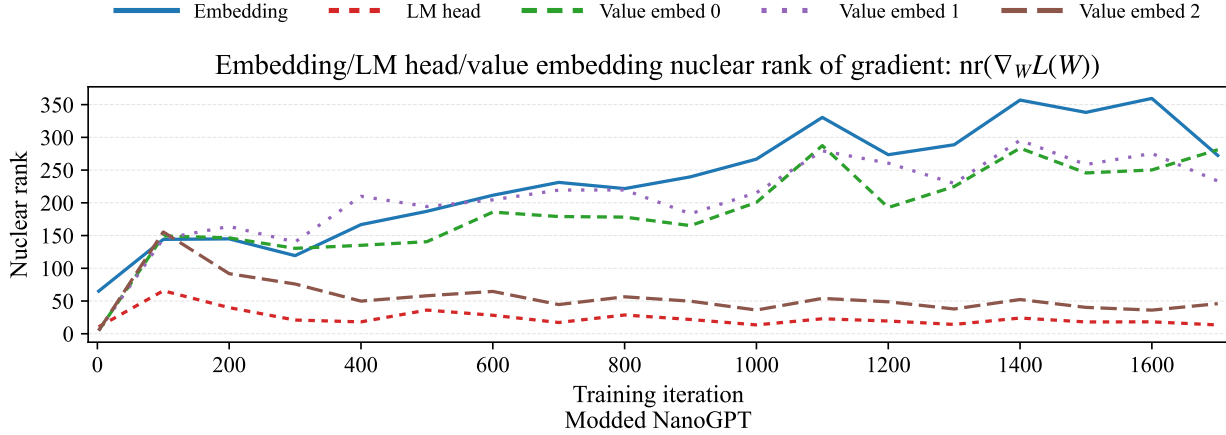


Figure 7: Gradient nuclear ranks for the token embedding and language-model head parameters in the same NanoGPT run. The mean ratio for the LM head over the last 1000 steps is approximately 42.68.

counterexample in which the nuclear-rank condition (1.5) fails and spectral updates are *slower* than Euclidean ones.

To demonstrate, we repeat the experiment from Figure 3, keeping the same dimensions, data distribution, and ground-truth matrix W_{\sharp} , but replacing the ReLU nonlinearity with a SwiGLU activation. Concretely, in this variant the random-feature matrix is

$$A = \text{SwiGLU}(W_1 X, W_2 X) := \text{SiLU}(W_1 X) \circ (W_2 X),$$

where $W_1, W_2 \in \mathbf{R}^{k \times d}$ are independent Gaussian weight matrices, the Hadamard product \circ is taken coordinatewise, and

$$\text{SiLU}(t) := t \cdot (1 + e^{-t})^{-1}$$

is the usual Swish/SiLU nonlinearity applied elementwise. Thus each feature coordinate is of the form

$$a_{ij} = \text{SiLU}((W_1 X)_{ij}) (W_2 X)_{ij},$$

in contrast to the ReLU experiment where $A = \sigma(W_1 X)$ depends on a single weight matrix. We will refer to such activations of the form $\phi(W_1 X) \circ (W_2 X)$ as *gated activations*.

In the ReLU experiment, the post-activation matrices A are empirically low-rank. One way to interpret this, developed in Section 2, is that non-centered activations such as ReLU and its variants produce a large rank-one spike in the Gram matrix AA^\top aligned with the mean vector $\mathbb{E}a$. This spike dominates the spectrum and keeps $\text{st}(A)$ bounded by a numerical constant even as the width grows. Gated activations like SwiGLU behave differently. At Gaussian initialization the mean vector $\mathbb{E}a$ is small, so the mean-induced spike in AA^\top is absent. The resulting Gram matrix has a more isotropic spectrum, and the stable rank $\text{st}(A)$ now grows proportionally with the width instead of remaining $O(1)$, while the nuclear rank $\text{nr}(\nabla \mathcal{L}(W))$ of the gradient remains modest. In the Gaussian random-feature experiment considered here this means that AA^\top has essentially no spike at initialization: its spectrum is bulk-only. For data that already carry a low-rank spike, however, certain centered activations are known to propagate that *informative* spike, as in the nonlinear spiked-covariance and conjugate-kernel analyses discussed in Section 1.3 [2, 59]; what

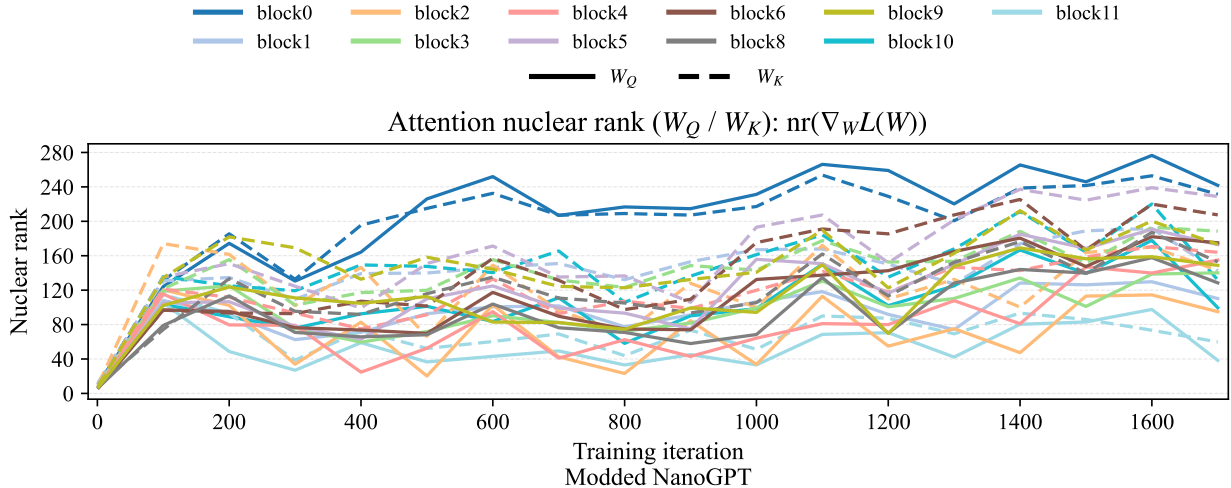


Figure 8: Gradient nuclear ranks for the attention parameters W_Q, W_K in the same NanoGPT run.

they avoid is exactly the large, uninformative mean-induced spike that drives the low-stable-rank regime in our ReLU examples.

In this regime the inequality

$$\text{nr}(\nabla \mathcal{L}(W)) \geq \text{st}(A)$$

is violated: the right-hand panel of Figure 11 shows the nuclear-rank curves dipping below the dashed stable-rank level. The one-step comparison in (1.5) therefore predicts that gradient descent should outperform spectral descent, and the left-hand panel confirms this prediction: GD reaches a much smaller objective value in far fewer iterations than SpecGD.

In Appendix A, we also repeat the sparse regression experiment of Figure 1 with a SwiGLU activation. There we see that SpecGD can still perform well at small batch sizes, where the post-activations remain moderately low-stable-rank, but that its advantage is quickly lost as the batch size (and hence the stable rank) increases.

Method	Non-gated MLP	Gated MLP
All Adam	3.9242	3.8837
Muon(W_{out} only)	3.7023	3.7843
Muon(All Attn, MLP)	3.5654	3.5125

Table 2: Validation loss at $10k$ training steps for the MLP ablations of Wang et al. [58]. The model is a 160M-parameter NanoGPT-style decoder-only transformer trained on FineWeb, with columns corresponding to standard (non-gated) and gated MLP variants as in Eqns. (3.2)–(3.3) of [58]. In the gated case, the MLP uses a gated activation of the form $\phi(W_{\text{in}}h) \circ (W_{\text{gate}}h)$ feeding W_{out} .

As a point of comparison, Table 2 summarizes the MLP ablations reported by Wang et al. [58]. For the non-gated MLP, switching only W_{out} from Adam to Muon reduces the validation loss from 3.9242 (All Adam) to 3.7023, while full Muon on all attention and MLP weights reaches 3.5654; thus about 62% of the total improvement from Adam to full Muon is already captured by changing W_{out} alone. In the gated MLP, the corresponding losses are 3.8837 (All Adam), 3.7843 (Muon on W_{out} only), and 3.5125 (Muon on all attention and MLP weights), so the change on W_{out} accounts for only about 27% of the full gain. One plausible interpretation, in light of the SwiGLU random-

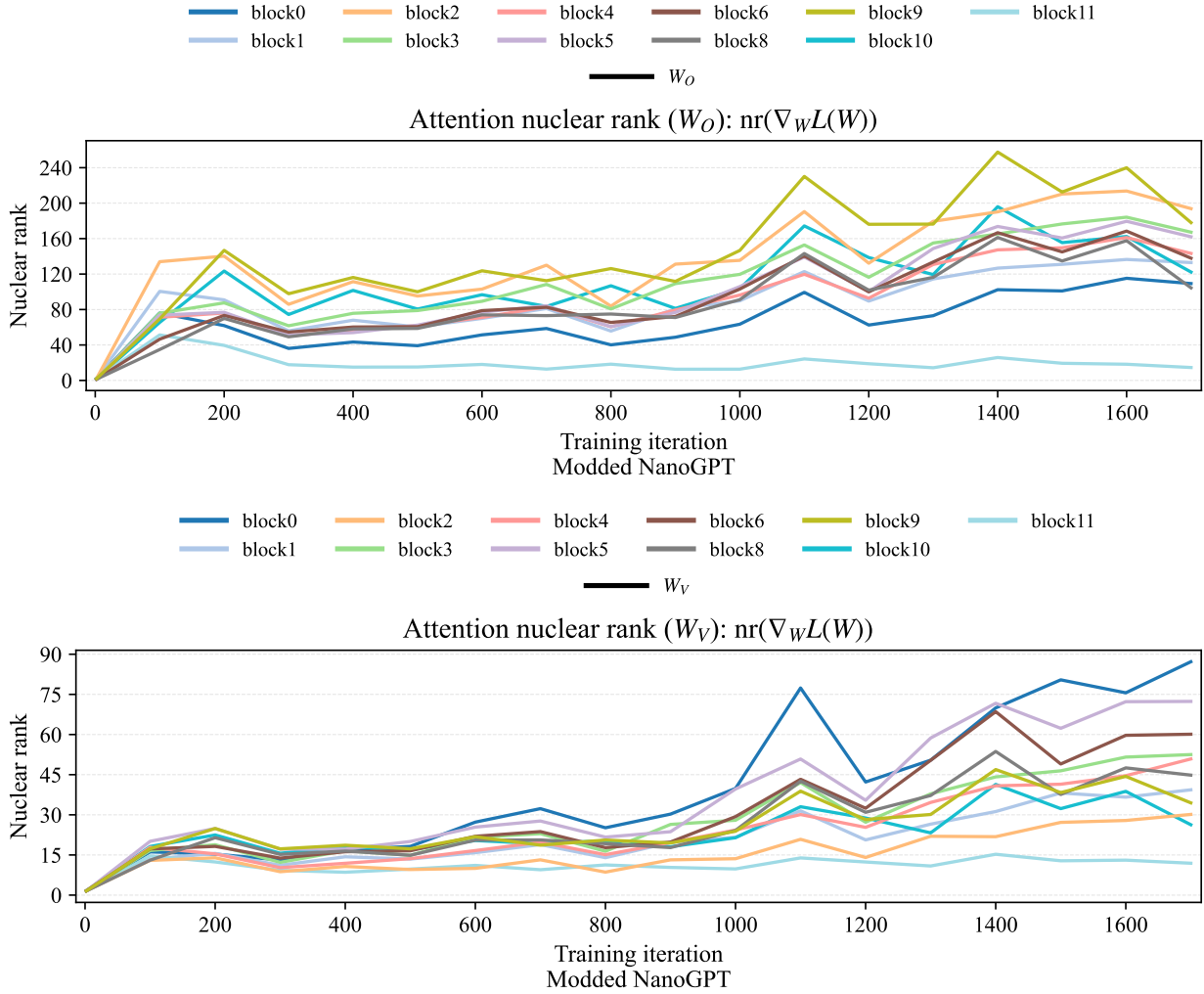


Figure 9: Gradient nuclear ranks for the attention parameters W_O, W_V in the same NanoGPT run.

feature example above, is that gated activations produce more nearly centered, higher-stable-rank post-activations feeding W_{out} , which makes Euclidean updates on that block better conditioned and leaves less room for a spectral update to help. A detailed verification of this mechanism in large transformers would require additional ablations and lies beyond our scope here.

1.3 Related literature

We briefly discuss work on (i) spectral and norm-constrained optimizers such as `SpecGD`, `Muon`, and `Scion`, and (ii) empirical and theoretical studies of low-rank structure in gradients and activations. We focus only on results that are relevant to the structural phenomena studied in this paper.

Spectral and norm-constrained optimizers. Preconditioned Spectral Descent (PSD) and Stochastic Spectral Descent (SSD) were among the first optimizers to use spectral geometry for training deep models. Carlson et al. formulate non-Euclidean gradient descent in general Schatten norms and show that for objectives built from log-sum-exp terms (including RBMs, feedforward networks, and CNNs), the loss admits a tighter majorization bound in the Schatten- ∞ norm than in

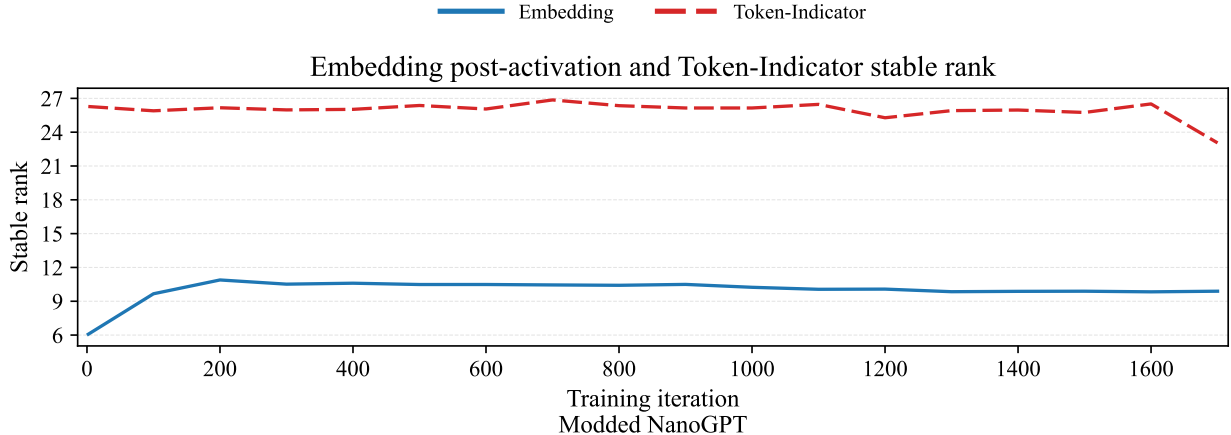


Figure 10: Embeddings matrix post-activation and Token-Indicator stable rank throughout training. See Section 2.2.1 for more on these matrices.

the Frobenius norm; this motivates steepest descent in the spectral norm rather than the Euclidean norm [7, 9]. Their analysis is entirely in terms of norm-dependent Lipschitz constants and matrix updates; they do not study nuclear ranks ratios of the gradient, nor connect the choice of geometry to the stable rank of the propagated data.

Muon [26] applies a similar spectral update—implemented with a Newton–Schulz approximation to the polar factor—to the hidden layers of modern architectures and has shown strong empirical performance for NanoGPT-scale models and other large-scale training tasks. Related work by Bernstein and collaborators has advocated norm-aware training via “modular norms” and “modular duality,” helping to popularize spectral and operator-norm updates in large-scale settings and providing practical Newton–Schulz-based orthogonalization routines used in **Muon** implementations [3, 4, 32]. A recent convergence analysis of **Muon** by Shen et al. [49] is particularly close in spirit to our work. In a general nonconvex setting, they derive iteration-complexity bounds for **Muon** and GD under various smoothness assumptions and identify two key quantities: a Hessian-based ratio J_t/L_t , and the gradient nuclear ranks $\text{nr}(\nabla f(W_t))$. Their central condition (Eq. (4) in [49]) is

$$\frac{J_t}{L_t} \lesssim \frac{\|\nabla f(W_t)\|_*^2}{\|\nabla f(W_t)\|_F^2}, \quad (1.9)$$

and they show that when (1.9) holds along the trajectory, **Muon** enjoys better convergence guarantees than GD for reaching a nuclear-norm stationary point. They also empirically track J_t , L_t , and the gradient nuclear ranks during GD and **Muon** training of a small MLP, and observe that (1.9) holds in the early and middle phases of training, consistent with **Muon**’s speedup.

Our analysis is complementary. We derive a *layerwise* inequality for **SpecGD** versus GD that has the same gradient ratio on the right-hand side as Shen et al. (1.9), but replaces the Hessian ratio J_t/L_t by the *stable rank of the post-activation matrices*:

$$\text{st}(A^{\ell-1}) \lesssim \text{nr}(\nabla_{W_\ell} \mathcal{L}(W))$$

We do not claim that it is conceptually novel that the nuclear rank of the gradient controls when spectral updates are better than Euclidean updates—this is already implicit in PSD/SSD and

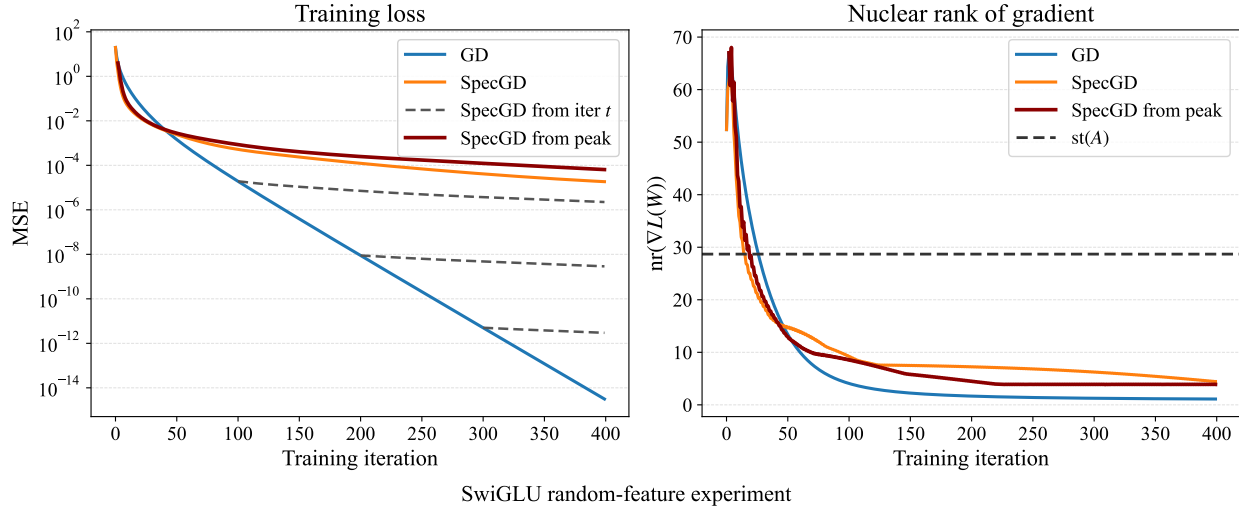


Figure 11: **A cautionary tail.** Random-feature regression with SwiGLU features $A = \text{SwiGLU}(W_1 X, W_2 X) = \text{SiLU}(W_1 X) \circ (W_2 X)$, in the same setup as Figure 3 but with the ReLU nonlinearity replaced by SwiGLU. *Left:* objective gap $\mathcal{L}(W) - \min \mathcal{L}$ along gradient descent (GD, solid blue) and spectral gradient descent (SpecGD, solid orange). Unlike the ReLU experiment in Figure 3, here SpecGD is *slower* than GD. *Right:* nuclear rank $\text{nr}(\nabla \mathcal{L}(W))$ of the gradient (solid curves) together with the stable rank $\text{st}(A)$ of the post-activations (black dashed line). Because SwiGLU produces post-activations with small mean at Gaussian initialization, the Gram matrix AA^\top lacks a large mean-induced spike and its stable rank scales with width. The inequality $\text{nr}(\nabla \mathcal{L}(W)) \gtrsim \text{st}(A)$ is more easily violated during training, and the one-step guarantees from Section 1.2 predict that Euclidean updates should outperform spectral ones.

explicit in the convergence bounds for **Muon** and related methods. Our contribution is to show that, in the setting of random-feature regression, deep neural networks, and transformers, the *left-hand side* of this inequality is naturally small (post-activations have low stable rank), while the *right-hand side* can be large (gradient nuclear rank is dimension-dependent), both theoretically (after a few GD steps in random-feature models) and empirically (in NanoGPT-scale training). This provides a concrete, data-driven explanation for the regimes where spectral updates outperform GD.

The **Scion** optimizer of Pethick et al. [44] builds a general framework of stochastic conditional gradient (LMO-based) methods with norm constraints, in which **Muon** is one special case and **Scion** corresponds to using operator norms (e.g., spectral and ℓ_∞ norms) for different layers. Their convergence guarantees are stated in terms of the dual norm of the gradient, $\|\nabla f(x)\|_*$, under L -smoothness in the corresponding primal norm, and in the spectral case this dual norm is exactly the nuclear norm. Thus their rates naturally control $\mathbb{E}\|\nabla f(x)\|_*$, while classical GD rates control $\mathbb{E}\|\nabla f(x)\|_F$. To compare these guarantees, one must again relate nuclear and Frobenius norms of the gradient, i.e., consider $\|\nabla f(x)\|_*/\|\nabla f(x)\|_F$. Pethick et al. focus on the algorithmic framework, norm choices, and hyperparameter transfer, and do not attempt to characterize when this ratio is large in neural networks.

Relation to nonlinear spiked covariance and conjugate kernel work. Our perspective is complementary to recent analyses of nonlinear spiked covariance matrices and conjugate kernels [2, 59]. There, the goal is to understand how a finite number of *informative* spikes in the input data propagate through random networks or how nonlinearity and non-Gaussianity affect the edge of the

spectrum, and for this reason the activations (and weights) are explicitly centered to suppress large, non-informative outliers. Earlier work by Pennington and Worah [43] analyzes the same one-layer Gram matrix $M = \frac{1}{m}YY^\top$ with $Y = f(WX)$ in a proportional random matrix limit and derives an explicit characterization of its limiting spectral density in terms of two Gaussian functionals of the activation; like [2, 59], they work with centered nonlinearities and focus on the bulk spectrum rather than on stable rank or mean-induced spikes. By contrast, we work with the non-centered activations used in practice (e.g. ReLU), for which even isotropic inputs generate mean-induced spikes in the post-activation covariances at every hidden layer. These spikes need not carry task-relevant signal, but they force the activation matrices to be intrinsically low-stable-rank, and it is precisely this degenerate geometry that makes spectral updates more effective than Euclidean ones in the regimes we study.

Low-rank structure in gradients and activations. There is a substantial literature documenting low-dimensional or low-rank structure in the gradients and representations of deep networks. Gur-Ari et al. [18] showed that during training, gradients quickly concentrate in a low-dimensional subspace spanned by the top Hessian eigenvectors—a “tiny subspace” whose dimension is often comparable to the number of classes [18]. This is a statement about *gradient subspace* dimension rather than nuclear rank, but it supports the general picture that most of the optimization geometry is captured by a small number of directions. More recent work in large-scale training leverages this low-rank structure explicitly: the GaLore algorithm [62] performs gradient low-rank projection to reduce optimizer memory while preserving pretraining performance, and reports empirical evidence that gradients of large language models admit very low-rank approximations; Sonthalia et al. [50] analyze low-rank gradients in two-layer networks in a spiked data model, proving that the gradient spectrum is sharply concentrated and identifying parameter and data regimes where gradient rank is small.

Huh et al. [22] empirically observe that the Gram matrix of the final-layer embeddings of deep networks has low effective rank (Observation 3.1 and 3.2), both at initialization and after training, and conjecture that deeper networks are biased toward lower effective-rank embeddings. In our notation, their Gram matrices are constructed from the columns of the post-activation matrix A_L , and effective rank is a soft-rank functional of the same spectrum as the stable rank $\text{st}(A_L)$. Our results are consistent with these observations and extend them in two directions: (i) we work with the stable rank $\text{st}(A_\ell)$ of the layerwise post-activation matrices, which is a closely related notion of effective dimensionality of the embeddings, and show theoretically in several random-feature and quadratic-activation models that $\text{st}(A_\ell)$ is bounded by a numerical constant independent of the layer width; and (ii) we verify empirically in realistic MLP and NanoGPT models that this low-stable-rank property holds across *all* intermediate layers, not only for the final embedding, and that it persists along the optimization trajectory. While we are mainly interested here in the stable rank, our results immediately imply that the “effective rank” in the sense of [22] is of order $\log(d)$.

A complementary line of work seeks to *remove* the kind of low-rank degeneracy we study by introducing normalization layers such as batch normalization [23]. For example, Daneshmand et al. [12] show that in deep *linear* networks (i.e., without nonlinear activations), batch normalization provably prevents rank collapse: the (soft) rank of the hidden activations remains of order d at all depths, whereas in the unnormalized case the representations become effectively rank one as depth grows. This line of work is complementary to ours: rather than modifying the architecture to avoid degeneracy, we take the activation matrices as they arise in standard, non-normalized networks with non-centered nonlinearities, and analyze how their low-stable-rank, spiked covariance structure influences optimization and favors spectral updates over Euclidean ones.

Finally, a parallel line of work examines the spectral structure of the Hessian itself and reports a similar ‘‘bulk + spikes’’ picture: Sagun et al. [48] and Papyan [42] find that deep networks have a large bulk of near-zero eigenvalues with a small number of large outliers, while Ghorbani et al. [16] show that these outliers appear rapidly during training and that the gradient concentrates in their eigenspaces. Our stable-rank perspective is consistent with this broader view of degenerate curvature, but focuses on the propagated data matrices that directly enter the layerwise Lipschitz constants relevant for spectral versus Euclidean updates.

Organization. Section 2 establishes our low-stable-rank results for post-activation matrices. Section 3 analyzes the random-feature regression model and proves that the nuclear-rank condition (3) is activated after a few gradient descent steps. Section 4 then formalizes a general layered model for deep architectures and derives a one-step descent comparison between Euclidean and spectral updates.

2 Controlling the stable rank: from samples to the population

In this section, we will establish sufficient conditions which ensure that the stable rank of post-activation matrices is indeed bounded by a numerical constant. Setting the stage, consider the post-activation matrices A_ℓ of neural networks defined recursively in (1.2). Recall that $X \in \mathbf{R}^{d \times n}$ is the initial data matrix, having the feature vectors as its columns and $\sigma: \mathbf{R} \rightarrow \mathbf{R}$ is some activation function. Observe that columns of the data X propagate independently, meaning we may write

$$A_\ell = [F(x_1), \dots, F(x_d)], \quad (2.1)$$

for some fixed map F . Now if the feature vectors x_i (columns of X) are iid copies of a random vector $x \in \mathbf{R}^d$, then the columns of A_ℓ are i.i.d. copies of the random vector $F(x)$. Consequently, we may invoke standard properties of random matrices to ensure that the stable rank $\text{sr}(A^{(\ell+1)})$ is controlled by the ratio of the trace/operator norm of the population second-moment matrix.

With this in mind, henceforth we consider a random matrix $Z_n = [z_1, \dots, z_d]$ with columns $z_i \in \mathbf{R}^d$ that are iid copies of a random vector z satisfying $0 < \mathbb{E}\|z\|_2^2 < \infty$. In the context of post-activation matrices (2.1), the vectors z_i stand for $F(x_i)$. We define the empirical second-moment matrix $M_n = \frac{1}{n}Z_n Z_n^\top = \frac{1}{n} \sum_{j=1}^n z_j z_j^\top$ and its expectation $M = \mathbb{E}[zz^\top]$. Throughout, we let $\text{er}(B) = \text{tr}(B)/\|B\|_{\text{op}}$ denote the *effective rank* of any positive semidefinite matrix. Note that the effective rank and the stable rank are related by the expression $\text{sr}(Z_n) = \text{er}(M_n)$, and therefore we expect $\text{sr}(Z_n)$ to be close to $\text{er}(M)$ when n is large. We begin formalizing this with the following rudimentary guarantee on asymptotic consistency.

Lemma 2.1 (Consistency of the stable rank). *The following holds:*

$$\text{sr}(Z_n) \xrightarrow{\text{a.s.}} \text{er}(M) \quad \text{as } n \rightarrow \infty.$$

Proof. The strong law of Large numbers applied entrywise directly implies that M_n converges almost surely to M as $n \rightarrow \infty$. Since both the operator norm and the trace are continuous functions, an application of the continuous mapping theorem shows that $\text{tr}(M_n)/\|M_n\|_{\text{op}}$ tends to $\text{tr}(M)/\|M\|_{\text{op}}$ almost surely as $n \rightarrow \infty$, as claimed. \square

We next would like to obtain nonasymptotic guarantees on the error $\text{sr}(Z_n) - \text{er}(M)$. Most important is an upper-bound on this error, since we want to upper bound $\text{sr}(Z_n)$. We now show that such an upper bound can be obtained under a mild small ball assumption (2.2) on the distribution of

z. Small ball conditions are standard in the literature and are closely related to the Paley–Zygmund inequality and lower bounds on the ratio of moments; see for example [31, 34–37, 40, 41].

Theorem 2.2 (Constant probability guarantees). *Suppose that there exists a unit vector $u_\star \in \mathbf{R}^d$ and constants $p_0 \in (0, 1)$ and $c_0 \in \mathbf{R}$ satisfying the small ball condition*

$$\mathbb{P}(\langle z, u_\star \rangle^2 \geq c_0 \|M\|_{\text{op}}) \geq p_0. \quad (2.2)$$

Then for any $c \in (0, \frac{1}{2})$, as long as $n \geq \frac{\log(1/2c)}{8p_0}$, the upper bound on the stable rank

$$\text{sr}(M_n) \leq \frac{2}{p_0 c_0 c} \cdot \text{er}(M), \quad (2.3)$$

holds with probability at least $1 - 2c$.

Proof. Trivially, equality holds $\mathbb{E} \text{tr}(M_n) = \text{tr}(M)$. Therefore, for any $c > 0$ Markov's inequality implies $\text{tr}(M_n) \leq c^{-1} \text{tr}(M)$ with probability at least $1 - c$. Next, we compute the lower-bound

$$\|M_n\|_{\text{op}} \geq u_\star^\top M_n u_\star^\top \geq \frac{1}{n} \sum_{i=1}^n \langle z_i, u_\star \rangle^2. \quad (2.4)$$

Taking into account the small ball condition (2.2), Chernoff's inequality implies that with probability at least $1 - \exp(-p_0 n/8)$ at least $\frac{p_0 n}{2}$ of the summands in (2.4) are bounded below by $c_0 \|M\|_{\text{op}}$. Therefore in this event, we have $\|M_n\|_{\text{op}} \geq \frac{p_0 c_0}{2} \|M\|_{\text{op}}$. Simple algebra completes the proof. \square

Next, we aim to boost the conclusion of Theorem 2.2 to hold with high probability and with the proportionality coefficient in (2.3) arbitrarily close to one. To this end, we will require the random vector z to be sub-Gaussian in an elliptical sense (2.5). The following theorem shows that with high probability, we have the bound $\text{sr}(Z_n) \lesssim (1 + \sqrt{\frac{\text{er}(M)}{n}}) \cdot \text{er}(M)$. Henceforth, we will be using standard definition of the sub-Gaussian and sub-exponential norms, $\|\cdot\|_{\psi_2}$ and $\|\cdot\|_{\psi_1}$, as described for example in the monograph [57, Chapter 2].

Theorem 2.3 (High probability). *Assume that the centered random vector $\tilde{z} := z - \mathbb{E}[z]$ satisfies the sub-Gaussian condition*

$$\|\langle \tilde{z}, u \rangle\|_{\psi_2} \leq K \sqrt{\langle Mu, u \rangle} \quad \forall u \in \mathbf{R}^d. \quad (2.5)$$

Then there exist constants $C, c > 0$ such that for any $u \geq 1$, the estimate

$$\frac{|\text{sr}(Z_n) - \text{er}(M)|}{\text{er}(M)} \leq CK^4 \sqrt{\frac{\text{er}(M) + u}{n}},$$

holds with probability at least $1 - 5e^{-cu}$, as long as $n \geq CK^8(\text{er}(M) + u)$.

Proof. Define the quantities $a_n := \text{tr}(M_n)$, $a := \text{tr}(M)$, $b_n := \|M_n\|_{\text{op}}$, $b := \|M\|_{\text{op}}$, and $\Delta := M_n - M$. Then we can compute

$$\frac{a_n}{b_n} - \frac{a}{b} = \frac{a_n - a}{b_n} + \frac{a(b_n - b)}{b b_n}.$$

Recall from Theorem B.2 that the estimate

$$\|\Delta\|_{\text{op}} \leq C_1 K^4 \left(\sqrt{\frac{\text{er}(M) + u}{n}} + \frac{\text{er}(M) + u}{n} \right) b \quad (2.6)$$

holds with probability at least $1 - 2e^{-u}$. In particular, within this event the estimate $\|\Delta\|_{\text{op}} \leq b/2$ holds as long as $n \geq C_2 K^8(\text{er}(M) + u)$ for some constant C_2 . Consequently, in this setting, by the triangle inequality we have $b_n \geq b/2$ and therefore

$$\left| \frac{a_n}{b_n} - \frac{a}{b} \right| \leq \frac{2|a_n - a|}{b} + \frac{2a}{b^2} |b_n - b| \leq \frac{2|a_n - a|}{b} + \frac{2a}{b^2} \|\Delta\|_{\text{op}}. \quad (2.7)$$

Applying Theorem B.1 we see that the estimate

$$\frac{|a_n - a|}{b} = \frac{a}{b} \frac{|a_n - a|}{a} \leq C_3 K^2 \frac{a}{b} \left(\sqrt{\frac{u}{n}} + \frac{u}{n} \right), \quad (2.8)$$

holds with probability at least $1 - 4e^{-cu}$. Combining the two bounds (2.6) and (2.8) with (2.7) directly gives

$$\left| \frac{a_n}{b_n} - \frac{a}{b} \right| \leq CK^4 \frac{a}{b} \left(\sqrt{\frac{\text{er}(M) + u}{n}} + \frac{\text{er}(M) + u}{n} \right),$$

for some constant C . By our assumption $n \geq C_2 K^8(\text{er}(M) + u)$, the first term on the right dominates. An application of the union bound completes the proof. \square

Example 2.1. As a concrete example, consider the setting of (2.1) corresponding to fixed weights W_1, W_2, \dots, W_ℓ and any 1-Lipschitz continuous activation function (e.g. ReLU). Then z has the form

$$z = F(x) = \sigma(W_\ell \sigma(W_{\ell-1} \dots \sigma(W_1 x))).$$

Clearly F is Lipschitz continuous with constant $\prod_{i=1}^\ell \|W_i\|_{\text{op}}$. Therefore if x is standard Gaussian $\mathcal{N}(0, I)$, Gaussian concentration [57, Theorem 5.2.3] shows $\|\langle z - \mathbb{E}z, u \rangle\|_{\psi_2} \leq C \prod_{i=1}^\ell \|W_i\|_{\text{op}} \cdot \|u\|_2$. Thus assumption (2.5) holds with $K = \frac{C \prod_{i=1}^\ell \|W_i\|_{\text{op}}}{\sqrt{\lambda_{\min}(M)}}$.

2.1 Controlling the effective rank of the population second-moment

In the previous section, we obtained a variety of conditions which ensured that the stable rank of the data matrix Z_n is bounded by a constant multiple of the effective rank of the population second-moment matrix $M = \mathbb{E}zz^\top$. In this section, we specialize the discussion to post-activation matrices and bound the effective rank of M in concrete cases of interest. All the computations will stem from the following elementary observation

$$\text{tr}(M) = \mathbb{E}\|z\|_2^2 \quad \text{and} \quad \|M\|_{\text{op}} \geq \|\mathbb{E}z\|_2^2.$$

Therefore we have the upper bound on the effective rank

$$\text{er}(M) \leq \frac{\mathbb{E}\|z\|_2^2}{\|\mathbb{E}z\|_2^2}.$$

We will abuse notation slightly and call the right side the noise-to-signal ratio $\text{NSR}(z) := \frac{\mathbb{E}\|z\|_2^2}{\|\mathbb{E}z\|_2^2}$.

We begin bounding $\text{NSR}(z)$ with the following rudimentary lemma, whose proof we omit.

Lemma 2.4 (Simple bound). *Consider a random vector $z = \sigma(Wx)$ for some fixed matrix $W \in \mathbf{R}^{k \times d}$, random vector $x \in \mathbf{R}^d$, and an activation function $\sigma: \mathbf{R} \rightarrow \mathbf{R}$. Suppose that there exist constants $\alpha, \beta > 0$ and a function $f: \mathbf{R}^d \rightarrow (0, \infty)$ such that for any $w \in \mathbf{R}^d$, the random variable $g = \langle w, x \rangle$ satisfies*

$$\alpha \cdot f(w) \leq (\mathbb{E}\sigma(g))^2 \quad \text{and} \quad \mathbb{E}\sigma(g)^2 \leq \beta \cdot f(w). \quad (2.9)$$

Then the inequality $\text{NSR}(z) \leq \beta/\alpha$ holds.

Let us now apply Lemma 2.4 to a single hidden layer neural networks with Gaussian data.

Example 2.2 (NSR for a single-hidden layer with centered Gaussian data). Consider the random vector $z = \sigma(Wx)$ where $x \sim \mathcal{N}(0, \Sigma)$ is a centered Gaussian with covariance $\Sigma > 0$. Figure 12 shows α , β , f , and the corresponding upper bound on $\text{NSR}(z)$ from Lemma 2.4 for common activations.

We next bound the empirical NSR by the population NSR, with the following elementary lemma.

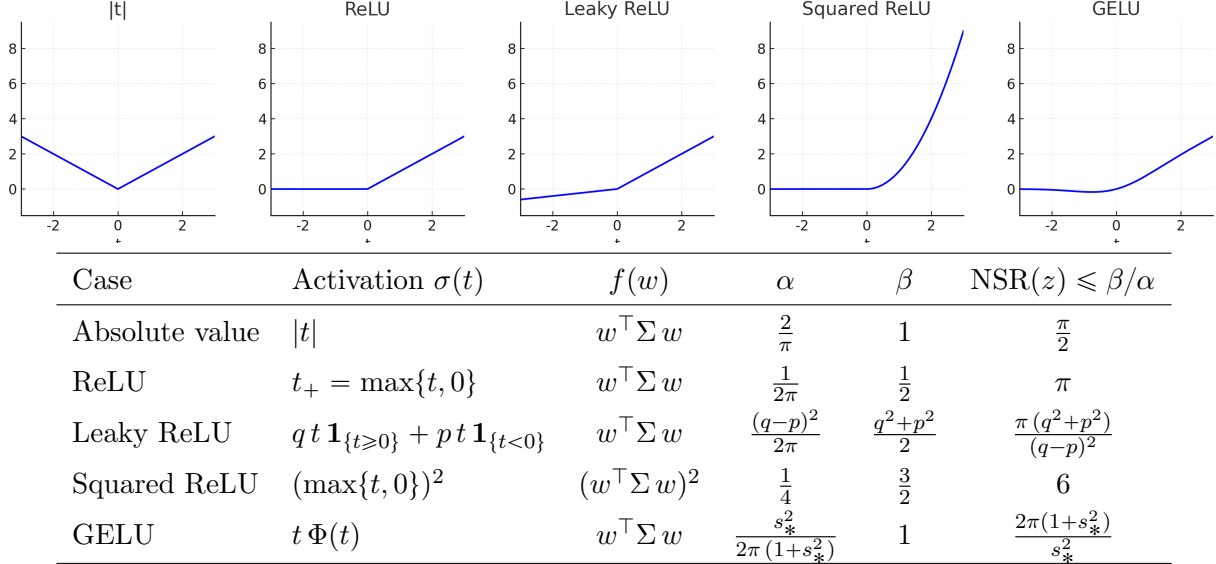


Figure 12: $\text{NSR}(z)$ for $z = \sigma(Wx)$ with different activation functions σ and with Gaussian data $x \sim \mathcal{N}(0, \Sigma)$. The table records the choices of f, α, β and the resulting NSR bound in Lemma 2.4. Here Φ is the standard normal CDF and $s_* = \min_i w_i^\top \Sigma w_i$ where w_i are the rows of W .

Lemma 2.5 (Consistency of the Empirical NSR). *Let $z \in \mathbf{R}^d$ be a random vector with mean $\mu := \mathbb{E}z \neq 0$ and finite second moment $m_2 := \mathbb{E}\|z\|_2^2$. Suppose that the random vector z is sub-Gaussian with parameter K , meaning $\|\langle z - \mu, u \rangle\|_{\psi_2} \leq K\|u\|_2$ for all vectors $u \in \mathbf{R}^d$. Moreover, let $L > 0$ denote a sub-exponential parameter for $\|z\|_2^2$, i.e. assume $\|\|z\|_2^2 - \mathbb{E}\|z\|_2^2\|_{\psi_1} \leq L$. Let z_1, \dots, z_n be iid copies of z , and define the empirical mean and the second moment:*

$$\hat{\mu} = \frac{1}{n} \sum_{i=1}^n z_i, \quad \hat{m}_2 = \frac{1}{n} \sum_{i=1}^n \|z_i\|_2^2.$$

Then there exist constants $c_1, c_2 > 0$ such that for any $0 < \varepsilon_1 \leq 1$ and $0 < \varepsilon_2 < 1$, the estimate

$$\frac{\hat{m}_2}{\|\hat{\mu}\|_2^2} \leq \frac{1 + \varepsilon_1}{(1 - \varepsilon_2)^2} \cdot \frac{m_2}{\|\mu\|_2^2}$$

holds with probability at least $1 - 2 \exp\left(-c_1 n \varepsilon_2^2 \frac{\|\mu\|_2^2}{K^2}\right) - 2 \exp\left(-c_2 n \min\left\{\frac{\varepsilon_1^2 m_2^2}{L^2}, \frac{\varepsilon_1 m_2}{L}\right\}\right)$.

Proof. We first control the empirical mean. Let $u_* := \mu/\|\mu\|_2$ be the unit vector in the direction of μ , and write

$$\hat{\mu} - \mu = \frac{1}{n} \sum_{i=1}^n (z_i - \mu).$$

Then $X_i := \langle z_i - \mu, u_\star \rangle$ are iid mean-zero sub-Gaussian random variables with parameter at most K . Standard concentration of centered sub-Gaussian random variables implies that for all $t > 0$, we have

$$\mathbb{P} \left(\left| \frac{1}{n} \sum_{i=1}^n X_i \right| \geq t \right) \leq 2 \exp \left(-c \frac{nt^2}{K^2} \right)$$

for some absolute constant $c > 0$. Setting $t = \varepsilon_2 \|\mu\|_2$ and using the estimate

$$\|\hat{\mu}\|_2 \geq \langle \hat{\mu}, u_\star \rangle = \|\mu\|_2 + \langle \hat{\mu} - \mu, u_\star \rangle,$$

we obtain

$$\mathbb{P}(\|\hat{\mu}\|_2 \leq (1 - \varepsilon_2) \|\mu\|_2) \leq 2 \exp \left(-c_1 n \varepsilon_2^2 \frac{\|\mu\|_2^2}{K^2} \right) \quad (2.10)$$

for some universal constant $c_1 > 0$.

We next control the empirical second moment. Define $Y_i := \|z_i\|_2^2 - m_2$. By assumption $\|Y_i\|_{\psi_1} \leq L$, so Y_i are iid centered sub-exponential random variables with parameter L . Bernstein's inequality for sub-exponential random variables guarantees that for all $t > 0$,

$$\mathbb{P} \left(\left| \frac{1}{n} \sum_{i=1}^n Y_i \right| \geq t \right) \leq 2 \exp \left(-c_2 n \min \left\{ \frac{t^2}{L^2}, \frac{t}{L} \right\} \right)$$

for some universal constant $c_2 > 0$. Substituting $t = \varepsilon_1 m_2$ yields

$$\mathbb{P}(\hat{m}_2 > (1 + \varepsilon_1) m_2) \leq 2 \exp \left(-c_2 n \min \left\{ \frac{\varepsilon_1^2 m_2^2}{L^2}, \frac{\varepsilon_1 m_2}{L} \right\} \right). \quad (2.11)$$

Combining (2.10) and (2.11) and taking a union bound over the two events completes the proof. \square

We are now ready to verify the three theorems announced in the introduction (Section 1.1). We begin by showing that for any fixed first-layer weights W_1 , the stable rank $\text{st}(A_1)$ of the second layer post-activation matrix is bounded by a small numerical constant independent of W_1 .

Theorem 2.6 (Stable rank for one-hidden layer NN). *Consider the post-activation matrix $A_1 = \sigma(WX)$ where $W \in \mathbf{R}^{m \times d}$ is fixed, $X \in \mathbf{R}^{d \times n}$ has iid standard Gaussian entries, and σ is the ReLU activation. Then there exists a constant $c > 0$ such that for any $\varepsilon_1, \varepsilon_2 \in (0, 1)$, the estimate holds:*

$$\text{sr}(A_1) \leq \frac{1 + \varepsilon_1}{(1 - \varepsilon_2)^2} \cdot \pi,$$

with probability at least $1 - 4 \exp(-c_1 n \min\{\varepsilon_1^2, \varepsilon_2^2 \text{st}(W)\})$. An analogous statement holds for the absolute value and Leaky ReLU with π replaced by the quantities in the last column of Figure 12.

Proof. This follows almost directly from Lemma 2.4 and Example 2.1. Indeed, with $z = \sigma(Wx)$ we may set $K \asymp \|W\|_{\text{op}}$, $\|\mu\|_2^2 \asymp \|W\|_F^2$, $m_2 \asymp \|W\|_F^2$, $L \asymp \|W\|_F^2$ (by the triangle inequality for the ψ_1 -norm). The result follows. \square

Next, we extend the previous theorem to the multilayer setting but where the last layer weights must be random.

Theorem 2.7 (Stable rank for any layer NN with random weights). *Consider the post-activation data matrix A_ℓ defined in (1.2) where the matrices $X, W_1, \dots, W_{\ell-1}$ are all fixed and σ is the ReLU activation function. Suppose the last layer weights $W_\ell \in \mathbf{R}^{m \times k}$ have iid standard Gaussian entries. Then there exists a constant $c > 0$ such that for any $\varepsilon_1, \varepsilon_2 \in (0, 1)$, the estimate holds:*

$$\text{sr}(A_\ell) \leq \frac{1 + \varepsilon_1}{(1 - \varepsilon_2)^2} \cdot \pi,$$

with probability at least $1 - 4 \exp(-c_1 n \min\{\varepsilon_1^2, \varepsilon_2^2 \text{st}(A_{\ell-1})\})$. An analogous statement holds for the absolute value and Leaky ReLU with π replaced by the quantities in the last column of Figure 12.

Proof. Observe that the stable rank of A_ℓ coincides with the stable rank of its transpose $\sigma(A_{\ell-1}^\top W_\ell^\top)$. Treating now $A_{\ell-1}^\top$ as fixed and $W_\ell^\top \in \mathbf{R}^{k \times m}$ as random we may apply Theorem 2.6 to directly deduce the result. \square

We now eliminate the randomness assumption on the weights when the activation functions are quadratic. Note that in this case, the bound we prove on the stable rank of the post-activation matrix (2.12) is dimension-independent but scales doubly exponentially with the depth. In our numerical experiments, however, we never observe such poor dependence on the depth.

Theorem 2.8 (Stable rank for any layer NN with quadratic activations). *Consider the post-activation data matrix A_ℓ defined in (1.2) for fixed matrices W_1, \dots, W_ℓ and where X has iid Gaussian columns $x_i \sim \mathcal{N}(\mu, \Sigma)$. Suppose that $\sigma(t) = t^2$ is the quadratic activation function. Then for any $c \in (0, \frac{1}{2})$, as long as $n \geq \frac{9 \cdot 3^{2\ell+1} \log(1/2c)}{32}$, the upper bound on the stable rank*

$$\text{sr}(A_\ell) \leq \frac{27 \cdot 3^{2\ell+2}}{2c}, \quad (2.12)$$

holds with probability at least $1 - 2c$.

Proof. We aim to apply Theorem 2.2. To this this end, we will repeatedly use the hypercontractivity property of Gaussians [38, Chapter 3.2]: any degree p polynomial $g: \mathbf{R}^d \rightarrow \mathbf{R}$ satisfies

$$(\mathbb{E}g(x)^q)^{1/q} \leq (q-1)^{p/2} (\mathbb{E}g(x)^2)^{1/2} \quad \forall q \geq 2,$$

where x is a Gaussian random vector. In particular setting $q = 4$ we have

$$\mathbb{E}g(x)^4 \leq 3^{2p} (\mathbb{E}g(x)^2)^2. \quad (2.13)$$

Let's first verify the small ball condition (2.2) for the random vector

$$z = F(x) = \sigma(W_\ell \sigma(W_{\ell-1} \dots \sigma(W_1 x))),$$

where x is a Gaussian random vector. Note that F is a degree 2^ℓ polynomial. Let u_\star be a unit norm eigenvector corresponding to the top eigenvalue of $M = \mathbb{E}zz^\top$. Then for any $c_0 \in (0, 1)$ the Paley–Zygmund inequality shows

$$\mathbb{P}(\langle z, u_\star \rangle^2 \geq c_0 \|M\|_{\text{op}}) \geq (1 - c_0)^2 \frac{(\mathbb{E}\langle z, u_\star \rangle^2)^2}{\mathbb{E}\langle z, u_\star \rangle^4} \geq (1 - c_0)^2 \cdot 3^{-2\ell+1},$$

where the last inequality follows from applying (2.13) with $g(x) = \langle F(x), u_\star \rangle$. Thus (2.2) holds with $p_0 = (1 - c_0)^2 \cdot 3^{-2\ell+1}$. An application of Theorem 2.2 therefore ensures that for any $c \in (0, \frac{1}{2})$, as long as $n \geq \frac{3^{2\ell+1} \log(1/2c)}{8(1-c_0)^2}$, the upper bound on the stable rank

$$\text{sr}(A_\ell) \leq \frac{2 \cdot 3^{2\ell+1}}{(1-c_0)^2 c_0 c} \cdot \text{er}(M), \quad (2.14)$$

holds with probability at least $1 - 2c$. It remains to upper bound $\text{er}(M)$. We will do so by upper bounding $\text{NSR}(z)$. To this end, we first estimate

$$\frac{\mathbb{E}\|z\|_2^2}{\|\mathbb{E}z\|_2^2} = \frac{\sum_i \mathbb{E}[z_i^2]}{\sum_i (\mathbb{E}z_i)^2} \leq \max_i \frac{\mathbb{E}[z_i^2]}{(\mathbb{E}z_i)^2},$$

where the last inequality follows algebraic manipulations. Observe now that for each coordinate i , we may write $z_i = (g(x))^2$ where g is a degree $2^{\ell-1}$ polynomial in x . Therefore we deduce

$$\frac{\mathbb{E}[z_i^2]}{(\mathbb{E}z_i)^2} = \frac{\mathbb{E}[g(x)^4]}{(\mathbb{E}g(x))^2} \leq 3^{2^\ell}.$$

Combining this estimate with (2.14) and setting $c_0 = 1/3$ completes the proof. \square

2.2 Low-stable-rank inputs in transformer blocks

In the layered viewpoint of Section 1.2.1, each trainable matrix W_ℓ interacts with an incoming feature matrix $A_{\ell-1}$ through a block of the form $X_\ell = W_\ell A_{\ell-1}$, and the relevant curvature constants are controlled by $\|A_{\ell-1}\|_F^2$ and $\|A_{\ell-1}\|_{\text{op}}^2$. For fully connected networks, $A_{\ell-1}$ is simply the post-activation matrix of the previous layer. In a transformer block, the matrices that play this role are more structured: they include the token embeddings, RMS-normalized hidden states, post-attention residuals, MLP inputs and MLP post-activations.

The goal of this section is threefold.

1. At initialization, we show that the *embedding activations* (and their RMS-normalized versions) already have low stable rank; in particular, their stable rank is controlled by the inverse frequency of the most common token in the sequence.
2. We then consider an *abstract transformer block* whose input $X \in \mathbf{R}^{d \times n}$ is allowed to be arbitrary, and prove that under mild regularity assumptions on X (notably, that its columns have Euclidean norm of order \sqrt{d}), all the relevant post-activation matrices that appear inside Table 1 have stable rank controlled by $\text{st}(X)$. Thus, if the block input has stable rank $O(1)$, then so do the RMS-normalized activations, the post-attention states, the MLP inputs, the MLP post-activations, and the block output.
3. As an immediate consequence, Corollary 2.15 shows that in an L -layer transformer the MLP post-activations $B^{(\ell)}$ have uniformly bounded stable rank (indeed $\text{st}(B^{(\ell)}) \leq 2\pi$ for all ℓ), that all other post-activations in the embedding layer $\ell = 0$ (e.g., $X^{(0)}$, $A^{\text{rms},(0)}$, $A^{\text{mlp},(0)}$) have stable rank controlled by the stable rank of the input data, and that for every deeper layer $\ell \geq 1$ all remaining post-activations at depth ℓ (including the various RMS-normalized states and the final representation fed to the language-model head) have stable rank bounded by a quadratic function of $1 + \ell$, independent of width and sequence length.

The embedding result provides a concrete instance of a low-stable-rank input to the first transformer block. The block-level result shows that, under Gaussian initialization of the trainable matrices, low-stable-rank structure is preserved through the attention and MLP sublayers, up to universal constants.

2.2.1 Embeddings at Gaussian initialization

As a warm up, we first begin with a simple observation about the stable rank of the token-indicator matrix associated with a fixed token sequence. Let (i_1, \dots, i_n) be a sequence of tokens with $i_t \in \{1, \dots, V\}$, and let $H \in \mathbf{R}^{V \times n}$ denote the matrix whose t -th column h_t is the standard basis vector with a single 1 in position i_t and zeros elsewhere. For each token $j \in \{1, \dots, V\}$, let

$$c_j := |\{t : i_t = j\}| \quad \text{and} \quad p_j := \frac{c_j}{n},$$

and set

$$p_{\max} := \max_{1 \leq j \leq V} p_j.$$

Then HH^\top is the diagonal matrix with entries c_1, \dots, c_V , so

$$\|H\|_{\text{op}}^2 = \lambda_{\max}(HH^\top) = \max_{1 \leq j \leq V} c_j = np_{\max}.$$

On the other hand, $\|H\|_F^2$ simply counts the number of nonzero entries of H , which is n , and therefore

$$\text{st}(H) = \frac{\|H\|_F^2}{\|H\|_{\text{op}}^2} = \frac{n}{np_{\max}} = \frac{1}{p_{\max}}. \quad (2.15)$$

Thus the stable rank of the raw token-indicator matrix is exactly the inverse of the empirical frequency of the most common token. In the NanoGPT experiment of Figure 10, we say that $\text{st}(H) \approx 26$ throughout training, and hence $p_{\max} \approx 1/26$. That this ratio is low is not so surprising. Indeed, this is consistent with a Zipf-type law $p_j \propto j^{-s}$ over a vocabulary of size $V = 50,257$, for which the observed p_{\max} corresponds to an exponent $s \approx 0.86$.

We now turn to the embedding matrix. Let $E \in \mathbf{R}^{d \times V}$ denote the embedding matrix, whose columns e_1, \dots, e_V are sampled independently from $\mathcal{N}(0, I_d)$. For the fixed sequence of n tokens (i_1, \dots, i_n) we form the embedded data matrix

$$X = [x_1, \dots, x_n] \in \mathbf{R}^{d \times n}, \quad x_t := e_{i_t}.$$

Recall that c_j and p_j denote the empirical counts and frequencies of token j , and $p_{\max} := \max_j p_j$. We write

$$S := \{j : c_j > 0\} \quad \text{and} \quad m := |S|$$

for the set of distinct tokens appearing in the sequence and its cardinality. We use $\text{st}(A) := \|A\|_F^2/\|A\|_{\text{op}}^2$ to denote the stable rank of a matrix A , as before.

Lemma 2.9 (Embeddings and RMS-normalized embeddings have low stable rank). *Fix $\varepsilon \in (0, 1)$. Let $E \in \mathbf{R}^{d \times V}$ be an embedding matrix whose columns e_1, \dots, e_V are sampled independently from $\mathcal{N}(0, I_d)$. For a fixed sequence of n tokens (i_1, \dots, i_n) form the embedded data matrix*

$$X = [x_1, \dots, x_n] \in \mathbf{R}^{d \times n}, \quad x_t := e_{i_t}.$$

Let c_j, p_j, S , and m be as above. Then there exist universal constants $c, C > 0$ such that, if

$$d \geq C \varepsilon^{-2} \log m,$$

then, with probability at least $1 - 2me^{-c\varepsilon^2 d}$, we have

$$(1 - \varepsilon)d \leq \|x_t\|_2^2 \leq (1 + \varepsilon)d \quad \text{for all } t = 1, \dots, n,$$

and

$$\text{st}(X) \leq \frac{1 + \varepsilon}{1 - \varepsilon} \frac{1}{p_{\max}}.$$

Proof. For each $j \in S$, $\|e_j\|_2^2$ has χ_d^2 distribution. By a standard χ^2 -concentration inequality (see, e.g., [57, Theorem 3.1.1]), there exist universal constants $c, C > 0$ such that

$$\mathbb{P}\left(\left|\|e_j\|_2^2 - d\right| \geq \varepsilon d\right) \leq 2e^{-c\varepsilon^2 d}$$

whenever $d \geq C\varepsilon^{-2}$. A union bound over $j \in S$ gives

$$(1 - \varepsilon)d \leq \|e_j\|_2^2 \leq (1 + \varepsilon)d \quad \text{for all } j \in S$$

with probability at least $1 - 2me^{-c\varepsilon^2 d}$.

On this event, the Gram matrix $G := XX^\top$ satisfies

$$\|X\|_F^2 = \text{tr}(G) = \sum_{j \in S} c_j \|e_j\|_2^2 \in [(1 - \varepsilon)dn, (1 + \varepsilon)dn],$$

since $\sum_{j \in S} c_j = n$. Let $j_\star \in S$ attain the maximum count $c_{j_\star} = np_{\max}$ and define $u := e_{j_\star}/\|e_{j_\star}\|_2$. Then

$$\lambda_{\max}(G) \geq u^\top Gu = \sum_{j \in S} c_j (e_j^\top u)^2 \geq c_{j_\star} (e_{j_\star}^\top u)^2 = c_{j_\star} \|e_{j_\star}\|_2^2 \geq (1 - \varepsilon)d np_{\max}.$$

Hence

$$\text{st}(X) = \frac{\|X\|_F^2}{\|X\|_{\text{op}}^2} = \frac{\text{tr}(G)}{\lambda_{\max}(G)} \leq \frac{(1 + \varepsilon)dn}{(1 - \varepsilon)d np_{\max}} = \frac{1 + \varepsilon}{1 - \varepsilon} \frac{1}{p_{\max}},$$

as desired. \square

Thus, under the Gaussian embedding model, the activations entering the *first* transformer block already have low stable rank whenever the empirical token distribution is not too uniform (equivalently, whenever p_{\max} is not too small). In particular, if p_{\max} is bounded below by a numerical constant, then both X and A^{rms} have stable rank $O(1)$ at initialization. Interestingly, even though $1/p_{\max}$ is an exact formula for $\text{st}(H)$, we see from Figure 10 that the bound $\text{st}(E) \leq 1/p_{\max}$ is generally loose.

2.2.2 Propagation of stable rank through a single transformer block

We now treat a single decoder block in abstraction. The input to the block is a matrix $X \in \mathbf{R}^{d \times n}$ whose columns we interpret as the hidden states for a sequence of length n and hidden dimension d . We are interested in how the stable rank of X is transformed by the attention and MLP sublayers. As in Section 1.2.1, we present the formulas for a single-head decoder block. We omit masking and positional encodings (RoPE) from the notation since they do not meaningfully change the proof nor the final bounds. Throughout this subsection, we fix input X and treat all trainable matrices inside the block as random (Gaussian) at initialization. Our goal is to show that, under Gaussian initialization of the block weights, the matrices that appear inside the block have stable rank controlled by $\text{st}(X)$.

We consider a single-head decoder block; see Figure 13 for an illustration. Ignoring masking

and positional encoding, the block acts on X by

$$\begin{aligned}
A^{\text{rms}} &= \text{RMSNorm}(X), \\
Q &= W_Q A^{\text{rms}}, \quad K = W_K A^{\text{rms}}, \quad V = W_V A^{\text{rms}}, \\
P &= \text{softmax}(d^{-1/2} K^\top Q), \\
H &= VP, \\
X^{\text{att}} &= X + W_O H, \\
A_{\text{mlp}}^{\text{rms}} &= \text{RMSNorm}(X^{\text{att}}), \\
B &= \sigma(W_1 A_{\text{mlp}}^{\text{rms}}), \\
X^+ &= X^{\text{att}} + W_2 B,
\end{aligned}$$

where $W_Q, W_K, W_V, W_O, W_1, W_2$ are trainable weight matrices, and σ is a pointwise nonlinearity (e.g. ReLU, absolute value, squared ReLU, GELU). We assume throughout that $W_1 \in \mathbb{R}^{k \times d}$ and $W_2 \in \mathbb{R}^{d \times k}$ for some fixed $k = \alpha d$, where $\alpha \geq 1$. In Proposition 2.14, we will prove that, under proper assumptions, A^{rms} , $A_{\text{mlp}}^{\text{rms}}$, B , and X^+ have stable rank bounded by a small multiple of $\text{st}(X)$ or a constant.

We make the following assumption for initialization.

Assumption A (Gaussian weight initialization). All trainable weight matrices in the block are initialized with independent Gaussian entries using the standard variance scaling $1/(\text{input dimension})$. Concretely,

$$(W_V)_{ij}, (W_O)_{ij}, (W_Q)_{ij}, (W_K)_{ij} \sim \mathcal{N}\left(0, \frac{1}{d}\right),$$

for the attention projections $W_Q, W_K, W_V, W_O \in \mathbb{R}^{d \times d}$, and

$$(W_1)_{ij} \sim \mathcal{N}\left(0, \frac{1}{d}\right), \quad (W_2)_{ij} \sim \mathcal{N}\left(0, \frac{1}{k}\right),$$

for the MLP weights $W_1 \in \mathbb{R}^{k \times d}$ and $W_2 \in \mathbb{R}^{d \times k}$. All entries are mutually independent, and all weight matrices are independent of the input X .

We begin by showing that the stable rank of the very first RMSNorm layer $\text{RMSNorm}(X)$ is controlled by the stable rank of X . See Appendix D for a proof.

Lemma 2.10 (RMSNorm preserves stable rank up to constants). *Let $X = [x_1, \dots, x_n] \in \mathbb{R}^{d \times n}$ be a deterministic matrix whose columns satisfy*

$$L \leq \|x_t\|_2^2 \leq U \quad \text{for all } t = 1, \dots, n,$$

for some $0 < L \leq U < \infty$. Define

$$A^{\text{rms}} := \text{RMSNorm}(X) \quad \text{with} \quad a_t := \sqrt{d} \frac{x_t}{\|x_t\|_2},$$

Then the estimate holds:

$$\text{st}(A^{\text{rms}}) \leq \frac{U}{L} \text{st}(X).$$

Analyzing the stable rank of the attention and MLP layers requires some further preparation. Our first technical tool will be the following simple fact about Gaussian perturbations. See Appendix C.1 for a proof.

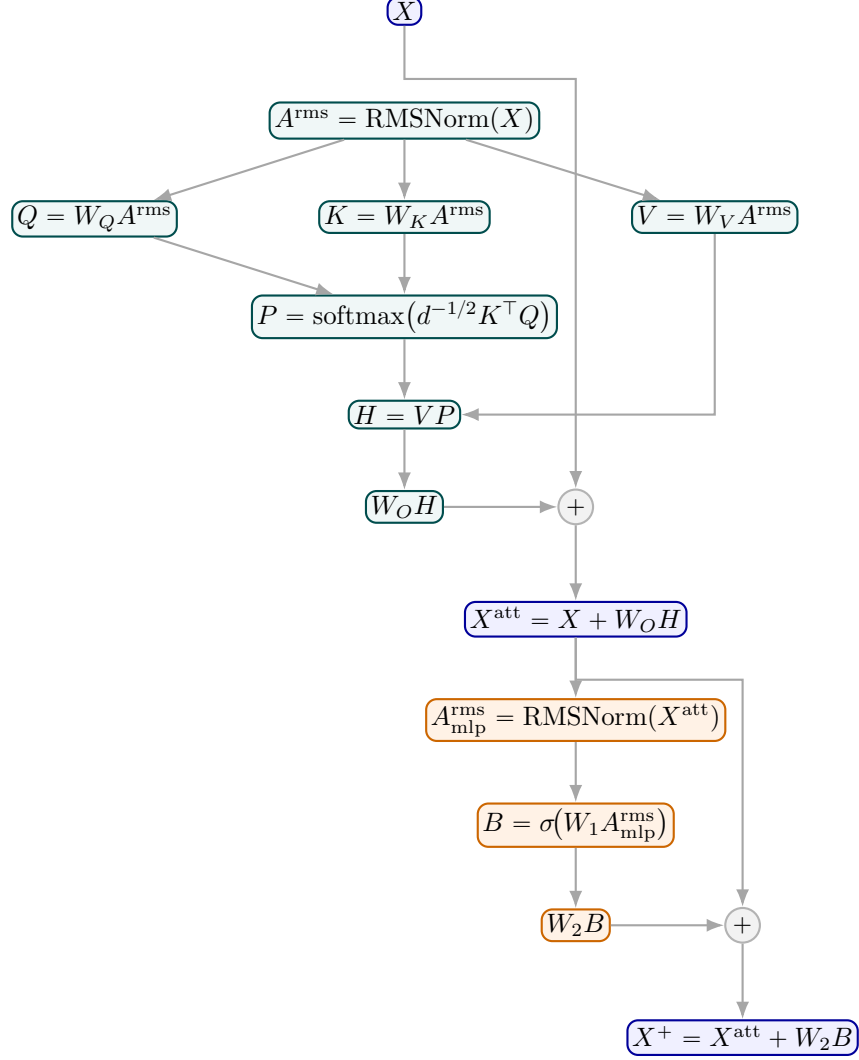


Figure 13: Single-head decoder block (masking and positional encodings omitted).

Lemma 2.11 (Gaussian perturbations preserve norms up to $(1 \pm \varepsilon)$). *Let $x \in \mathbf{R}^d$ be deterministic and let $g \sim \mathcal{N}(0, \sigma^2 I_d)$ for some $\sigma > 0$. Then for any $\varepsilon \in (0, \frac{1}{2})$ we have*

$$\mathbb{P}\left((1 - \varepsilon)(\|x\|_2^2 + \|g\|_2^2) \leq \|x + g\|_2^2 \leq (1 + \varepsilon)(\|x\|_2^2 + \|g\|_2^2)\right) \geq 1 - 4 \exp\left(-\frac{\varepsilon^2 d}{64}\right).$$

Next, we introduce the following assumption, which in particular is valid for ReLU. Indeed, for ReLU, Assumption B holds with $\tau_\sigma = 1$ and $p_\sigma = \mathbb{P}(G \geq 1) = 1 - \Phi(1) \approx 0.1587$, since for any $\tau > 0$ and $G \sim \mathcal{N}(0, 1)$ we have $\mathbb{P}(|\sigma(G)| \geq \tau) = \mathbb{P}(G \geq \tau)$.

Assumption B (Small-ball condition for the activation). *Let $\sigma : \mathbf{R} \rightarrow \mathbf{R}$ be an activation function. We assume there exist constants $\tau_\sigma > 0$ and $p_\sigma \in (0, 1)$ such that*

$$\mathbb{P}(|\sigma(G)| \geq \tau_\sigma) \geq p_\sigma \quad \text{for} \quad G \sim \mathcal{N}(0, 1).$$

We will use this assumption to prove the following lower bound; the proof appears in Section D.1.

Lemma 2.12 (Gaussian block does not strongly contract the Frobenius norm). *Assume $\sigma : \mathbf{R} \rightarrow \mathbf{R}$ satisfies Assumption B. Let $W \in \mathbf{R}^{k \times d}$ have i.i.d. entries $W_{ij} \sim \mathcal{N}(0, 1/d)$, and let $A = [a_1, \dots, a_n] \in \mathbf{R}^{d \times n}$ be independent of W with*

$$\|a_t\|_2^2 = d \quad \text{for all } t = 1, \dots, n.$$

Then there exist constants $\tilde{c}_\sigma, c_1 > 0$ depending only on σ such that, for every $\varepsilon \in (0, 1)$,

$$\mathbb{P}\left(\|\sigma(WA)\|_F^2 \geq (1 - \varepsilon) c_\sigma \frac{k}{d} \|A\|_F^2\right) \geq 1 - 2n \exp(-c_1 \varepsilon^2 k), \quad (2.16)$$

where one may take $c_\sigma = \frac{1}{2} \tau_\sigma^2 p_\sigma$. In particular, if $\sigma(t) = \max\{0, t\}$ is the ReLU activation, then $c_\sigma = (1/2)(1 - \Phi(1))$, where Φ is the Gaussian CDF.

The final preparatory result is the following lemma, which will be key to handling the stable rank of matrices formed by adding from the residual stream. We place the proof in Appendix D.2

Lemma 2.13. *Let $X \in \mathbf{R}^{d \times n}$ and $H \in \mathbf{R}^{k \times n}$ be fixed matrices, and assume $k \geq \alpha d$ for some constant $\alpha \geq 1$. Let $W \in \mathbf{R}^{d \times k}$ have independent entries*

$$W_{ij} \sim \mathcal{N}\left(0, \frac{1}{k}\right).$$

Then there exist absolute constants $c, C > 0$ such that the following holds. For every $\delta \in (0, 1)$, if

$$d \geq C \delta^{-2} \log(n + 2),$$

then with probability at least $1 - C \exp(-c\delta^2 d)$ we have

$$\text{st}(X + WH) \leq \frac{1 + \delta}{1 - \delta} \cdot \frac{\|X\|_F^2 + \frac{d}{k} \|H\|_F^2}{\max\left\{\|X\|_{\text{op}}^2, \frac{d}{k} \|H\|_{\text{op}}^2\right\}}. \quad (2.17)$$

We are now ready to analyze the stable rank of the attention and MLP sublayers. We will need the make the following assumption on the input vectors.

Assumption C (Column norms of the block input). *There exist constants $0 < c_- \leq c_+ < \infty$ such that the columns x_t of $X = [x_1, \dots, x_n] \in \mathbf{R}^{d \times n}$ satisfy*

$$c_- d \leq \|x_t\|_2^2 \leq c_+ d \quad \text{for all } t = 1, \dots, n.$$

Under the Gaussian embedding model of Lemma 2.9, this assumption holds with $c_+/c_- \asymp 1$ for X at initialization, and therefore also for the input to the first transformer block.

The proof of the following proposition appears in Section E. The proof is not difficult, but requires careful bookkeeping, so we present a sketch just after the statement of the proposition.

Proposition 2.14 (Stable rank through a single transformer block). *Assume Assumption A and C are in force. Let $\sigma(t) := \max\{0, t\}$ be the ReLU activation. Fix $\delta \in (0, \frac{1}{4})$ and set*

$$c_-^+ := (1 - \delta)^2 c_-, \quad c_+^+ := (1 + \delta)^2 (c_+ + 2).$$

Then there exist universal constants $c, C > 0$ (independent of d, n) such that, whenever $d \geq C\delta^{-2} \log(n)$, the following holds with probability at least $1 - Ce^{-c\delta^2 d}$.

(i) **Column norms of the block output.** For every t , the column x_t^+ of X^+ satisfy

$$c_-^+ d \leq \|x_t^+\|_2^2 \leq c_+^+ d.$$

(ii) **Stable ranks.** We have the explicit bounds

$$\begin{aligned} \text{st}(A^{\text{rms}}) &\leq \frac{c_+}{c_-} \text{st}(X), \\ \text{st}(X^{\text{att}}) &\leq \frac{1+\delta}{1-\delta} \left(1 + \frac{2}{c_-}\right) \text{st}(X), \\ \text{st}(A_{\text{mlp}}^{\text{rms}}) &\leq \frac{(1+\delta)^2}{(1-\delta)^2} \frac{c_+ + 1}{c_-} \left(1 + \frac{2}{c_-}\right) \text{st}(X), \\ \text{st}(B) &\leq 2\pi, \\ \text{st}(X^+) &\leq 2\pi \frac{1+\delta}{1-\delta} \cdot \left(1 + \frac{(1+\delta)(c_+ + 1)}{\frac{1}{2}(1-\Phi(1))(1-\delta)}\right), \end{aligned}$$

where Φ is the standard Gaussian CDF.

Proof sketch. The argument proceeds by tracking, through a single block, both (i) column-wise ℓ_2 norms and (ii) Frobenius/operator norms in the feature seminorm $\sum_\ell \|\Delta W_\ell A_{\ell-1}\|_F^2$. The RMS-normalization steps are easy: by Lemma 2.10, if the input columns satisfy $c_- d \leq \|x_t\|_2^2 \leq c_+ d$, then $\text{st}(\text{RMSNorm}(X)) \leq (c_+/c_-)\text{st}(X)$, and every column of the RMS output has norm exactly \sqrt{d} . For the attention sublayer, we first note that $Y = A^{\text{rms}}P$ has columns of norm at most \sqrt{d} (since P is column-stochastic), so $H = W_V Y$ has Frobenius norm and column norms controlled by those of A^{rms} via a χ^2 argument. Adding the residual X and $W_O H$ is then treated as a Gaussian perturbation: Lemma 2.11 shows that each column norm of $X^{\text{att}} = X + W_O H$ remains in $[c_-^{\text{att}} d, c_+^{\text{att}} d]$ for explicit c_\pm^{att} , while Lemma 2.13 and the bound $\|H\|_F^2 \lesssim \|X\|_F^2$ yield $\text{st}(X^{\text{att}}) \lesssim (1 + 2/c_-)\text{st}(X)$. A second RMS-normalization step then multiplies the stable rank by at most $c_+^{\text{att}}/c_-^{\text{att}}$, giving the stated bound on $\text{st}(A^{\text{rms}})$ in terms of $\text{st}(X)$ and the ratio c_+/c_- .

For the MLP block, the key inputs are (a) the random-weights stable-rank bound (Theorem 2.7), which yields $\text{st}(B) \leq 2\pi$ for $B = \sigma(W_1 A_{\text{mlp}}^{\text{rms}})$, and (b) the lower bound on the Frobenius norm in Lemma 2.12, which shows that $\|B\|_F^2 \gtrsim (k/d)\|A_{\text{mlp}}^{\text{rms}}\|_F^2 \gtrsim (k/d)\|X^{\text{att}}\|_F^2$. Together with $\text{st}(B) \leq 2\pi$, this implies that $(k/d)\|X^{\text{att}}\|_F^2/\|B\|_{\text{op}}^2$ is bounded by a numerical constant, so Lemma 2.13 applied to X^{att} and $W_2 B$ gives $\text{st}(X^+) \lesssim \text{st}(B)$ up to an explicit factor depending only on c_\pm and δ . The column norms of X^+ are controlled exactly as in the attention case: we first bound $\|b_t\|_2^2$ by $O(k)$ using subgaussian concentration for $W_1 A_{\text{mlp}}^{\text{rms}}$, then apply Lemma 2.11 to X^{att} and $W_2 B$ and use a χ^2 lower bound for $\|r'_t\|_2^2$ to obtain a new interval $[c_-^+ d, c_+^+ d]$ for the column norms of X^+ . All events of the form ‘‘column norms/Frobenius norms stay within constants’’ occur with probability at least $1 - Ce^{-c\delta^2 d}$, and a union bound over the finitely many steps in the block yields the stated high-probability bounds. \square

In summary, the block-level analysis shows that, under Gaussian initialization and mild regularity of the input column norms, the stable ranks of all matrices that appear inside a transformer block are controlled by the stable rank of the block input. In particular, if the input X to a block has $\text{st}(X) = O(1)$ (as in the Gaussian embedding model of Lemma 2.9), then the RMS-normalized activations, attention outputs, MLP inputs, MLP post-activations, and block outputs all have stable rank $O(1)$ as well.

2.2.3 Multiple transformer layers

Lemma 2.9 provides a low-stable-rank input at initialization: the embedding matrix $X^{(0)}$ has column norms of order \sqrt{d} and stable rank $\text{st}(X^{(0)}) \lesssim 1/p_{\max}$. Proposition 2.14, applied to a single block, shows that if the block input has column norms of order \sqrt{d} and finite stable rank, then all internal post-activations in that block (RMS-normalized states, post-attention states, MLP inputs, and MLP post-activations) have column norms of the same order (up to layer-dependent constants), and their stable ranks are controlled in terms of that of the input. Iterating this layer by layer, and starting from the Gaussian embedding model, yields global bounds summarized in Corollary 2.15: the MLP post-activations $B^{(\ell)}$ enjoy a uniform $O(1)$ bound ($\text{st}(B^{(\ell)}) \leq 2\pi$ for all ℓ), the embedding-layer activations are controlled by C_{in}/p_{\max} , and all remaining post-activations at depth $\ell \geq 1$ (including the various RMS-normalized states and the final representation fed to the language-model head) have stable rank bounded by a quadratic function of $1 + \ell$, independently of width and sequence length. We now formalize the L -layer model and state the corollary precisely.

Assumption D (L -layer ReLU transformer). Fix an integer depth $L \geq 1$. Let $X^{(0)} \in \mathbf{R}^{d \times n}$ be the (pre-normalization) embedding matrix for a fixed token sequence, constructed from a Gaussian embedding as in Lemma 2.9, with empirical token frequencies $p_j = c_j/n$ and $p_{\max} := \max_j p_j$.

For each layer $\ell = 0, \dots, L-1$, let $X^{(\ell+1)}$ be the hidden state obtained by applying one transformer block as in Proposition 2.14 to $X^{(\ell)}$. In particular, each block uses the ReLU activation $\sigma(t) = \max\{0, t\}$ and Gaussian initialization as in Assumption A. Within each block we write

$$A^{\text{rms},(\ell)}, \quad X^{\text{att},(\ell)}, \quad A_{\text{mlp}}^{\text{rms},(\ell)}, \quad B^{(\ell)}$$

for the attention RMS activations, post-attention states, MLP RMS activations, and MLP post-activations at layer ℓ , respectively. Finally, set

$$A_{\text{final}}^{\text{rms}} := \text{RMSNorm}(X^{(L)}).$$

Then based on this assumption we have the following theorem. We place the proof in Appendix F because it is a simple bookkeeping exercise. Note that we also have not tried to optimize the constants in the theorem.

Corollary 2.15 (Low-stable-rank representations in an L -layer ReLU transformer). *Suppose that Assumption D holds. Then there exist numerical constants $C_{\text{in}}, C > 0$ such that, for all $d \geq CL^2 \log n$, with probability at least $1 - e^{-cd}$ the following holds: we have $\text{st}(B^{(\ell)}) \leq 2\pi$ for $\ell = 0, \dots, L$, and*

$$\text{st}(M) \leq \frac{C_{\text{in}}}{p_{\max}} \quad \text{for all } M \in \{X^{(0)}, A^{\text{rms},(0)}, A_{\text{mlp}}^{\text{rms},(0)}\}$$

and

$$\text{st}(M) \leq C(1 + \ell)^2 \quad \text{for all } M \in \{A^{\text{rms},(\ell)}, A_{\text{mlp}}^{\text{rms},(\ell)}\} \quad \text{for } \ell = 1, \dots, L.$$

Finally, we have $\text{st}(A_{\text{final}}^{\text{rms}}) \leq C(1 + L)^2$.

3 Nuclear Rank in random feature models

The layerwise criterion (1.5) shows that spectral updates are most advantageous precisely when the nuclear rank of the gradient is large compared to the stable rank of the incoming activations. At the same time, there is no a priori reason for the gradient nuclear rank to be large early on in training; in fact, we will see that it can be bounded by a numerical constant in simple, yet representative,

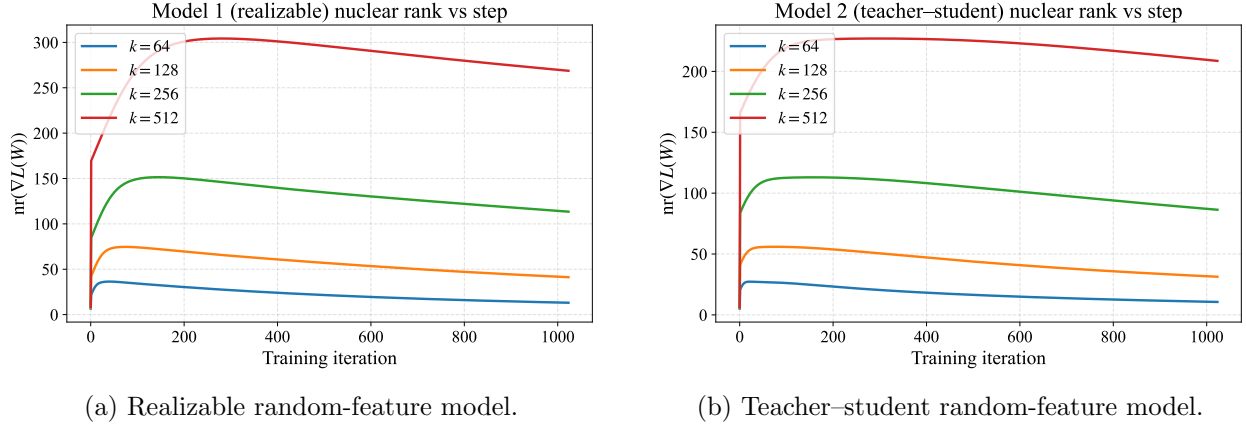


Figure 14: Gradient nuclear rank as a function of the gradient step. We plot $\text{nr}(\nabla_W \mathcal{L}(W_t))$ for several feature dimensions k . Here $n = 2k$ and $d = k/2$. In both the realizable (left) and teacher–student (right) models, the nuclear rank grows rapidly in the first few steps and does so more strongly for larger $k = 2d$, indicating that spectral updates become increasingly advantageous as the feature dimension grows.

random-feature models. The goal of this section is to show that a *few* gradient steps are already enough to change this picture entirely leading to a nuclear rank that scales linearly with dimension.

Throughout the section, we consider the quadratic random-feature objective

$$\mathcal{L}(W) := \frac{1}{2} \|WA - Y\|_F^2 \quad \text{for} \quad W \in \mathbf{R}^{m \times k},$$

and study two choices of labels Y . In the first model, the “realizable” case, the labels are generated by a ground-truth matrix W_{\sharp} via $Y = W_{\sharp}A$, and the Gram matrix $B := AA^{\top}$ follows the rank-one spike–plus–bulk structure in Assumption E. The main difficulty here is spectral: at initialization the gradient is $-W_{\sharp}B$ and inherits the poor conditioning of B , so its nuclear rank is small, whereas after a few steps the relevant block becomes $W_{\sharp}(I - \eta B)^t B$, and we must show that the polynomial $(I - \eta B)^t B$ flattens the spectrum of B : it squeezes the top spike down to constant scale while leaving the bulk eigenvalues at constant scale, so that the nuclear rank of the resulting gradient grows with the feature dimension. In the second model, a teacher–student setup, the labels are generated by a different feature map \bar{A} as $Y = \bar{W}\bar{A}$ with

$$A = \sigma(VX), \quad \bar{A} = \sigma(\bar{V}X),$$

so the gradient involves the cross-Gram matrix $\bar{A}A^{\top}$. Here we work under the spiked assumptions E and G, which encompass both the basic rank-one random-feature setting and its multi-spike extensions, and we show that these models are realized with high probability for ReLU random features with Gaussian inputs and weights: the gradient nuclear rank is $O(1)$ at initialization but becomes dimension-dependent (of order $\Theta(d)$) after a few gradient steps. Moreover, we show that it then remains $\Omega(d)$ over a window of at least $\Theta(d)$ gradient-descent iterates (Theorems 3.6 and 3.11); a refinement of the same arguments yields longer $\Theta(d \log d)$ windows at the cost of a slightly lower nuclear rank, as explained in the subsequent remark.

Before turning to the formal statements, we illustrate these effects numerically in both random-feature models. Figures 14 and 15 show how the gradient nuclear rank evolves over the first few gradient steps and how its first-step value scales with the feature dimension k .

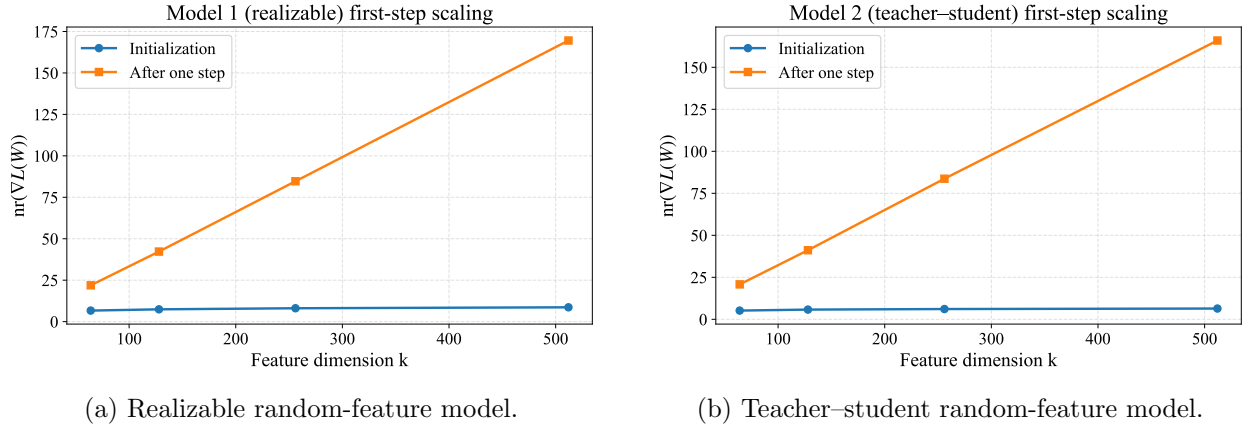


Figure 15: First-step scaling of the gradient nuclear rank with feature dimension. For each feature dimension k we plot the nuclear rank at initialization, $\text{nr}(\nabla_W \mathcal{L}(W_0))$, and after one gradient step, $\text{nr}(\nabla_W \mathcal{L}(W_1))$. Here $n = 2k$ and $d = k/2$. In both the realizable (left) and teacher–student (right) models, the initialization nuclear rank is essentially independent of k , while the post-first-step nuclear rank grows approximately linearly with k . This illustrates the regime captured by our theory: the condition $\text{nr}(\nabla_W \mathcal{L}(W_1)) \gg \text{st}(A)$ is increasingly activated as the feature dimension increases.

Notation. For any $V \in \mathbf{R}^{m \times k}$ we order its singular values as $s_1(V) \geq s_2(V) \geq \dots \geq s_{\min\{k,m\}}(V)$. Similarly, the eigenvalues of any symmetric matrix $B \in \mathbf{R}^{k \times k}$ are $\lambda_1(B) \geq \lambda_2(B) \geq \dots \geq \lambda_k(B)$.

3.1 Random feature model I

In this section, we consider the problem of random feature regression, discussed in Section 1.2 of the introduction. We show two interesting facts that hold under mild assumptions: (1) when initializing at the origin W_0 , the nuclear rank $\text{nr}(\nabla \mathcal{L}(W_0))$ is upper bounded by a numerical constant and (2) after a single gradient step the nuclear rank $\text{nr}(\nabla \mathcal{L}(W_1))$ grows with the dimension. Together these facts show that one can expect the nuclear rank to be large at least early on in training and therefore for spectral descent to outperform the Euclidean gradient method.

Setting the stage, consider the problem

$$\min_{W \in \mathbf{R}^{m \times k}} \mathcal{L}(W) := \frac{1}{2n} \|WA - Y\|_F^2 \quad \text{where} \quad Y = W_{\sharp} A. \quad (3.1)$$

The dimensions of the involved matrices are $W, W_{\sharp} \in \mathbf{R}^{m \times k}$ and $A \in \mathbf{R}^{k \times n}$ and we will be interested in the proportionate regime

$$d \asymp k \quad \text{as} \quad d \rightarrow \infty.$$

We will focus on the setting when the Gram matrix $B := \frac{1}{n} AA^{\top}$ has a “spike+bulk” structure:

Assumption E (Spiked model). Suppose that we may write

$$B = uu^{\top} + \Sigma, \quad (3.2)$$

for some vector $u \in \mathbf{R}^k$ satisfying $\|u\|_2^2 \asymp d$ and a positive definite matrix $\Sigma \in \mathbf{R}^{k \times k}$ satisfying $c_1 I_k \leq \Sigma \leq c_2 I_k$ for some constants $0 < c_1 \leq c_2 < \infty$.

In particular, the rank-one interlacing theorem [19, Chapter 4] implies separation of eigenvalues:

$$\lambda_1(B) \asymp d \quad \text{and} \quad \lambda_i(B) \in [c_1, c_2] \quad \forall i \geq 2.$$

Spiked data matrices play an prominent role in random matrix theory [1, 24]. The main example of spiked data matrices for us is the post-activation matrix generated from random data. For the sake of concreteness, we focus on the ReLU activation function, although many other activation functions elicit the same phenomenon.

3.1.1 ReLU post-activation matrices follow the spiked model

Consider the matrix $A = \sigma(VX)$ for some fixed matrix $V \in \mathbf{R}^{k \times d}$ and where $X \in \mathbf{R}^{d \times n}$ is a random matrix with iid standard Gaussian entries $\mathcal{N}(0, 1)$ and σ is the ReLU activation function. We will show that under a mild incoherence condition on the rows of V , the post-activation matrix A indeed follows the spiked model (Assumption E). To see this, we first analyze the expectation of AA^T . Observe that setting $a := \sigma(Vx)$ for a standard Gaussian random vector $x \in \mathbf{R}^d$, we may write

$$\mathbb{E} \left[\frac{1}{n} AA^T \right] = \mathbb{E}[aa^T] = \mu\mu^T + \Sigma,$$

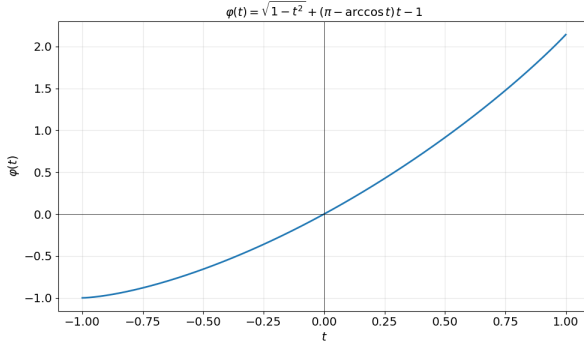
where we define

$$\mu := \mathbb{E}[a] \quad \text{and} \quad \Sigma := \text{Cov}(a) = \mathbb{E}(a - \mu)(a - \mu)^T.$$

A standard computation shows the explicit formulas:

$$\mu = \frac{1}{2\pi} \begin{bmatrix} \|v_1\|_2 & \dots & \|v_k\|_2 \end{bmatrix}^\top \quad \text{and} \quad \Sigma_{ij} = \frac{\|v_i\|_2 \|v_j\|_2}{2\pi} \varphi \left(\frac{\langle v_i, v_j \rangle}{\|v_i\|_2 \|v_j\|_2} \right),$$

where we set $\varphi(t) = (\sqrt{1-t^2} + (\pi - \arccos t)t - 1)$; see Figure 16a for an illustration of φ .



(a) The reparametrizing function φ

Figure 16: Illustration of φ .

Thus $\mathbb{E}[\frac{1}{n} AA^T]$ has the spike+bulk structure (3.10) with $\|\mu\|_2^2 = \frac{1}{4\pi^2} \|V\|_F^2$. Now in order to estimate the extremal eigenvalues of Σ , we will have to assume that the rows of V have roughly the same norm and are nearly orthogonal—a form of incoherence. This is the content of Theorem 3.2. The proof of Theorem 3.2 relies on the following lemma describing a few standard properties of the Hadamard product. Namely, item 1 is elementary, item 2 appears in [5, Thm. 1.4.1], and item 3 is the Schur product theorem [5, Sec. 1.2].

Lemma 3.1 (Properties of Hadamard products). *For any two matrices $Q, P \in \mathbf{R}^{k \times k}$, it holds:*

1. $\|Q \odot P\|_{\text{op}} \leq \max_{ij} |Q_{ij}| \cdot \|P\|_F$
2. $\|Q \odot P\|_{\text{op}} \leq \max_i Q_{ii} \cdot \|P\|_{\text{op}}$ if $Q \succeq 0$.
3. $Q \odot P \succeq 0$ if $Q \succeq 0$ and $P \succeq 0$.

Theorem 3.2 (Perfect conditioning of the covariance). *Suppose that the rows v_i of V are incoherent in the following sense: there exist constants $\varepsilon \in (0, 1)$ and $c > 0$ satisfying*

$$1 - \varepsilon \leq \|v_i\|_2^2 \leq 1 + \varepsilon \quad \text{and} \quad \frac{|\langle v_i, v_j \rangle|}{\|v_i\| \|v_j\|} \leq c \sqrt{\frac{\log(k)}{d}} \quad \forall i \neq j. \quad (3.3)$$

Then Σ satisfies the two-sided bound:

$$\left(\frac{1 + \pi^{-1}(1-\varepsilon)^{-1}}{4} \|V\|_{\text{op}}^2 + \frac{(\pi-3)(1+\varepsilon)}{4\pi} + O\left(\frac{k \log^2(k)}{d^2}\right) \right) I_k \succeq \Sigma \succeq \frac{1}{4} VV^\top + \left(\frac{(\pi-3)(1-\varepsilon)}{4\pi} + O\left(\frac{k \log^2(k)}{d^2}\right) \right) I_k. \quad (3.4)$$

Proof. Notice that we may write

$$\Sigma = \frac{1}{2\pi} \Lambda K \Lambda$$

where the entries of K are $K_{ij} = \varphi\left(\frac{\langle v_i, v_j \rangle}{\|v_i\|_2 \|v_j\|_2}\right)$ and Λ is a diagonal matrix with $\Lambda_{ii} = \|v_i\|$. We define $\hat{V} \in \mathbf{R}^{k \times d}$ to be a matrix whose i 'th row is the normalized vector $v_i / \|v_i\|_2$. We will treat K first and deal with Λ at the end of the argument.

The proof proceeds by carefully Taylor expanding φ and treating diagonal and off-diagonal elements separately. First, a quick computation yields the derivatives:

$$\varphi(0) = 0, \quad \varphi'(0) = \frac{\pi}{2}, \quad \varphi''(0) = 1, \quad \varphi^{(3)}(0) = 0, \quad \varphi^{(4)}(0) = 1, \quad \varphi^{(5)}(0) = 0.$$

For any square matrix Q , let $\text{offDiag}(Q)$ denote the matrix obtained by zeroing out the diagonal of Q , that is $\text{offDiag}(Q) = Q - \text{Diag}(Q)$. Using Taylor's theorem with remainder, we may write

$$\text{offDiag}(K) = \frac{\pi}{2} \text{offDiag}(\hat{V} \hat{V}^\top) + \frac{1}{2} \text{offDiag}((\hat{V} \hat{V}^\top)^{\odot 2}) + \frac{1}{4!} D \odot \text{offDiag}((\hat{V} \hat{V}^\top)^{\odot 4}), \quad (3.5)$$

where the entries of D are fourth-order derivatives of φ at some points in the interval $[-\frac{c}{\sqrt{d}}, \frac{c}{\sqrt{d}}]$ and are therefore bounded by some numerical constant. Using Lemma 3.1 (Item 1), we deduce

$$\left\| D \odot \text{offDiag}((\hat{V} \hat{V}^\top)^{\odot 4}) \right\|_{\text{op}} \leq \max_{ij} |D_{ij}| \cdot \left\| \text{offDiag}((\hat{V} \hat{V}^\top)^{\odot 4}) \right\|_F = O(k \log^2(k) d^{-2}),$$

where the last equality follows from the fact that each entry of $\text{offDiag}((\hat{V} \hat{V}^\top)^{\odot 4})$ is bounded by $O(\log^2(k) d^{-2})$. Adding back the diagonal $\text{Diag}(K) = (\pi - 1) I_k$ to (3.5) we therefore obtain

$$K = \frac{\pi}{2} \hat{V} \hat{V}^\top + \frac{1}{2} (\hat{V} \hat{V}^\top)^{\odot 2} + \frac{\pi-3}{2} I_k + E$$

where the error term satisfies $\|E\|_{\text{op}} = O(k \log^2(k) d^{-2})$. Conjugating by Λ and multiplying by $\frac{1}{2\pi}$ yields the expression

$$\Sigma = \frac{1}{4} VV^\top + \frac{1}{4\pi} \Lambda^{-1} (VV^\top)^{\odot 2} \Lambda^{-1} + \frac{\pi-3}{4\pi} \Lambda^2 + \frac{1}{2\pi} E. \quad (3.6)$$

Using Lemma 3.1 (Item 3) we see that $(VV^\top)^{\odot 2}$ is positive semidefinite, and therefore we obtain the claimed lower bound:

$$\Sigma \succeq \frac{1}{4} VV^\top + \frac{(\pi-3)(1-\varepsilon)}{4\pi} I_k + \frac{1}{2\pi} E.$$

Conversely, using Lemma 3.1 (Item 2), we see that $\|(VV^\top)^{\odot 2}\|_{\text{op}} \leq \|VV^\top\|_{\text{op}}$ and therefore from (3.6) we deduce

$$\Sigma \leq \left(\frac{1+\pi^{-1}(1-\varepsilon)^{-1}}{4} \|V\|_{\text{op}}^2 + \frac{(\pi-3)(1+\varepsilon)}{4\pi} + O(k \log^2(k) d^{-2}) \right) I_k,$$

which completes the proof. \square

In words, Theorem 3.2 shows that under the incoherence condition (3.3) and in the regime $k/d^2 \rightarrow 0$ as k and d tend to infinity, $\mathbb{E}[nB]$ follows the spiked model (3.10) with $\|u\|_2^2 \asymp \|V\|_F^2$ and Σ satisfying $c_1 \leq \Sigma \leq c_2(1 + \|V\|_{\text{op}}^2)$ where $c_1, c_2 > 0$ are numerical constants. Reassuringly random matrices V with iid Gaussian entries $\mathcal{N}(0, \frac{1}{d}I)$ satisfy the incoherence condition (3.3) and moreover $\|V\|_{\text{op}}$ has order $O(1)$ in the regime $k \asymp d$ while the spike has order $\|\mu\|_2^2 \asymp d$. This is the content of the following lemma; we omit the proof since it is standard.

Lemma 3.3 (Incoherence with random V). *Let $v_1, \dots, v_n \in \mathbb{R}^d$ be independent random vector with $v_i \sim \mathcal{N}(0, \frac{1}{d}I_d)$ and suppose $\frac{\log k}{d} \leq \frac{1}{4}$. Then we have*

$$\mathbb{P} \left(\max_{i \neq j} \left| \frac{\langle v_i, v_j \rangle}{\|v_i\|_2 \|v_j\|_2} \right| \leq 4\sqrt{\frac{\log k}{d}} \quad \text{and} \quad \max_{i \leq k} \left| \|v_i\|_2^2 - 1 \right| \leq 4\sqrt{\frac{\log k}{d}} \right) \geq 1 - \frac{4}{k}. \quad (3.7)$$

Moreover, with probability at least $1 - 4e^{-c\delta^2 d}$ it holds:

$$\|V\|_{\text{op}} \leq \sqrt{\frac{k}{d}} + (1 + \delta) \quad \text{and} \quad (1 - \delta)k \leq \|V\|_F^2 \leq (1 + \delta)k. \quad (3.8)$$

It remains to take into account concentration of $\frac{1}{n}AA^\top$ around its mean in order to deduce that it follows the spiked model. This is the content of the following theorem, which is immediate from standard results on concentration of covariance matrices. In the theorem, we denote the i 'th column of A by a_i .

Theorem 3.4 (Spiked model from Gaussian initialization). *Let $V \in \mathbb{R}^{k \times d}$ have iid Gaussian entries $\mathcal{N}(0, \frac{1}{d}I_d)$. Then there exist constants $C_0, C_1, C_2 > 0$ such that in the regime $k \asymp d$ and $n \geq C_0 d$, with probability tending to one as $d \rightarrow \infty$, we may write*

$$\frac{1}{n}AA^\top = \bar{\mu}\bar{\mu}^\top + \bar{\Sigma},$$

where the empirical mean $\bar{\mu} = \frac{1}{n} \sum_{i=1}^n a_i$ and the empirical covariance $\bar{\Sigma} = \frac{1}{n} \sum_{i=1}^n (a_i - \bar{\mu})(a_i - \bar{\mu})^\top$ satisfy $\|\bar{\mu}\|^2 \asymp d$ and $C_1 I \leq \bar{\Sigma} \leq C_2 I$.

Proof. Suppose that the events (3.7) and (3.8) hold, which occurs with probability at least $1 - \frac{4}{k} - 4\exp(-c\delta^2 d)$. Then Theorem 3.2 implies that the bound (3.4) holds say for $\varepsilon = 1/2$ as long as $d \geq c \log(k)$ for some constant c .

Define the empirical mean $\bar{\mu} = \frac{1}{n} \sum_{i=1}^n a_i$ and the empirical covariance $\bar{\Sigma} = \frac{1}{n} \sum_{i=1}^n (a_i - \bar{\mu})(a_i - \bar{\mu})^\top$ and note the equality:

$$\frac{1}{n}AA^\top = \bar{\mu}\bar{\mu}^\top + \bar{\Sigma}.$$

Recall from Example 2.1 that the estimate holds:

$$\|\langle a - \mathbb{E}a, u \rangle\|_{\psi_2} \lesssim \underbrace{\|V\|_{\text{op}}}_{\lesssim 1} \|u\|_2 \quad \forall u.$$

Moreover, the minimal eigenvalues of Σ is bounded from below by a constant (3.4) and therefore we may write

$$\|\langle a - \mathbb{E}a, u \rangle\|_{\psi_2} \lesssim \sqrt{\langle \Sigma u, u \rangle} \quad \forall u.$$

Appealing to concentration of covariance matrices [57, Remark 9.2.3], we deduce that there exist universal constants $c, C > 0$ such that for all $u \geq 1$, with probability at least $1 - 2e^{-d}$, it holds:

$$\|\bar{\Sigma} - \Sigma\|_{\text{op}} \lesssim \left(\sqrt{\frac{d}{n}} + \frac{d}{n} \right) \underbrace{\|\Sigma\|_{\text{op}}}_{\lesssim 1}.$$

Appealing to concentration of the mean [20, Theorem 1], we also obtain:

$$\|\bar{\mu} - \mu\|_2 \lesssim \sqrt{\frac{d}{n}},$$

with probability $1 - e^{-d}$. In particular, taking into account (3.8) in this event we may estimate

$$\sqrt{k} - \sqrt{\frac{d}{n}} \lesssim \|\bar{\mu}\|_2 \lesssim \sqrt{k} + \sqrt{\frac{d}{n}},$$

which completes the proof. \square

3.1.2 The nuclear rank at initialization is constant

We now look at the consequences of the spiked model (3.10) on the nuclear rank of the gradient. Namely, consider initializing gradient descent on the problem (3.1) at W_0 . Then taking into account the expression for the gradient

$$\nabla \mathcal{L}(W) = (W - W_{\sharp})B \quad \text{with} \quad B := \frac{1}{n}AA^{\top},$$

we have

$$\nabla \mathcal{L}(W_0) = -W_{\sharp}B. \quad (3.9)$$

Now suppose that the ground truth matrix W_{\sharp} does not eliminate the spike in the following sense:

$$\|W_{\sharp}\|_{\text{op}} \leq C \quad \text{and} \quad \|W_{\sharp}u\|_2 \geq \kappa \cdot \|u\|_2,$$

where C and κ are numerical constants. This is indeed the case for example if the singular values $s_1(W_{\sharp})$ and $s_k(W_{\sharp})$ are bounded from above and below by a numerical constant or is true with high probability if the entries of $W_{\sharp} \in \mathbf{R}^{m \times k}$ are iid Gaussian $\mathcal{N}(0, \frac{1}{m})$ and $m \gtrsim k$. Then we can estimate the nuclear rank of the gradient as:

$$\sqrt{\text{nr}(W_{\sharp}B)} = \frac{\|W_{\sharp}B\|_*}{\|W_{\sharp}B\|_F} \leq \frac{C\|B\|_*}{\|W_{\sharp}uu^{\top}\|_F - \|W_{\sharp}\Sigma\|_F} \leq \frac{C\|u\|_2^2 + C\|\Sigma\|_*}{\kappa\|u\|_2^2 - C\|\Sigma\|_F} \lesssim \frac{d}{d - \sqrt{d}} \asymp 1.$$

Thus indeed the nuclear rank of the gradient $\nabla \mathcal{L}(W_0)$ is bounded by a constant.

3.1.3 The nuclear rank after one gradient step scales with dimension.

Let us now analyze what happens after a single gradient step $W_1 = W_0 - \eta \nabla \mathcal{L}(W_0)$. Observe the gradient of the objective function at W_1 is

$$\nabla \mathcal{L}(W_1) = (\eta W_{\sharp} B - W_{\sharp}) B = -W_{\sharp} \underbrace{(I - \eta B) B}_{=: T_{\eta}}.$$

We will now see that although B is a poorly conditioned matrix, T_{η} is perfectly conditioned for any stepsize $\eta = \frac{1}{c + \|B\|_{\text{op}}}$ with constant $c > 0$.

Lemma 3.5 (Nuclear rank after one iteration grows with dimension). *Suppose that Assumption E holds and fix a step-size $\eta = \frac{1}{c + \|B\|_{\text{op}}}$ for any constant $c > 0$. Then the condition number of T_{η} is bounded by a numerical constant in the regime $k \asymp d$ as $d \rightarrow \infty$, and consequently, we have*

$$\text{nr}(\nabla \mathcal{L}(W_1)) \gtrsim \text{nr}(W_{\sharp}).$$

Proof. The eigenvalues of T_{η} have the form $\lambda_i \left(1 - \frac{\lambda_i}{c + \lambda_1}\right)$ where λ_i is the i 'th largest eigenvalue of B . Now clearly, we have $\lambda_1(B) \geq \|u\|_2^2 \asymp d$. Moreover by the rank one interlacing theorem we have

$$\lambda_i(\Sigma) \geq \lambda_{i+1}(B) \geq \lambda_{i+1}(\Sigma) \quad \forall i = 1, \dots, d-1.$$

Consequently, the eigenvalues $\lambda_i(B)$ for $i = 2, \dots, d$ all lie in the interval $[c_1, c_2]$. We therefore deduce for $i \geq 2$ the estimates:

$$1 \lesssim c_1 \left(1 - \frac{c_2}{c + \lambda_1}\right) \leq \lambda_i \left(1 - \frac{\lambda_i}{c + \lambda_1}\right) \leq c_2.$$

Moreover, for $i = 1$ we have $\lambda_1 \left(1 - \frac{\lambda_1}{c + \lambda_1}\right) = \frac{c\lambda_1}{c + \lambda_1} \asymp 1$. Thus T_{η} is bounded by a numerical constant in the regime $k \asymp d$ as $d \rightarrow \infty$. Using the elementary observation $\text{nr}(W_{\sharp} T_{\eta}) \gtrsim \left(\frac{\lambda_k(T_{\eta})}{\lambda_1(T_{\eta})}\right)^2 \text{nr}(W_{\sharp})$ completes the proof. \square

Since typical ground truth matrices W_{\sharp} (e.g. Gaussian) have nuclear rank that grows with dimension, Lemma 3.5 shows that the nuclear rank of $\nabla \mathcal{L}(W_1)$ grows with dimension as well.

3.1.4 Multi-step and Multi-spike

The results in the previous section established that, under a spiked model and for a specific choice of stepsize, the nuclear rank of the gradient is initially small at W_0 and becomes large already at W_1 . There are, however, two serious simplifications in this setup. First, we assumed a stepsize of the form $\eta = 1/(c + \|B\|_{\text{op}})$, whereas in practice it is more natural to consider the choice $\eta = 1/(c\|B\|_{\text{op}})$ with $c \geq 1$. Second, we worked with a single spike uu^{\top} , while random feature Gram matrices in applications often exhibit multiple prominent directions (e.g, [2, 59]). In this subsection, we show that both of these limitations can be removed simultaneously: under a multi-spiked model and with the more realistic stepsize $\eta = 1/(c\|B\|_{\text{op}})$, the same qualitative conclusions on the growth of nuclear rank continue to hold. The main difference is that the phenomenon no longer occurs at the very first update; instead, after a short burn-in period, gradient descent produces iterates W_t for which $\nabla \mathcal{L}(W_t)$ has large nuclear rank over a long time window.

Assumption F (Multi-spiked model). Suppose that we may write

$$B = S + \Sigma, \quad (3.10)$$

for some symmetric matrices $S, \Sigma \in \mathbf{R}^{k \times k}$ with S having rank $r \in \mathbb{N}$ and satisfying $c_1 d^\ell I_k \leq S \leq c_2 d^u I_k$ and $c_1 I_k \leq \Sigma \leq c_2 I_k$ for some constants $0 < c_1 \leq c_2 < \infty$ and $\ell, u > 0$.

In words, Assumption F asserts that the matrix B can be decomposed into a low-rank “signal” part S and a full-rank, well-conditioned “bulk” part Σ . The matrix S has rank r and eigenvalues that grow polynomially with d , between $c_1 d^\ell$ and $c_2 d^u$, so there are only r directions in feature space along which B is very large. In contrast, Σ has all of its eigenvalues uniformly bounded above and below by numerical constants, so it behaves like a well-conditioned background covariance on the remaining $k - r$ directions. Thus, this assumption generalizes the rank-one spiked model considered earlier: instead of a single prominent direction u , we now allow a low-dimensional subspace of “spiky” directions with substantially larger eigenvalues than the bulk. The parameters ℓ and u control how quickly the spike eigenvalues can grow, while a small rank r ensures that the spiky subspace remains negligible in dimension compared to the overall ambient dimension.

We now turn to the dynamics of gradient descent with stepsize η , given by

$$W_{t+1} = W_t - \eta \nabla \mathcal{L}(W_t) = W_t - \eta (W_t - W_\sharp) B.$$

Recall that we initialize the algorithm at the all zero-matrix W_0 . Introducing the error matrix $E_t := W_t - W_\sharp$, this recursion becomes

$$E_{t+1} = E_t (I - \eta B) = E_0 (I - \eta B)^t.$$

Substituting this into the expression for the gradient, we obtain the convenient expression

$$\nabla \mathcal{L}(W_t) = (W_t - W_\sharp) B = -W_\sharp \underbrace{(I - \eta B)^t B}_{=: T_{\eta, t}}.$$

The following is the main result of the section. It shows that under Assumption F, after a short burn-in period of $d^{u-\ell} \log(d)$, the gradient’s nuclear rank is lower-bounded by the dimension $\text{nr}(\nabla \mathcal{L}(W_t)) \gtrsim d$ until iteration $t = Cd^u$ where C is an arbitrary numerical constant.⁵ In particular, in the setting $\ell = u$ the burn-in period is of logarithmic size $\log(d)$ while the time-window of the large nuclear ranks is linear in d . To get a better sense of the scaling, recall that gradient descent will find an ε -optimal solution to the problem after order $d^u \log(\frac{d}{\varepsilon})$ many steps. Thus, if we treat the accuracy ε as being constant, the time window when the nuclear rank of the gradient is large (order d) is shorter than the full run of the algorithm only by a $\log(d)$ factor.

Theorem 3.6 (Multi-step gradient descent). *Suppose that Assumption F holds. Fix $\eta = \frac{1}{c\|B\|_{\text{op}}}$ for any constant $c \geq 1$ and suppose that $\|W_\sharp\|_{\text{op}} \lesssim 1$. Let $\bar{M} \in \mathbf{R}^{k \times (k-r)}$ be the matrix consisting of the last $k - r$ columns of the matrix product $W_\sharp U$, where $U \in \mathbf{R}^{k \times k}$ is the orthogonal factor in the (decreasing) ordered eigenvalue decomposition of B . Then there exists a constant $C_1 > 0$ such that for any constant $C_2 > 0$ the two estimates hold:*

$$\begin{aligned} \|\nabla \mathcal{L}(W_t)\|_* &\gtrsim \|\bar{M}\|_* - r \\ \|\nabla \mathcal{L}(W_t)\|_F &\lesssim \|\bar{M}\|_F + \sqrt{r}. \end{aligned} \quad (3.11)$$

⁵Note in this statement, we choose $C > 0$ first and then let d tend to infinity.

for any t satisfying $C_1 d^{u-\ell} \log(d) \leq t \leq C_2 d^u$. In particular, if W_\sharp has iid Gaussian entries $\mathcal{N}(0, \frac{1}{d})$ independent of A , then in the regime $m = k = d$ there exists a constant C_3 such that conditionally on the realizations of A , with probability tending to one as d tends to infinity, the estimate

$$\text{nr}(\mathcal{L}(W_t)) \geq C_3 d \quad \text{holds for any } t \text{ satisfying } C_1 d^{u-\ell} \log(d) \leq t \leq C_2 d^u.$$

Proof. The eigenvalues of $T_{\eta,t}$ have the form $\lambda_i \left(1 - \frac{\lambda_i}{c\lambda_1}\right)^t$ where λ_i is the i 'th largest eigenvalue of B . Let us next describe the asymptotic growth of the eigenvalues of B . Clearly, we have $\lambda_1(B) \lesssim d^u$ and the condition $B \succeq S$ ensures $\lambda_r(B) \gtrsim \lambda_r(S) \gtrsim d^\ell$. Now the rank r interlacing theorem shows that for every j with $1 \leq j \leq k-r$ we have

$$\lambda_{j+r}(\Sigma) \leq \lambda_j(B) \leq \lambda_{j-r}(\Sigma).$$

In particular, we deduce $\lambda_{r+1}(B) \leq \lambda_1(\Sigma) \lesssim 1$. Moreover, the condition $B \succeq \Sigma$ ensures $\lambda_k(B) \geq \lambda_k(\Sigma) \gtrsim 1$. Summarizing, we have

$$d^\ell \lesssim \lambda_i(B) \lesssim d^u \quad \forall i \in [1 : r] \quad \text{and} \quad c_1 \leq \lambda_i(B) \leq c_2 \quad \forall i \in [r+1 : k].$$

Let us now look at how the eigenvalues of T_η depend on the iteration counter t . For any $i \in [1 : r]$, using the standard inequality $1 - x \leq \exp(-x)$, we have

$$\lambda_i \left(1 - \frac{\lambda_i}{c\lambda_1}\right)^t \leq e^{u \log(d) - t\Omega(d^{\ell-u})} \quad (3.12)$$

Consequently, as soon as $t \geq cd^{u-\ell} \log(d)$ for a sufficiently large constant c , the right side of (3.12) is bounded by a numerical constant uniformly over all $i \in [1 : r]$. Now for all $i \in [r+1 : k]$, using the inequality $1 - x \geq \exp(-2x)$ for $x \in [0, 0.8]$, we have the lower bound

$$\lambda_i \left(1 - \frac{\lambda_i}{c\lambda_1}\right)^t \geq c_1 e^{-O(2td^{-u})}. \quad (3.13)$$

Consequently, as long as $t \leq Cd^u$ for any constant C , the right side of (3.13) is lower bounded by a positive numerical constant uniformly over all $i \in [r+1 : k]$. Let us now form an eigenvalue decomposition of $T_\eta = U\Lambda U^\top$ where the diagonal matrix Λ contains the eigenvalues of T_η according to the increasing order of λ_i . We now decompose U as $U = [U_1 \ U_2]$ where U_1 has r columns and U_2 has $k-r$. Similarly we decompose Λ into two diagonal matrices Λ_1 and Λ_2 . We then compute

$$\begin{aligned} \|W_\sharp T_\eta\|_* &\geq \|W_\sharp U_2 \Lambda_2 U_2^\top\|_* - \|W_\sharp U_1 \Lambda_1 U_1^\top\|_* \\ &\gtrsim \|W_\sharp U_2 \Lambda_2\|_* - \|U_1 \Lambda_1 U_1^\top\|_* \\ &\gtrsim \|W_\sharp U_2 \Lambda_2\|_* - r \\ &\gtrsim \|W_\sharp U_2\|_* - r. \end{aligned}$$

Similarly we compute

$$\|W_\sharp T_\eta\|_F \leq \|W_\sharp U_2 \Lambda_2 U_2^\top\|_F + \|W_\sharp U_1 \Lambda_1 U_1^\top\|_F \lesssim \|W_\sharp U_2\|_F + \sqrt{r}.$$

Suppose now that W_\sharp has iid Gaussian entries $\mathcal{N}(0, \frac{1}{d})$ independent of A . Note that $\bar{M} \in \mathbf{R}^{k \times r}$ has iid Gaussian entries $\mathcal{N}(0, \frac{1}{d})$ and therefore conditionally on realizations of A we have $\|\bar{M}\|_{\text{op}} = O_{d,\mathbb{P}}(1)$, $\|\bar{M}\|_F = O_{d,\mathbb{P}}(\sqrt{d})$, and $\|\bar{M}\|_* = \Omega_{d,\mathbb{P}}(d)$. The result follows. \square

Remark 1 (Extending the window to $d^u \log d$). In Theorem 3.6 we showed that, under Assumption F and the Gaussian ground-truth model for W_\sharp , there exist constants $C_1, C_2, C_3 > 0$ such that with probability tending to one,

$$\text{nr}(\nabla \mathcal{L}(W_t)) \geq C_3 d \quad \text{for all } t \in [C_1 d^{u-\ell} \log d, C_2 d^u].$$

Thus on this window the gradient nuclear rank is actually linear in d .

The same bulk-versus-spike analysis used in the proof of Theorem 3.6 yields a slightly larger window (by a logarithmic factor) of large nuclear ranks. Namely, for any $\varepsilon > 0$ there exist constants c_0 and $c = c(\varepsilon) > 0$ such that, with probability tending to one as $d \rightarrow \infty$, we have

$$\text{nr}(\nabla \mathcal{L}(W_t)) \geq d^{1-\varepsilon} \quad \text{for all } t \in [c_0 d^{u-\ell} \log d, c d^u \log d].$$

The only required modification to the proof is to realize that by setting the end horizon to be $c d^u \log(d)$ for a sufficiently small constant $c(\varepsilon)$, we can be sure that the right side of (3.13) is lower bounded by $d^{-\varepsilon}$. The rest of the proof proceeds unchanged.

3.2 Random feature model II

Next, we consider a modification of the random feature model (3.1) corresponding to a “teacher-student setup”:

$$\min_{W \in \mathbb{R}^{m \times k}} \mathcal{L}(W) := \frac{1}{2n} \|WA - Y\|_F^2 \quad \text{where} \quad Y = \overline{W} \overline{A}, \quad \overline{A} = \sigma(\overline{V}X), \quad A = \sigma(VX). \quad (3.14)$$

Here, the dimensions of the involved matrices are $W, \overline{W} \in \mathbb{R}^{m \times k}$ and $V, \overline{V} \in \mathbb{R}^{k \times d}$ and $X \in \mathbb{R}^{d \times n}$. Problem (3.1) corresponds exactly to the setting $V = \overline{V}$, that is when the first layer weights have been learned perfectly and only the second layer weights need to be trained. As in the previous section, we will be interested in the proportional regime

$$k \asymp d \quad \text{as} \quad d \rightarrow \infty.$$

Analogously to Assumption E, we will assume that both matrices $\frac{1}{n}AA^\top$ and $\frac{1}{n}\overline{A}\overline{A}^\top$ follow a spiked model in the sense of Assumption G. Note that we stipulate that the spike for both matrices has the same right singular vector.

Assumption G (Spiked model). Suppose that we may write

$$\frac{1}{n}AA^\top = uu^\top + \Gamma \quad \text{and} \quad \frac{1}{n}\overline{A}\overline{A}^\top = vu^\top + \Sigma, \quad (3.15)$$

for some vector $u, v \in \mathbb{R}^k$ satisfying $\|v\|_2 \asymp \|u\|_2 \asymp \sqrt{d}$ and matrices $\Gamma, \Sigma \in \mathbb{R}^{k \times k}$. Suppose moreover:

- Γ is symmetric and for some constants $0 < c_1 \leq c_2 < \infty$, we have $c_1 I_k \leq \Gamma \leq c_2 I_k$,
- there exists $r \asymp d$ satisfying $c_2 \geq s_1(\Sigma) \geq s_r(\Sigma) \geq c_1$.

In particular, as we have already seen, the rank one interlacing theorem [19, Chapter 4] implies separation of eigenvalues

$$\lambda_1(\frac{1}{n}AA^\top) \asymp d \quad \text{and} \quad \lambda_i(\frac{1}{n}AA^\top) \in [c_1, c_2] \quad \forall i \geq 2.$$

Weyl inequality [19, 7.3.P16] and the interlacing theorem for singular values [52, Theorem 1] imply:

$$\begin{aligned} s_1(\frac{1}{n}\overline{A}\overline{A}^\top) &\asymp d \\ s_i(\frac{1}{n}\overline{A}\overline{A}^\top) &\in [c_1, c_2] \quad \forall i \in [2 : r]. \end{aligned}$$

The main example of spiked data matrices for us is the post-activation matrix generated from random data. This is the content of the following section.

3.2.1 ReLU post-activation matrices follow the spiked model

Consider the matrices $A = \sigma(VX)$ and $\bar{A} = \sigma(\bar{V}X)$, where the matrices $V, \bar{V} \in \mathbf{R}^{k \times d}$ have iid Gaussian entries $\mathcal{N}(0, \frac{1}{d})$ and $X \in \mathbf{R}^{d \times n}$ has iid standard Gaussian entries $\mathcal{N}(0, 1)$. Recall as before σ is the ReLU activation function. We will show that Assumption G indeed holds with probability tending to one in the proportionate regime $d \asymp k$. Since the requisite properties of AA^T have already been established in Theorem 3.4, it only remains to analyze $\bar{A}A^T$. To this end, we first focus on the expectation of $\bar{A}A^T$. Define $a := \sigma(Vx)$ and $\bar{a} := \sigma(\bar{V}x)$ where $x \sim \mathcal{N}(0, I_d)$ is a standard Gaussian random vector. Then, we may write

$$\mathbb{E}_x \left[\frac{1}{n} \bar{A} A^T \right] = \mathbb{E}_x [\bar{a}a^T] = \mu \nu^T + \Sigma,$$

where we define

$$\nu := \mathbb{E}_x [\bar{a}], \quad \mu = \mathbb{E}_x [a] \quad \text{and} \quad \Sigma := \mathbb{E}_x (\bar{a} - \mu)(a - \nu)^T.$$

Letting v_i and \bar{v}_i denote the rows of V and \bar{V} , respectively, a standard computation shows the explicit formulas:

$$\begin{aligned} \mu &= \frac{1}{2\pi} \begin{bmatrix} \|v_1\|_2 & \dots & \|v_k\|_2 \end{bmatrix}^T, \\ \nu &= \frac{1}{2\pi} \begin{bmatrix} \|\bar{v}_1\|_2 & \dots & \|\bar{v}_k\|_2 \end{bmatrix}^T, \\ \Sigma_{ij} &= \frac{\|\bar{v}_i\|_2 \|v_j\|_2}{2\pi} \varphi \left(\frac{\langle \bar{v}_i, v_j \rangle}{\|\bar{v}_i\|_2 \|v_j\|_2} \right), \end{aligned}$$

where we set $\varphi(t) = (\sqrt{1-t^2} + (\pi - \arccos t)t - 1)$; see Figure 16a for an illustration of φ . The next theorem establishes the asymptotics of Σ in the proportionate regime $k \asymp d$ as $d \rightarrow \infty$. Although, this result can be directly proved using the seminar work of [10, 27], we provide a short self-contained argument here based on the hypercontractivity of Gaussian random vectors.

Theorem 3.7 (Asymptotics). *Consider the regime where k and d tend to infinity with $\sqrt{k}/d \rightarrow 0$. Assume that V and \bar{V} are matrices with iid Gaussian entries with variance $1/d$. Then for any $\epsilon > 0$ it holds:*

$$\|\Sigma - \left(\frac{1}{2\pi} \bar{V}V^T + \frac{1}{d} \mathbf{1}\mathbf{1}^T \right) \|_{\text{op}} = O_{d,\mathbb{P}} \left(\frac{k^{\frac{1}{2}+\epsilon}}{d} \right).$$

Proof. The proof begins in the same way as the proof of Theorem 3.2. Namely, we write

$$\Sigma = \frac{1}{2\pi} \bar{\Lambda} K \Lambda$$

where the entries of K are $K_{ij} = \varphi \left(\frac{\langle \bar{v}_i, v_j \rangle}{\|\bar{v}_i\|_2 \|v_j\|_2} \right)$ and $\bar{\Lambda}$ and Λ are diagonal matrices with $\bar{\Lambda}_{ii} = \|\bar{v}_i\|$ and $\Lambda_{ii} = \|v_i\|$, respectively. We define $\bar{U} \in \mathbf{R}^{k \times d}$ to be a matrix whose i 'th row is the normalized vector $\bar{v}_i/\|\bar{v}_i\|_2$ and similarly we define $U \in \mathbf{R}^{k \times d}$ to be a matrix whose i 'th row is the normalized vector $v_i/\|v_i\|_2$. We will treat K first and deal with $\Lambda, \bar{\Lambda}$ at the end of the argument. Performing the same Taylor expansion as in the proof of Theorem 3.2 we arrive at the expression

$$K = \frac{\pi}{2} \bar{U} U^T + \frac{1}{2} (\bar{U} U^T)^{\odot 2} + \frac{1}{4!} D \odot (\bar{U} U^T)^{\odot 4}, \quad (3.16)$$

where the entries of D and of $\bar{U}U^\top$ are bounded in absolute value by $c_1\sqrt{\frac{\log k}{d}}$ with probability at least $1 - \frac{c_2}{k}$. In this event, using Lemma 3.1 (Item 1), we may bound the last term in (3.16) as

$$\|D \odot (\bar{U}U^\top)^{\odot 4}\|_{\text{op}} \leq \max_{ij} |D_{ij}| \cdot \|(\bar{U}U^\top)^{\odot 4}\|_F \lesssim k \log^2(k) d^{-2}.$$

Next, we deal with the term $(\bar{U}U^\top)^{\odot 2}$ in (3.16). To this end, let us first estimate $(\bar{V}V^\top)^{\odot 2}$. We compute $\mathbb{E}(\bar{V}V^\top)^{\odot 2} = \frac{1}{d}\mathbf{1}\mathbf{1}^\top$. Let z_i be the i 'th row of $(\bar{V}V^\top)^{\odot 2} - \frac{1}{d}\mathbf{1}\mathbf{1}^\top$. Note that conditionally on v_1, \dots, v_k , the vectors z_i are independent and identically distributed. Let \mathbb{E}_v be conditional expectation on v_1, \dots, v_k . Then using [55, Theorem 5.48], we deduce

$$\sqrt{\mathbb{E}_v \|(\bar{V}V^\top)^{\odot 2} - \frac{1}{d}\mathbf{1}\mathbf{1}^\top\|_{\text{op}}^2} \leq \|\Sigma\|_{\text{op}}^{1/2} d^{1/2} + Cm^{1/2} \log^{1/2}(\min\{k, d\})$$

where $\Sigma = \mathbb{E}_v z_i z_i^\top$ is the conditional second moment for any index i and $m = \mathbb{E}_v [\max_{i=1, \dots, k} \|z_i\|_2^2]$. Now a straightforward computation shows that the (j, l) entry of Σ is given by $\frac{\|v_j\|_2^2 \|v_l\|_2^2 + 2\langle v_j, v_l \rangle^2 - \|v_j\|_2^2 - \|v_l\|_2^2 + 1}{d^2}$. Thus we may write

$$\Sigma = \frac{1}{d^2} (2(VV^\top)^{\odot 2} + (q - \mathbf{1})(q - \mathbf{1})^\top),$$

where we define the vector $q = (\|v_1\|_2^2, \dots, \|v_k\|_2^2)$. Thus we deduce

$$\|\Sigma\|_{\text{op}} \leq \frac{2\|(VV^\top)^{\odot 2}\|_{\text{op}} + \|q - \mathbf{1}\|_2^2}{d^2}.$$

Now elementary algebra shows $\mathbb{E}\|q - \mathbf{1}\|^2 = \frac{2k}{d}$. Now we break up $(VV^\top)^{\odot 2}$ into the diagonal and off-diagonal parts:

$$\begin{aligned} (VV^\top)^{\odot 2} &= \|\text{Diag}(q^2) + ((VV^\top)^{\odot 2} - \text{Diag}(q^2))\|_{\text{op}} \\ &\leq \|\text{Diag}(q^2)\|_{\text{op}} + \|((VV^\top)^{\odot 2} - \text{Diag}(q^2))\|_F \\ &\leq \max_i \|v_i\|_2^4 + \sqrt{\sum_{i \neq j} \langle v_i, v_j \rangle^4}. \end{aligned}$$

Now simple algebra shows $\mathbb{E} \sum_{i \neq j} \langle v_i, v_j \rangle^4 \lesssim \frac{k^2}{d^2}$ and a standard concentration argument shows $\mathbb{E} \max_i \|v_i\|_2^4 \lesssim \left(1 + \frac{\log k}{d}\right)^2$. Thus we deduce $\mathbb{E}\|\Sigma\|_{\text{op}} \lesssim \frac{1 + \frac{k}{d}}{d^2}$. Next, we compute

$$m = \mathbb{E}_v \left[\max_{i=1, \dots, k} \|z_i\|_2^2 \right] \leq [\mathbb{E}_v \max_{i=1, \dots, k} \|z_i\|_2^{2p}]^{1/p} \leq [\mathbb{E}_v \sum_{i=1}^k \|z_i\|_2^{2p}]^{1/p} = k^{1/p} (\mathbb{E}_v \|z_i\|_2^{2p})^{1/p}.$$

Observe that $\|z_i\|_2^2$ is a degree 4 polynomial of a Gaussian and therefore by Gaussian hypercontractivity [38, Chapter 3.2] satisfies $(\mathbb{E}_v \|z_i\|_2^{2p})^{1/p} \leq (p-1)^2 (\mathbb{E}_v \|z_i\|_2^4)^{1/2}$. Taking the expectation now with respect to v_1, \dots, v_k , we deduce $\mathbb{E}m \leq k^{1/p} (p-1)^2 (\mathbb{E}\|z_i\|_2^4)^{1/2} \lesssim k^{1/p} (p-1)^2 \frac{k}{d^2}$. Thus we deduce

$$\mathbb{E}\|(\bar{V}V^\top)^{\odot 2} - \frac{1}{d}\mathbf{1}\mathbf{1}^\top\|_{\text{op}}^2 \lesssim \frac{1 + \frac{k}{d}}{d^2} + k^{2/p} (p-1)^4 \frac{k \log(\min\{k, d\})}{d^2}.$$

Applying Markov's inequality completes the proof. \square

Finally, we pass from the expectation $\mathbb{E}[\bar{A}A^\top]$ to its empirical version $\frac{1}{n}\bar{A}A^\top$.

Corollary 3.8 (Spiked model from Gaussian initialization). *Assume that $V, \bar{V} \in \mathbf{R}^{k \times d}$ are matrices with iid Gaussian entries $\mathcal{N}(0, \frac{1}{d})$ and let $X \in \mathbf{R}^{k \times n}$ be an independent matrix with iid Gaussian entries $\mathcal{N}(0, 1)$. Then in the regime $\frac{k}{d} \rightarrow \gamma \in (1, \infty)$ and $n \geq C_0 d$, with probability tending to one as $d \rightarrow \infty$, Assumption G holds.*

Proof. Let a_i and \bar{a}_i denote the i 'th rows of A and \bar{A} , respectively. We have already seen in Theorem 3.4 that there exist constants $C_0, C_1, C_2 > 0$ such that in the regime $k \asymp d$ and $n \geq C_0 d$, with probability tending to one as $d \rightarrow \infty$, we may write

$$\frac{1}{n} A A^\top = \bar{\mu} \bar{\mu}^\top + \bar{\Sigma},$$

where the empirical mean $\bar{\mu} = \frac{1}{n} \sum_{i=1}^n a_i$ and the empirical covariance $\bar{\Sigma} = \frac{1}{n} \sum_{i=1}^n (a_i - \bar{\mu})(a_i - \bar{\mu})^\top$ satisfy $\|\bar{\mu}\|^2 \asymp d$ and $C_1 I \leq \bar{\Sigma} \leq C_2 I$. Therefore we now focus on $\frac{1}{n} \bar{A} A^\top$. To this end, define the empirical means

$$\bar{\mu} := \frac{1}{n} \sum_{i=1}^n a_i, \quad \bar{\nu} := \frac{1}{n} \sum_{i=1}^n \bar{a}_i,$$

and the empirical cross-covariance

$$\bar{\Sigma} := \frac{1}{n} \sum_{i=1}^n (\bar{a}_i - \bar{\nu})(a_i - \bar{\mu})^\top.$$

A simple expansion shows that

$$\bar{B} = \frac{1}{n} \bar{A} A^\top = \bar{\nu} \bar{\mu}^\top + \bar{\Sigma},$$

so \bar{B} already has the desired rank-one plus bulk structure with right spike vector $\bar{\mu}$.

Exactly as in the proof of Theorem 3.4, Example 2.1 and the bounds (3.8) imply that both a and \bar{a} are subgaussian:

$$\|\langle a - \mathbb{E}a, u \rangle\|_{\psi_2} \lesssim \|u\|_2, \quad \|\langle \bar{a} - \mathbb{E}\bar{a}, u \rangle\|_{\psi_2} \lesssim \|u\|_2 \quad \forall u \in \mathbf{R}^k.$$

Applying the covariance concentration inequality [57, Remark 9.2.3] to the joint vector $(a^\top, \bar{a}^\top)^\top \in \mathbf{R}^{2k}$ and reading off the off-diagonal blocks yields, for $n \geq C_0 d$, the estimate

$$\|\bar{\Sigma} - \Sigma\|_{\text{op}} \lesssim \sqrt{\frac{d}{n}} + \frac{d}{n},$$

with probability at least $1 - 2e^{-d}$. Similarly, by [20, Theorem 1] we obtain

$$\|\bar{\mu} - \mu\|_2 \lesssim \sqrt{\frac{d}{n}}, \quad \|\bar{\nu} - \nu\|_2 \lesssim \sqrt{\frac{d}{n}},$$

so that $\|\bar{\mu}\|_2 \asymp \|\bar{\nu}\|_2 \asymp \sqrt{d}$ whenever $n \geq C_0 d$. Now Theorem 3.7 showed

$$\|\Sigma - \left(\frac{1}{2\pi} \bar{V} V^\top + \frac{1}{d} \mathbf{1} \mathbf{1}^\top \right)\|_{\text{op}} = o_d(1).$$

Now observe that

$$\left\| \frac{1}{d} \mathbf{1} \mathbf{1}^\top - \frac{1}{d} \bar{\nu} \bar{\mu}^\top \right\|_{\text{op}} \leq \left\| \frac{1}{d} \mathbf{1} \mathbf{1}^\top - \frac{1}{d} \nu \mu^\top \right\|_{\text{op}} + \left\| \frac{1}{d} \nu \mu^\top - \frac{1}{d} \bar{\nu} \bar{\mu}^\top \right\|_{\text{op}} \leq o_d(1) + \sqrt{\frac{d}{n}}.$$

Thus we may write

$$\frac{1}{n} \bar{A} A^\top = (1 + \frac{1}{d}) \bar{\nu} \bar{\mu}^\top + \frac{1}{2\pi} \bar{V} V^\top + E$$

where $\|E\|_{\text{op}} \lesssim o_d(1) + \sqrt{\frac{d}{n}}$. Now observe $\bar{V}V^\top(\bar{V}V^\top)^\top \geq \lambda_d(V^\top V)\bar{V}\bar{V}^\top$. Thus standard results [55, Theorem 4.6.1] on the extremal singular values of tall Gaussian matrices (recall we are in the regime $k/d \rightarrow \gamma \in (1, \infty)$) imply that there exist constants $0 < c_1 \leq c_2 < \infty$ such that with probability tending to one as $d \rightarrow \infty$, we have

$$c_2 \geq s_1(\bar{V}V^\top) \geq s_d(\bar{V}V^\top) \geq c_1. \quad (3.17)$$

Therefore after possibly inflating the constants $c_1, c_2 > 0$ the bulk $Q := \frac{1}{2\pi}\bar{V}\bar{V}^\top + E$ satisfies

$$c_2 \geq s_1(Q) \geq s_d(Q) \geq c_1 \quad \text{and} \quad s_{d+1} \lesssim o_{d,\mathbb{P}}(1) + O_{d,\mathbb{P}}\left(\sqrt{\frac{d}{n}}\right).$$

Thus the proof is complete. \square

3.2.2 The nuclear rank at initialization is constant.

We now look at the consequences of the spiked model (3.23) on the nuclear rank of the gradient. Namely, consider initializing gradient descent on the problem (3.14) at the all-zero matrix $W_0 = 0$. Then taking into account the expression for the gradient

$$\nabla \mathcal{L}(W) = \frac{1}{n}(WA - \bar{W}\bar{A})A^\top,$$

we have

$$\nabla \mathcal{L}(W_0) = -\bar{W}\bar{B} \quad \text{where} \quad \bar{B} := \frac{1}{n}\bar{A}A^\top. \quad (3.18)$$

Now suppose that the ground truth matrix \bar{W} does not eliminate the spike in the following sense:

$$\|\bar{W}\|_{\text{op}} \leq C \quad \text{and} \quad \|\bar{W}u\|_2 \geq \kappa \cdot \|u\|_2.$$

This is indeed the case for example if the singular values $s_1(\bar{W})$ and $s_k(\bar{W})$ are bounded from above and below by a numerical constant or is true with high probability if the entries of $\bar{W} \in \mathbf{R}^{m \times k}$ are iid Gaussian $\mathcal{N}(0, \frac{1}{m})$ and $m \gtrsim k$. Then we can estimate the nuclear rank of the gradient as:

$$\sqrt{\text{nr}(\bar{W}\bar{B})} = \frac{\|\bar{W}\bar{B}\|_*}{\|\bar{W}\bar{B}\|_F} \leq \frac{C\|\bar{B}\|_*}{\|\bar{W}uv^\top\|_F - \|\bar{W}\Sigma\|_F} \leq \frac{C\|u\|_2\|v\|_2 + C\|\Sigma\|_*}{\kappa\|u\|_2\|v\|_2 - C\|\Sigma\|_F} \lesssim \frac{d}{d - \sqrt{d}} \asymp 1.$$

Thus indeed the nuclear rank of the gradient $\nabla \mathcal{L}(W_0)$ is bounded by a constant.

3.2.3 The nuclear rank after one gradient step scales with dimension.

Let us now analyze what happens after a single gradient step $W_1 = W_0 - \eta \nabla \mathcal{L}(W_0)$. Observe the gradient of the objective function at W_1 is

$$\nabla \mathcal{L}(W_1) = -\bar{W} \underbrace{\bar{B}(I - \eta B)}_{=: T_\eta},$$

where recall that we set $\bar{B} = \frac{1}{n}\bar{A}A^\top$ and $B = \frac{1}{n}AA^\top$. We will now show that for any stepsize $\eta = \frac{1}{c + \|B\|_{\text{op}}}$ under natural randomness assumptions, the nuclear rank of $\nabla \mathcal{L}(W_1)$ grows with dimension—the main result of the section.

Theorem 3.9 (Nuclear rank after one iteration grows with dimension). *Suppose that Assumption G holds and fix $\eta = \frac{1}{c + \|\bar{B}\|_{\text{op}}}$ for any constant $c > 0$. Let $\bar{M} \in \mathbf{R}^{k \times r}$ be the matrix consisting of the first r columns of $\bar{W} \bar{L}$, where $\bar{L} \in \mathbf{R}^{k \times k}$ is the left orthogonal factor in the ordered singular value decomposition of \bar{B} . Then the following estimates hold in the regime $k = d$ for all large d :*

$$\text{nr}(\nabla \mathcal{L}(W_1)) \geq \frac{\|\bar{M}\|_*}{\|\bar{W}\|_F}. \quad (3.19)$$

In particular, if \bar{W}, \bar{V}, V have iid Gaussian entries $\mathcal{N}(0, \frac{1}{d})$, and we are in the regime $m = d$ and $\frac{k}{d} \rightarrow \gamma \in (1, \infty)$, then there exists a constant C such that as long as $n \geq Cd$ we have

$$\text{nr}(\mathcal{L}(W_1)) \geq \Omega_{d, \mathbb{P}}(d). \quad (3.20)$$

Proof. Let us write the singular value decompositions

$$B = L S L^\top \quad \text{and} \quad \bar{B} = \bar{L} \bar{S} \bar{R}^\top,$$

where $S, \bar{S} \in \mathbf{R}^{k \times k}$ are diagonal matrices with non-negative decreasing entries (singular values), and $L, \bar{L} \in \mathbf{R}^{k \times k}$ and $\bar{R} \in \mathbf{R}^{k \times k}$ are orthogonal matrices. We then compute

$$\bar{L}^\top T_\eta L = \bar{S} \bar{R}^\top L (I - \eta S).$$

The goal is now to show that the product $\bar{R}^\top L$ nearly has a block form. To this end, let us write

$$\bar{R} = [r_0 \quad R_0] \quad \text{and} \quad L = [\ell_0 \quad L_0]$$

for some vectors $r_0, \ell_0 \in \mathbf{R}^k$. Now the Davis-Kahan Theorem [14] applied to the two matrices AA^\top and uu^\top shows that the corresponding top eigenvectors are close

$$\underset{q \in \{\pm 1\}}{\text{argmin}} \|\hat{u} - q\ell_0\|_2 \lesssim \frac{1}{d}, \quad (3.21)$$

where we set $\hat{u} = u/\|u\|_2$. Without loss of generality, we may assume the optimal orientation is $q = 1$. Similarly, applying the Davis-Kahan theorem for singular values [60] to the right singular vectors of $\bar{A}A^\top$ and vu^\top , we deduce

$$\underset{q \in \{\pm 1\}}{\text{argmin}} \|\hat{u} - qr_0\|_2 \lesssim \frac{1}{d}. \quad (3.22)$$

Again without loss of generality, we may assume that $q = 1$ is optimal. Let us now write $\bar{R}^\top L$ in block form:

$$\bar{R}^\top L = \begin{bmatrix} r_0^\top \ell_0 & r_0^\top L_0 \\ R_0^\top \ell_0 & R_0^\top L_0 \end{bmatrix}$$

Now using equations (3.21) and (3.22) we deduce

$$|r_0^\top \ell_0 - 1| \lesssim \frac{1}{d}, \quad \|r_0^\top L_0\|_2 \lesssim \frac{1}{d}, \quad \|R_0^\top \ell_0\|_2 \lesssim \frac{1}{d}.$$

Moreover, by standard principal-angle arguments, the singular values of $R_0^\top L_0$ are the cosines of the principal angles between the subspaces r_0^\perp and ℓ_0^\perp (see, e.g., [6] or [61]). Thus we deduce

$$s_{k-1}(R_0^\top L_0) = |r_0^\top \ell_0| \gtrsim 1 - \frac{1}{d}.$$

Thus writing $S = \text{Diag}(s)$ and $\bar{S} = \text{Diag}(\bar{s})$ for some vectors s and \bar{s} we deduce

$$\bar{S} \bar{R}^\top L(I - \eta S) = \text{Diag}(1, \bar{s}_{\geq 2}) \cdot \underbrace{\begin{bmatrix} \bar{s}_1(1 - \eta s_1)r_0^\top \ell_0 & \bar{s}_1 r_0^\top L_0(I - \eta \text{Diag}(s_{\geq 2})) \\ (1 - \eta s_1)R_0^\top \ell_0 & R_0^\top L_0(I - \eta \text{Diag}(s_{\geq 2})) \end{bmatrix}}_{=:Q},$$

where $s_{\geq 2}$ and $\bar{s}_{\geq 2}$ denote, respectively, the vectors s and \bar{s} with the first coordinate removed. Now observe $\bar{s}_1 \asymp d$ and $1 - \eta s_1 \asymp \left(1 - \frac{\|A\|_{\text{op}}^2}{c + \|A\|_{\text{op}}^2}\right) \asymp \frac{1}{d}$. Therefore we may write

$$Q = \begin{bmatrix} a & z^\top \\ 0 & D \end{bmatrix} + E,$$

where $a \asymp 1$, $\|z\|_2 \lesssim 1$, $\|E\|_{\text{op}} \lesssim \frac{1}{d^2}$, and $1 \lesssim s_{k-1}(D) \leq s_1(D) \lesssim 1$. It follows immediately that the operator norm of the blocked matrix is bounded by a constant, while its minimal singular value is bounded away from zero due to the standard linear algebraic Lemma G.1. Thus we deduce

$$1 \lesssim s_k(Q) \lesssim s_1(Q) \lesssim 1.$$

We therefore deduce

$$\text{nr}(\nabla \mathcal{L}(W_1)) = \text{nr}(\bar{W} \bar{L} \bar{L}^\top T_\eta L) = \text{nr}(\bar{W} \bar{L} \text{Diag}(1, \bar{s}_{\geq 2}) Q) \asymp \text{nr}(\bar{W} \bar{L} \text{Diag}(1, \bar{s}_{\geq 2})).$$

Using the linear algebra Lemma G.2 with $P = [1 : r]$ we immediately deduce

$$\|\bar{W} \bar{L} \text{Diag}(1, \bar{s}_{\geq 2})\|_* \gtrsim \|\bar{M}\|_*,$$

while the inequality $\|\bar{W} \bar{L} \text{Diag}(1, \bar{s}_{\geq 2})\|_F \lesssim \|\bar{W}\|_F$ holds trivially. The claimed estimate (3.19) follows immediately.

Suppose now that \bar{W}, V, \bar{V} have iid Gaussian entries $\mathcal{N}(0, \frac{1}{d})$. Then we have already seen in Corollary 3.8 that Assumption G is satisfied with $r = d$. Note that $\bar{M} \in \mathbf{R}^{k \times r}$ has iid Gaussian entries $\mathcal{N}(0, \frac{1}{d})$ and therefore we have $\|\bar{W}\|_F = O_{d, \mathbb{P}}(\sqrt{d})$, $\|\bar{M}\|_* = \Omega_{d, \mathbb{P}}(d)$, and $\|\bar{W}\|_{\text{op}} = O_{d, \mathbb{P}}(1)$. The claimed estimate (3.20) follows immediately. \square

3.2.4 Multi-step and multi-spike for the teacher–student model

Theorem 3.9 shows that, under the rank-one spiked model of Assumption G, the nuclear rank of the gradient in the teacher–student random feature model jumps from $O(1)$ at initialization to order d after a single gradient step. In the realizable model, we further saw in Section 3.1.4 that a similar phenomenon persists for multi-spiked Gram matrices and over many gradient steps (Theorem 3.6). The goal of this section is to develop an analogous multi-step, multi-spike theory in the teacher–student setting. The main technical difference compared to the realizable case is that the gradient now contains the cross-Gram matrix $\bar{B} := \frac{1}{n} \bar{A} \bar{A}^\top$, rather than the symmetric Gram matrix $B = \frac{1}{n} A A^\top$ alone. As a result, the gradient at time t takes the form $\bar{W} \bar{B}$ multiplied by a polynomial in B , and the relevant spectrum is that of the non-symmetric matrix $\bar{B}(I - \eta B)^t$. We will see, however, that under a natural multi-spiked generalization of Assumption G, the same qualitative picture holds: after a short burn-in period the gradient nuclear rank is of order d for a long time window, so that the spectral-versus-Euclidean advantage is again visible.

We continue to work in the proportional regime $k \asymp d$ as $d \rightarrow \infty$ and we use the same notation as in the rest of this section. In particular,

$$B := \frac{1}{n} A A^\top \in \mathbf{R}^{k \times k}, \quad \bar{B} := \frac{1}{n} \bar{A} \bar{A}^\top \in \mathbf{R}^{k \times k},$$

and gradient descent on the objective (3.14) satisfies

$$W_{t+1} = W_t - \eta \nabla \mathcal{L}(W_t), \quad \nabla \mathcal{L}(W_t) = \frac{1}{n} (W_t A - \bar{W} \bar{A}) A^\top = W_t B - \bar{W} \bar{B}.$$

We first formulate a multi-spiked analogue of Assumption G. As in the realizable case, we assume that B decomposes into a low-rank “signal” part and a well-conditioned bulk, as in Assumption F, and we impose a compatible structure on the cross-Gram matrix \bar{B} .

Assumption H (Multi-spiked teacher–student model). Suppose that we may write

$$\frac{1}{n} A A^\top = H_1 + \Gamma \quad \text{and} \quad \frac{1}{n} \bar{A} \bar{A}^\top = H_2 + \Sigma, \quad (3.23)$$

for some matrices $H_1, H_2 \in \mathbf{R}^{k \times k}$. Suppose that the following conditions are true.

- **Spike properties** H_1 and H_2 have rank $p = o(d)$, the matrix H_1 is symmetric positive semidefinite, and the singular values of H_1 and H_2 lie in the interval $[d^\ell, d^u]$ for some constants $u, \ell \in (0, 1]$. Moreover, H_1 and H_2 admit compact singular value decompositions

$$H_1 = U Q U^\top \quad \text{and} \quad H_2 = V \bar{Q} U^\top$$

for orthogonal matrices $U, V \in \mathbf{R}^{k \times p}$ and nonnegative diagonal matrices $Q, \bar{Q} \in \mathbf{R}^{p \times p}$ with non-increasing diagonal entries. Note that the right orthogonal factors of H_1 and H_2 coincide.

- **Bulk properties.** The matrix Γ is symmetric and for some constants $0 < c_1 \leq c_2 < \infty$, we have $c_1 I_k \leq \Gamma \leq c_2 I_k$. Additionally, there exists $r \asymp d$ satisfying $c_2 \geq s_1(\Sigma) \geq s_r(\Sigma) \geq c_1$.

In words, Assumption G ensures that the matrices $\frac{1}{n} A A^\top$ and $\frac{1}{n} \bar{A} \bar{A}^\top$ decompose into a low-rank *signal* (or “spike”) part H_1, H_2 plus a *bulk* part Γ, Σ . The spike matrices H_1, H_2 have rank $p = o(d)$, so the signal concentrates in a low-dimensional subspace compared to the ambient dimension, and their nonzero singular values grow like a power of d ; moreover, the right singular vectors of H_1 and H_2 in an ordered SVD coincide, so both spikes are aligned in the same latent directions. The bulk matrix Γ is well-conditioned (its eigenvalues are bounded above and below by fixed constants), while Σ has $r \asymp d$ singular values of constant order. Overall, this is a multi-spike teacher–student model in which a small number of strong signal directions are embedded in an otherwise well-behaved high-dimensional bulk. In particular it is straightforward to check that Assumption G is a strict generalization of the rank-one teacher–student model in Assumption G.

We begin analyzing gradient descent in the multi-spiked student–teacher setting by deriving a simple expression for the gradient of \mathcal{L} along the iterates. This is the content of the following lemma which parallels the realizable case.

Lemma 3.10 (Gradient recursion). *Let $W_{t+1} = W_t - \eta \nabla \mathcal{L}(W_t)$ be the gradient descent iterates on the objective (3.14), initialized at $W_0 = 0$. Then the gradients satisfy*

$$\nabla \mathcal{L}(W_t) = -\bar{W} \bar{B} (I - \eta B)^t \quad \text{for all } t \geq 0.$$

Proof. Recall that $\nabla \mathcal{L}(W) = WB - \bar{W} \bar{B}$. Define $G_t := \nabla \mathcal{L}(W_t)$. Then

$$G_0 = \nabla \mathcal{L}(W_0) = W_0 B - \bar{W} \bar{B} = -\bar{W} \bar{B}.$$

Moreover, using the update $W_{t+1} = W_t - \eta G_t$ we obtain

$$G_{t+1} = W_{t+1} B - \bar{W} \bar{B} = (W_t - \eta G_t) B - \bar{W} \bar{B} = G_t - \eta G_t B = G_t (I - \eta B).$$

By induction this yields $G_t = G_0 (I - \eta B)^t = -\bar{W} \bar{B} (I - \eta B)^t$ for all $t \geq 0$. \square

Thus, the time- t gradient is obtained by multiplying the initial gradient $-\overline{W}\overline{B}$ on the right by the polynomial $(I - \eta B)^t$. In particular, the spectral properties of the family of matrices

$$T_{\eta,t} := \overline{B}(I - \eta B)^t$$

control the evolution of $\nabla \mathcal{L}(W_t)$. We are now ready to estimate the nuclear rank of the gradient after a short burn-in period. This is the content of the following theorem, which closely parallels Theorem 3.6 in the realizable case. Henceforth, for any matrix M we let $M_{i:j}$ denote the submatrix formed by columns i through j .

Theorem 3.11 (Nuclear rank for multi-step GD). *Suppose that Assumption G holds and that $\|\overline{W}\|_{\text{op}} \lesssim 1$. Let \overline{M} consist of the columns $p+1$ through $r-p$ of the matrix $\overline{W}\overline{L}$, where \overline{L} is the left orthogonal factor in the ordered (decreasing) singular values decomposition of \overline{B} . Then for any constants $q, C_3 > 0$ there exists a constant constant $C_1 > 0$ such that the following estimates hold*

$$\begin{aligned} \|\nabla \mathcal{L}(W_t)\|_* &\gtrsim \|\overline{M}\|_* - pd^{u-\ell} - d^{-q} \\ \|\nabla \mathcal{L}(W_t)\|_F &\lesssim \|\overline{W}\|_F + \sqrt{pd}^{u-\ell} + d^{-q}, \end{aligned}$$

for all t in the interval $[C_1 d^{u-\ell} \log(d), C_3 d^u]$.

Proof. First, recall that eigenvalue interlacing directly implies

$$d^\ell \lesssim \lambda_i(B) \lesssim d^u \quad \forall i \in [1 : r] \quad \text{and} \quad c_1 \leq \lambda_i(B) \leq c_2 \quad \forall i \in [r+1 : k].$$

Moreover, interlacing of singular values [52] shows:

$$s_{i+p}(\Sigma) \leq s_i(\overline{B}) \leq s_{i-p}(\Sigma).$$

In particular, we deduce

$$s_i(\overline{B}) \in [c_1, c_2] \quad \forall i \in [p+1, r-p].$$

Let us now write the singular value decompositions

$$B = LSL^\top \quad \text{and} \quad \overline{B} = \overline{L}\overline{S}\overline{R}^\top,$$

where $S, \overline{S} \in \mathbf{R}^{k \times k}$ are diagonal matrices with non-negative decreasing entries (singular values), and $L, \overline{L} \in \mathbf{R}^{k \times k}$ and $\overline{R} \in \mathbf{R}^{k \times k}$ are orthogonal matrices. We then compute

$$\overline{L}^\top T_{\eta,t} L = \overline{S}\overline{R}^\top L(I - \eta S)^t.$$

The goal is now to show that the product $\overline{R}^\top L$ nearly has a block form. To this end, let us write

$$\overline{R} = [R_1 \quad R_2] \quad \text{and} \quad L = [L_1 \quad L_2]$$

for some matrices $R_1, L_1 \in \mathbf{R}^{k \times p}$ and $R_2, L_2 \in \mathbf{R}^{k \times (k-p)}$. Now the Davis-Kahan Theorem [14] applied to the two matrices AA^\top and UQU^\top shows that

$$\|UU^\top - L_1 L_1^\top\|_{\text{op}} \leq \frac{\|\Gamma\|_{\text{op}}}{d^\ell} \lesssim \frac{1}{d^\ell}, \quad (3.24)$$

Applying the Davis-Kahan theorem for singular values [60] to the right singular vectors of $\overline{A}A^\top$ and $V\overline{Q}U^\top$, we deduce

$$\|UU^\top - R_1 R_1^\top\|_{\text{op}} \leq \frac{\|\Sigma\|_{\text{op}}}{d^\ell} \lesssim \frac{1}{d^\ell}. \quad (3.25)$$

Let us now write $\bar{R}^\top L$ in block form:

$$\bar{R}^\top L = \begin{bmatrix} R_1^\top L_1 & R_1^\top L_2 \\ R_2^\top L_1 & R_2^\top L_2 \end{bmatrix}.$$

Let us now partition $S = \begin{bmatrix} S_1 & 0 \\ 0 & S_2 \end{bmatrix}$ and $\bar{S} = \begin{bmatrix} \bar{S}_1 & 0 \\ 0 & \bar{S}_2 \end{bmatrix}$ in the obvious way. Thus we deduce

$$\bar{S} \bar{R}^\top L (I - \eta S)^t = \begin{bmatrix} \bar{S}_1 R_1^\top L_1 (I - \eta S_1)^t & \bar{S}_1 R_1^\top L_2 (I - \eta S_2)^t \\ \bar{S}_2 R_2^\top L_1 (I - \eta S_1)^t & \bar{S}_2 R_2^\top L_2 (I - \eta S_2)^t \end{bmatrix}. \quad (3.26)$$

Now for any constant $a > 0$, we can choose a constant $C > 0$ such that for $t \geq Cd^{u-\ell} \log(d)$ we have $\|(I - \eta S_1)^t\|_{\text{op}} \leq d^{-a}$. Therefore, the first column on the right side of (3.26) is small in operator norm and we may estimate

$$\left\| \bar{S} \bar{R}^\top L (I - \eta S)^t - \begin{bmatrix} 0 & \bar{S}_1 R_1^\top L_2 (I - \eta S_2)^t \\ 0 & \bar{S}_2 R_2^\top L_2 (I - \eta S_2)^t \end{bmatrix} \right\|_{\text{op}} \lesssim d^{-(a-u)}.$$

Recalling the equality $\nabla \mathcal{L}(W_t) = -\bar{W} T_{\eta,t}$, we therefore deduce

$$\left\| \nabla \mathcal{L}(W_t) - \bar{W} \bar{L} \begin{bmatrix} 0 & -\bar{S}_1 R_1^\top L_2 (I - \eta S_2)^t \\ 0 & -\bar{S}_2 R_2^\top L_2 (I - \eta S_2)^t \end{bmatrix} L \right\|_{\text{op}} \lesssim \|\bar{W}\|_{\text{op}} \cdot d^{-(a-u)}.$$

It remains therefore to estimate the nuclear and Frobenius norms of

$$\bar{W} \bar{L} \begin{bmatrix} 0 & -\bar{S}_1 R_1^\top L_2 (I - \eta S_2)^t \\ 0 & -\bar{S}_2 R_2^\top L_2 (I - \eta S_2)^t \end{bmatrix} L \quad \text{or equivalently} \quad \bar{W} \bar{L} \begin{bmatrix} \bar{S}_1 R_1^\top L_2 \\ \bar{S}_2 R_2^\top L_2 \end{bmatrix} (I - \eta S_2)^t.$$

Now observe that as long as $t \leq Cd^u$ for any constant C , the diagonal entries of $(I - \eta S_2)^t$ are bounded from above and below by positive numerical constants. Therefore it remains to estimate the nuclear and Frobenius norms of the matrix

$$M = \bar{W} \bar{L} Q \quad \text{where} \quad Q := \begin{bmatrix} \bar{S}_1 R_1^\top L_2 \\ \bar{S}_2 R_2^\top L_2 \end{bmatrix}.$$

Using (3.24) and (3.25) we have $\|L_1 L_1^\top - R_1 R_1^\top\|_{\text{op}} \lesssim d^{-\ell}$. Now a standard argument based on principal angles shows the estimates

$$\|L_1 L_1^\top - R_1 R_1^\top\|_{\text{op}} = \|R_1^\top L_2\|_{\text{op}} \quad \text{and} \quad s_{k-p}(R_2^\top L_2) = \sqrt{1 - \|L_1 L_1^\top - R_1 R_1^\top\|_{\text{op}}^2}.$$

In particular, we deduce $\|\bar{S}_1 R_1^\top L_2\|_{\text{op}} \lesssim d^{u-\ell}$. Therefore, we obtain the upper bound on the Frobenius norm

$$\begin{aligned} \|Q\|_* &\geq \left\| \bar{W} \bar{L} \begin{bmatrix} 0 \\ \bar{S}_2 R_2^\top L_2 \end{bmatrix} \right\|_* - \left\| \bar{W} \bar{L} \begin{bmatrix} \bar{S}_1 R_1^\top L_2 \\ 0 \end{bmatrix} \right\|_* \\ &\geq \|[\bar{W} \bar{L}]_{p+1:k} \bar{S}_2 R_2^\top L_2\|_* - pd^{u-\ell} \\ &\gtrsim \|[\bar{W} \bar{L}]_{p+1:k} \bar{S}_2\|_* - pd^{u-\ell} \\ &\gtrsim \|[\bar{W} \bar{L}]_{p+1:r-p}\|_* - pd^{u-\ell}, \end{aligned}$$

where the last inequality follows from applying the linear algebraic Lemma G.2 with $P = [p+1 : r-p]$. Similarly, we obtain the bound on the Frobenius norm:

$$\begin{aligned} \|Q\|_F &\leq \left\| \bar{W} \bar{L} \begin{bmatrix} 0 \\ \bar{S}_2 R_2^\top L_2 \end{bmatrix} \right\|_F - \left\| \bar{W} \bar{L} \begin{bmatrix} \bar{S}_1 R_1^\top L_2 \\ 0 \end{bmatrix} \right\|_F \\ &\lesssim \|[\bar{W} \bar{L}]_{p+1:k} \bar{S}_2 R_2^\top L_2\|_F + \sqrt{p} d^{u-\ell} \\ &\lesssim \|[\bar{W} \bar{L}]_{p+1:k} \bar{S}_2\|_F + \sqrt{p} d^{u-\ell} \\ &\lesssim \|\bar{W}\|_F + \sqrt{p} d^{u-\ell}. \end{aligned}$$

The two claimed estimates follow directly. \square

Theorem 3.11 thus shows that after a burn-in of length $d^{u-\ell} \log d$ and up to iteration d^u , the gradient along the iterations satisfies

$$\text{nr}(W_t) \gtrsim \frac{\|[\bar{W} \bar{L}]_{p+1:r-p}\|_*^2}{\|\bar{W}\|_*^2},$$

assuming that the error terms in the numerator and denominator are negligible. Consequently, under a natural incoherence condition

$$\|[\bar{W} \bar{L}]_{p+1:r-p}\|_* \gtrsim \|\bar{W}\|_*,$$

we get the desired conclusion $\text{nr}(W_t) \gtrsim \text{nr}(\bar{W})$. Intuitively, the incoherence condition holds if the spectrum of W_t is well-spread across the columns, and is true for example if \bar{W} has iid Gaussian entries. This is the content of the following Corollary, which is the main result of the section.

Corollary 3.12 (Nuclear rank with multiple spikes). *Suppose that Assumption G holds. Suppose moreover that the entries of \bar{W} are iid Gaussian $\mathcal{N}(1/d)$ and are independent of A and \bar{A} , and we are in the regime $u - \ell < \frac{1}{2}$, $p = o_d(d^{1-2(u-\ell)})$, and $r \asymp d \asymp m \asymp k$ with $k/d \rightarrow \gamma \in (0, \infty)$ as $d \rightarrow \infty$. Then there exist constants $C_1, C_2 > 0$ such that for any constant $C_3 > 0$ the probability conditioned on (A, \bar{A}) of the event*

$$\text{nr}(\nabla \mathcal{L}(W_t)) \gtrsim d \quad \text{holds for all } t \in [C_1 d^{u-\ell} \log(d), C_3 d^u], \quad (3.27)$$

tends to one as d tends to infinity.

Proof. The proof follows immediately from Theorem 3.11 upon noting that the entries of $\bar{M} = [\bar{W} \bar{L}]_{p+1:r-p}$ are iid Gaussian $\mathcal{N}(1/d)$ and therefore standard Gaussian estimates show $\|\bar{W}\|_F = O_{d,\mathbb{P}}(\sqrt{d})$ and $\|\bar{M}\|_* = \Omega_{d,\mathbb{P}}(k(r-2p+1)) = \Omega_{d,P}(d)$. \square

Thus, under a random teacher setting the nuclear rank of $\nabla \mathcal{L}(W_t)$ is linear in d throughout the entire time window $t \in [C_1 d^{u-\ell} \log d, C_3 d^u]$. This confirms that the spectral-versus-Euclidean separation identified in the realizable multi-spike setting persists in the teacher-student regime.

Remark 2. Just as in the realizable case, the window of large nuclear ranks can be extended by a logarithmic factor: Namely, for any $\varepsilon > 0$ there exist constants c_0 and $c = c(\varepsilon) > 0$ such that, with probability tending to one as $d \rightarrow \infty$, we have

$$\text{nr}(\nabla \mathcal{L}(W_t)) \geq d^{1-\varepsilon} \quad \text{for all } t \in [c_0 d^{u-\ell} \log d, c d^u \log d].$$

The only required modification to the proof is to realize that by setting the horizon to be $c d^u \log(d)$ for a sufficiently small constant $c(\varepsilon)$, we can be sure that the diagonal entries of $(I - \eta S_2)^t$ are lower bounded by $d^{-\varepsilon}$. The proof then proceeds similarly, while taking this observation into account.

4 A General Layered Model and Spectral Descent

The theoretical and empirical results in the earlier sections suggest that spectral updates should be particularly effective when the features seen by each block have low stable rank and the corresponding gradients have large nuclear/Frobenius ratios. Until now, this discussion has been framed in terms of specific architectures (e.g., MLPs) and random-feature models. In this section we formulate a general layered model that captures a broad class of neural architectures and show that, under mild smoothness assumptions, the same spectral-versus-Euclidean descent tradeoff holds for a *full* gradient step. The key ingredient is a layerwise Hessian bound involving a dominant feature term $\sum_\ell \|\Delta W_\ell A_{\ell-1}\|_F^2$ and a smaller parameter-only term $\sum_\ell \|\Delta W_\ell\|_{\text{op}}^2$, and a one-block comparison which pulls in both the stable rank of the incoming features and the stable rank and nuclear rank of the gradient. The model is designed to encompass:

- **Fully-connected networks (MLPs):** each block is a dense matrix W_ℓ , and the activation A_ℓ is obtained by applying a (possibly vector-valued) nonlinearity to the current preactivation X_ℓ and, optionally, combining it with earlier preactivations and activations (residual/skip connections).
- **Convolutional networks:** after flattening, each convolutional or projection layer can be viewed as a matrix W_ℓ acting on an unfolded feature map $A_{\ell-1}$, with A_ℓ produced by pointwise nonlinearities, pooling, and residuals that are smooth functions of (X_1, \dots, X_ℓ) .
- **Transformers and attention-based models:** multihead attention, feedforward sublayers, and output projections are linear maps W_ℓ applied to token/head features $A_{\ell-1}$; the resulting activations A_ℓ are smooth functions of all previous preactivations through attention, normalization, and residual mixing.

In all of these cases, each block is (affine) linear in its parameters W_ℓ , and the nonlinear structure is captured by smooth activation maps Φ_ℓ that depend on the preactivations (X_1, \dots, X_ℓ) . We will show that the curvature of the composite loss can be bounded in a layer-wise fashion by a feature term plus a smaller parameter-only term, and that, once this bound is established, the spectral-versus-Euclidean comparison essentially reduces to the same nuclear-rank versus stable-rank inequality as in the random-feature model, with an additional dependence on the stable rank of the gradient.

4.1 Model and smoothness assumptions

Fix an integer $L \geq 1$. For each layer $\ell = 1, \dots, L$ we have dimensions d_ℓ (output) and $d_{\ell-1}$ (input). We also fix a column dimension n and think of all activations $A_\ell(W) \in \mathbf{R}^{d_\ell \times n}$ as stacking n data points in columns. Let $W_\ell \in \mathbf{R}^{d_\ell \times d_{\ell-1}}$ be the learnable weight matrix at layer ℓ . We denote the collection of all weights by $W = (W_1, \dots, W_L)$.

Preactivations and activations. We define preactivations and activations recursively as follows:

- The input feature $A_0 \in \mathbf{R}^{d_0 \times n}$ is fixed (e.g., the current minibatch).
- For each $\ell = 1, \dots, L$, the preactivation at layer ℓ is

$$X_\ell(W) := W_\ell A_{\ell-1}(W) \in \mathbf{R}^{d_\ell \times n}.$$

- For each $\ell = 1, \dots, L$, the activation at layer ℓ is given by a C^2 -smooth map

$$A_\ell(W) := \Phi_\ell(X_1(W), \dots, X_\ell(W)) \in \mathbf{R}^{d_\ell \times n}.$$

Thus each $A_\ell(W)$ depends only on the previous preactivations $(X_1(W), \dots, X_\ell(W))$, and each $X_\ell(W)$ depends linearly on W_ℓ and on $A_{\ell-1}(W)$.

Outer loss. We assume a C^2 -smooth outer loss

$$f: \mathcal{X}_1 \times \dots \times \mathcal{X}_L \rightarrow \mathbf{R}, \quad \mathcal{X}_\ell = \mathbf{R}^{d_\ell \times n},$$

and define the composite loss

$$\mathcal{L}(W) := f(X_1(W), \dots, X_L(W)).$$

We denote by $G_\ell(W) := \nabla_{W_\ell} \mathcal{L}(W)$ the gradient with respect to block W_ℓ .

4.2 Layerwise Hessian bound

In the previous subsection we introduced the layered model

$$X_\ell(W) = W_\ell A_{\ell-1}(W), \quad A_\ell(W) = \Phi_\ell(X_1(W), \dots, X_\ell(W)), \quad \ell = 1, \dots, L,$$

with A_0 fixed, and the composite loss

$$\mathcal{L}(W) := f(X_1(W), \dots, X_L(W)).$$

We now fix a parameter $W = (W_1, \dots, W_L)$ and study the Hessian quadratic form

$$Q_W(\Delta W) := \langle \Delta W, \nabla^2 \mathcal{L}(W) \Delta W \rangle$$

for perturbations $\Delta W = (\Delta W_1, \dots, \Delta W_L)$. The goal is to show that Q_W is bounded by a feature term $\sum_\ell \|\Delta W_\ell A_{\ell-1}(W)\|_F^2$ and a parameter-only term $\sum_\ell \|\Delta W_\ell\|_{\text{op}}^2$, with constants depending only on local derivative bounds and on the depth L , and *not* on the layer widths.

Notation. At the fixed parameter W , we introduce the following quantities:

$$\begin{aligned} J_{\Phi, \ell} &:= \sup_{\|U\|_F=1} \|D\Phi_\ell(X)[U]\|_F, \\ H_{\Phi, \ell} &:= \sup_{\|U\|_F=1} \|D^2\Phi_\ell(X)[U, U]\|_F, \\ J_\Phi &:= \max_{1 \leq \ell \leq L} J_{\Phi, \ell}, \quad H_\Phi := \max_{1 \leq \ell \leq L} H_{\Phi, \ell}, \\ J_f &:= \|\nabla f(X_1, \dots, X_L)\|_F, \\ H_f &:= \sup_{\|U\|_F=1} |D^2 f(X_1, \dots, X_L)[U, U]|, \\ W_* &:= \max_{1 \leq \ell \leq L} \|W_\ell\|_{\text{op}}, \\ B_\ell &:= \Delta W_\ell A_{\ell-1}(W), \quad \|B^{(\ell)}\|_F^2 := \sum_{i=1}^{\ell} \|B_i\|_F^2, \\ \Gamma &:= \sqrt{2} (1 + 2J_\Phi^2 W_*^2)^{\frac{L}{2}}, \\ \Theta &:= (1 + J_\Phi W_*)^{L-1}. \end{aligned}$$

Here $X = (X_1(W), \dots, X_L(W))$ denotes the collection of preactivations at W .

We parameterize the perturbation along the path $W(t) = W + t\Delta W$ and define

$$X_\ell(t) := X_\ell(W(t)), \quad A_\ell(t) := A_\ell(W(t)).$$

We then write

$$U_\ell := \dot{X}_\ell(0), \quad \tilde{U}_\ell := \ddot{X}_\ell(0), \quad U^{(\ell)} := (U_1, \dots, U_\ell), \quad \tilde{U}^{(\ell)} := (\tilde{U}_1, \dots, \tilde{U}_\ell),$$

and similarly

$$V_\ell := \dot{A}_\ell(0), \quad \tilde{V}_\ell := \ddot{A}_\ell(0).$$

The next two lemmas bound the first and second derivatives of the preactivations in terms of the feature perturbations B_ℓ and the parameter perturbations ΔW_ℓ .

Lemma 4.1 (First-order propagation). *For every $1 \leq \ell \leq L$ we have*

$$\|U^{(\ell)}\|_F \leq \Gamma \|B^{(\ell)}\|_F. \quad (4.1)$$

Proof. Differentiating $X_\ell(t) = W_\ell(t)A_{\ell-1}(t)$ at $t = 0$ yields

$$U_1 = \Delta W_1 A_0 = B_1, \quad U_\ell = B_\ell + W_\ell V_{\ell-1} \quad (\ell \geq 2),$$

where $V_{\ell-1} := \dot{A}_{\ell-1}(0)$. Differentiating $A_\ell(t) = \Phi_\ell(X^{(\ell)}(t))$ at $t = 0$ and using the definition of $J_{\Phi, \ell}$ gives

$$V_\ell = D\Phi_\ell(X)[U^{(\ell)}], \quad \|V_\ell\|_F \leq J_{\Phi, \ell} \|U^{(\ell)}\|_F \leq J_\Phi \|U^{(\ell)}\|_F.$$

Define the quantities

$$S_\ell := \sum_{i=1}^{\ell} \|U_i\|_F^2, \quad b_\ell^2 := \sum_{i=1}^{\ell} \|B_i\|_F^2.$$

Then $S_1 = \|B_1\|_F^2 \leq b_1^2$. For $\ell \geq 2$ we have

$$\|U_\ell\|_F \leq \|B_\ell\|_F + \|W_\ell\|_{\text{op}} \|V_{\ell-1}\|_F \leq \|B_\ell\|_F + W_* J_\Phi \|U^{(\ell-1)}\|_F,$$

and hence

$$\|U_\ell\|_F^2 \leq 2\|B_\ell\|_F^2 + 2W_*^2 J_\Phi^2 S_{\ell-1}.$$

Therefore

$$S_\ell = S_{\ell-1} + \|U_\ell\|_F^2 \leq (1 + 2W_*^2 J_\Phi^2) S_{\ell-1} + 2\|B_\ell\|_F^2.$$

Setting $a := 1 + 2W_*^2 J_\Phi^2$ and iterating from $\ell = 1$ gives $S_\ell \leq 2a^{\ell-1} b_\ell^2 \leq 2a^{L-1} b_\ell^2$. Thus, we deduce

$$\|U^{(\ell)}\|_F = \sqrt{S_\ell} \leq \sqrt{2} a^{L/2} \|B^{(\ell)}\|_F = \Gamma \|B^{(\ell)}\|_F,$$

as claimed. \square

Lemma 4.2 (Second-order propagation). *The following estimate holds:*

$$\|\tilde{U}^{(L)}\|_F \leq 2\Theta J_\Phi \Gamma \sqrt{L} \left(\sum_{\ell=1}^L \|\Delta W_\ell\|_{\text{op}}^2 \right)^{\frac{1}{2}} \|B^{(L)}\|_F + \Theta W_* H_\Phi \Gamma^2 L \|B^{(L)}\|_F^2. \quad (4.2)$$

Proof. Differentiating $X_\ell(t) = W_\ell(t)A_{\ell-1}(t)$ twice at $t = 0$ gives

$$\tilde{U}_1 = 0, \quad \tilde{U}_\ell = 2\Delta W_\ell V_{\ell-1} + W_\ell \tilde{V}_{\ell-1} \quad (\ell \geq 2),$$

where $V_\ell := \dot{A}_\ell(0)$ and $\tilde{V}_\ell := \ddot{A}_\ell(0)$. For $A_\ell(t) = \Phi_\ell(X^{(\ell)}(t))$, the second-order chain rule yields

$$\tilde{V}_\ell = D^2\Phi_\ell(X)[U^{(\ell)}, U^{(\ell)}] + D\Phi_\ell(X)[\tilde{U}^{(\ell)}].$$

By the definitions of $H_{\Phi,\ell}$ and $J_{\Phi,\ell}$, we have

$$\|D^2\Phi_\ell(X)[U^{(\ell)}, U^{(\ell)}]\|_F \leq H_{\Phi,\ell} \|U^{(\ell)}\|_F^2 \leq H_\Phi \|U^{(\ell)}\|_F^2,$$

and

$$\|D\Phi_\ell(X)[\tilde{U}^{(\ell)}]\|_F \leq J_{\Phi,\ell} \|\tilde{U}^{(\ell)}\|_F \leq J_\Phi \|\tilde{U}^{(\ell)}\|_F.$$

Using the triangle inequality, we obtain

$$\|\tilde{V}_\ell\|_F \leq H_\Phi \|U^{(\ell)}\|_F^2 + J_\Phi \|\tilde{U}^{(\ell)}\|_F \quad \text{for all } \ell. \quad (4.3)$$

Define now $M_\ell := \|\tilde{U}^{(\ell)}\|_F$ for $\ell = 1, \dots, L$. Then $M_1 = \|\tilde{U}_1\|_F = 0$. For $\ell \geq 2$ we have

$$M_\ell = \|\tilde{U}^{(\ell)}\|_F \leq \|\tilde{U}^{(\ell-1)}\|_F + \|\tilde{U}_\ell\|_F = M_{\ell-1} + \|\tilde{U}_\ell\|_F.$$

Using the expression for \tilde{U}_ℓ and the bound (4.3) for $\tilde{V}_{\ell-1}$ yields

$$\begin{aligned} \|\tilde{U}_\ell\|_F &\leq 2\|\Delta W_\ell\|_{\text{op}} \|V_{\ell-1}\|_F + \|W_\ell\|_{\text{op}} \|\tilde{V}_{\ell-1}\|_F \\ &\leq 2\|\Delta W_\ell\|_{\text{op}} \|V_{\ell-1}\|_F + W_* (H_\Phi \|U^{(\ell-1)}\|_F^2 + J_\Phi \|\tilde{U}^{(\ell-1)}\|_F), \end{aligned}$$

and hence

$$M_\ell \leq (1 + W_* J_\Phi) M_{\ell-1} + 2\|\Delta W_\ell\|_{\text{op}} \|V_{\ell-1}\|_F + W_* H_\Phi \|U^{(\ell-1)}\|_F^2.$$

From Lemma 4.1 we have $\|V_{\ell-1}\|_F \leq J_\Phi \Gamma \|B^{(\ell-1)}\|_F$ and $\|U^{(\ell-1)}\|_F \leq \Gamma \|B^{(\ell-1)}\|_F$, so

$$M_\ell \leq (1 + W_* J_\Phi) M_{\ell-1} + 2J_\Phi \Gamma \|\Delta W_\ell\|_{\text{op}} \|B^{(\ell-1)}\|_F + W_* H_\Phi \Gamma^2 \|B^{(\ell-1)}\|_F^2.$$

Unrolling this recursion from $\ell = 2$ to $\ell = L$ and using $M_1 = 0$ and $(1 + W_* J_\Phi)^{L-k} \leq \Theta$ for all k gives

$$M_L \leq \Theta \sum_{k=2}^L \left(2J_\Phi \Gamma \|\Delta W_k\|_{\text{op}} \|B^{(k-1)}\|_F + W_* H_\Phi \Gamma^2 \|B^{(k-1)}\|_F^2 \right).$$

We bound the two sums separately. First,

$$\sum_{k=2}^L \|B^{(k-1)}\|_F^2 = \sum_{k=2}^L \sum_{i \leq k-1} \|B_i\|_F^2 = \sum_{i=1}^{L-1} (L-i) \|B_i\|_F^2 \leq L \sum_{i=1}^L \|B_i\|_F^2 = L \|B^{(L)}\|_F^2.$$

Second, by Cauchy–Schwarz,

$$\sum_{k=2}^L \|\Delta W_k\|_{\text{op}} \|B^{(k-1)}\|_F \leq \sqrt{L} \left(\sum_{\ell=1}^L \|\Delta W_\ell\|_{\text{op}}^2 \right)^{\frac{1}{2}} \|B^{(L)}\|_F.$$

Substituting these bounds into the expression for M_L gives

$$\|\tilde{U}^{(L)}\|_F = M_L \leq 2\Theta J_\Phi \Gamma \sqrt{L} \left(\sum_{\ell=1}^L \|\Delta W_\ell\|_{\text{op}}^2 \right)^{\frac{1}{2}} \|B^{(L)}\|_F + \Theta W_* H_\Phi \Gamma^2 L \|B^{(L)}\|_F^2,$$

which is exactly (4.2). \square

We can now state the layerwise Hessian bound, which is the main conclusion of this subsection.

Proposition 4.3 (Layerwise Hessian bound). *Let W be fixed and consider the layered model and loss \mathcal{L} described above. Then there exist finite constants $C_F(W), C_{\text{op}}(W) > 0$, depending only on J_Φ, H_Φ, J_f, H_f , on the block operator norms $\|W_\ell\|_{\text{op}}$ (through W_*), and on the depth L , such that for every perturbation $\Delta W = (\Delta W_1, \dots, \Delta W_L)$, we have*

$$|\langle \Delta W, \nabla^2 \mathcal{L}(W) \Delta W \rangle| \leq C_F(W) \sum_{\ell=1}^L \|\Delta W_\ell A_{\ell-1}(W)\|_F^2 + C_{\text{op}}(W) \sum_{\ell=1}^L \|\Delta W_\ell\|_{\text{op}}^2. \quad (4.4)$$

Moreover, one can take for example

$$C_F(W) := \Gamma^2 H_f + J_f \Theta W_* H_\Phi \Gamma^2 L + J_f^2 \Theta \Gamma^2 L, \quad C_{\text{op}}(W) := \Theta J_\Phi^2. \quad (4.5)$$

Proof. Along the path $W(t) = W + t\Delta W$, the chain rule for $\mathcal{L}(W(t)) = f(X_1(t), \dots, X_L(t))$ gives

$$\frac{d^2}{dt^2} \Big|_{t=0} \mathcal{L}(W(t)) = D^2 f(X)[U^{(L)}, U^{(L)}] + \langle \nabla f(X), \tilde{U}^{(L)} \rangle.$$

By the definitions of H_f and J_f , we have

$$|\langle \Delta W, \nabla^2 \mathcal{L}(W) \Delta W \rangle| \leq H_f \|U^{(L)}\|_F^2 + J_f \|\tilde{U}^{(L)}\|_F. \quad (4.6)$$

Lemma 4.1 yields $\|U^{(L)}\|_F \leq \Gamma \|B^{(L)}\|_F$, and Lemma 4.2 yields

$$\|\tilde{U}^{(L)}\|_F \leq 2\Theta J_\Phi \Gamma \sqrt{L} \left(\sum_{\ell=1}^L \|\Delta W_\ell\|_{\text{op}}^2 \right)^{\frac{1}{2}} \|B^{(L)}\|_F + \Theta W_* H_\Phi \Gamma^2 L \|B^{(L)}\|_F^2.$$

Substituting these bounds into (4.6) and collecting terms gives

$$|\langle \Delta W, \nabla^2 \mathcal{L}(W) \Delta W \rangle| \leq A_B(W) \|B^{(L)}\|_F^2 + 2C_c(W) a b,$$

where

$$A_B(W) := \Gamma^2 H_f + J_f \Theta W_* H_\Phi \Gamma^2 L, \quad C_c(W) := J_f \Theta J_\Phi \Gamma \sqrt{L},$$

and

$$a := \left(\sum_{\ell=1}^L \|\Delta W_\ell\|_{\text{op}}^2 \right)^{\frac{1}{2}}, \quad b := \|B^{(L)}\|_F.$$

Using the inequality

$$2C_c(W) a b \leq A a^2 + B b^2 \quad \text{for any } A, B > 0 \text{ with } AB \geq C_c(W)^2,$$

and choosing, for instance,

$$A = \Theta J_\Phi^2, \quad B = \frac{C_c(W)^2}{A} = J_f^2 \Theta \Gamma^2 L,$$

we obtain

$$|\langle \Delta W, \nabla^2 \mathcal{L}(W) \Delta W \rangle| \leq (A_B(W) + B) \|B^{(L)}\|_F^2 + A \sum_{\ell=1}^L \|\Delta W_\ell\|_{\text{op}}^2.$$

Since equality $\|B^{(L)}\|_F^2 = \sum_{\ell=1}^L \|\Delta W_\ell A_{\ell-1}(W)\|_F^2$ holds, this is exactly (4.4) with $C_F(W)$ and $C_{\text{op}}(W)$ as in (4.5). \square

Scaling with the number of samples. For averaged losses such as the squared loss $f(X_1, \dots, X_L) = \frac{1}{2n} \|X_L - Y\|_F^2$, we have

$$J_f = \|\nabla f(X)\|_F = \frac{1}{n} \|X_L - Y\|_F, \quad H_f = \frac{1}{n},$$

as we will verify below. If, in addition, the average loss f remains $O(1)$ along training so that typically $\|X_L - Y\|_F^2 = O(n)$, then $J_f = O(1/\sqrt{n})$ and $H_f = O(1/n)$. A completely analogous scaling holds for softmax cross-entropy: the per-example gradients are uniformly bounded, so for the averaged loss one has $J_f = O(1/\sqrt{n})$ and $H_f = O(1/n)$ regardless of the size of the prediction errors. These factors appear only in $C_F(W)$, which multiplies the feature term $\sum_\ell \|\Delta W_\ell A_{\ell-1}(W)\|_F^2$. Since $\|A_{\ell-1}(W)\|_F^2$ is of order n when $A_{\ell-1}$ stacks n data points in columns, the resulting curvature contribution is of order one in n . In particular, the constants $C_F(W)$ and $C_{\text{op}}(W)$ in Proposition 4.3 do not grow with the number of samples n , nor with the layer widths.

4.2.1 Derivative constants for MLPs and transformer blocks

To interpret the layerwise Hessian bound in concrete architectures, it is useful to understand the size of the derivative constants $J_{\Phi,\ell}$, $H_{\Phi,\ell}$ and J_f , H_f . In this subsubsection we sketch how these constants are instantiated in multilayer perceptrons and transformer blocks. Throughout, all implicit constants depend only on the choice of nonlinearities and loss, and not on the dimensions d_ℓ or n .

MLPs. Consider a fully-connected network with layers

$$X_1 = W_1 A_0, \quad A_1 = \sigma(X_1), \quad X_2 = W_2 A_1, \quad A_2 = \sigma(X_2), \quad \dots,$$

and a fixed elementwise activation $\sigma : \mathbf{R} \rightarrow \mathbf{R}$. In the layered notation above, the nonlinear map at layer ℓ is simply

$$\Phi_\ell(X_1, \dots, X_\ell) = \sigma(X_\ell) \quad (\text{applied entrywise}).$$

Assume that σ is C^2 -smooth with

$$\sup_{t \in \mathbf{R}} |\sigma'(t)| \leq L_1, \quad \sup_{t \in \mathbf{R}} |\sigma''(t)| \leq L_2.$$

Then for the Jacobian we have

$$D\Phi_\ell(X)[U] = \sigma'(X_\ell) \odot U, \quad \|D\Phi_\ell(X)[U]\|_F \leq L_1 \|U\|_F.$$

Therefore we deduce

$$J_{\Phi,\ell} \leq L_1 \quad \text{and hence} \quad J_\Phi = \max_\ell J_{\Phi,\ell} \leq L_1.$$

Similarly, the second derivative takes the form

$$D^2\Phi_\ell(X)[U, U] = \sigma''(X_\ell) \odot U \odot U,$$

and

$$\|D^2\Phi_\ell(X)[U, U]\|_F \leq L_2 \|U \odot U\|_F \leq L_2 \|U\|_F^2,$$

Therefore, we deduce

$$H_{\Phi,\ell} \leq L_2, \quad H_\Phi \leq L_2.$$

Thus, for MLPs with a fixed smooth activation, the activation-side constants $J_{\Phi,\ell}$, $H_{\Phi,\ell}$ are controlled entirely by scalar bounds on σ' , σ'' and do not depend on width.

For the outer loss f , the squared loss and softmax cross-entropy examples in the scaling paragraph above already show that J_f and H_f inherit only the $1/n$ factors coming from the averaging in the loss, and do not introduce any additional dependence on the layer widths.

Transformer blocks and the layered model. We now make the structure of a single decoder block explicit in the layered notation. Fix a block input $X^{(0)} \in \mathbf{R}^{d_{\text{model}} \times T}$ (hidden dimension d_{model} , sequence length T). We enumerate the trainable matrices inside the block as

$$W_1 = W_Q, \quad W_2 = W_K, \quad W_3 = W_V, \quad W_4 = W_O, \quad W_5 = W_1, \quad W_6 = W_2,$$

corresponding to the attention projections and MLP weights. Following the layered model convention $X_\ell(W) = W_\ell A_{\ell-1}(W)$ and $A_\ell(W) = \Phi_\ell(X_1(W), \dots, X_\ell(W))$, we introduce the following internal variables and maps.

Block structure. Define first the RMS-normalized input

$$A_0(W) := A^{\text{rms}}(W) := \text{RMSNorm}(X^{(0)}(W)),$$

so that the first three preactivations are

$$X_1(W) = W_1 A_0(W) = W_Q A^{\text{rms}}, \quad X_2(W) = W_2 A_0(W) = W_K A^{\text{rms}}, \quad X_3(W) = W_3 A_0(W) = W_V A^{\text{rms}}.$$

Next, we form the scaled attention scores and probabilities

$$S(W) := d_{\text{model}}^{-1/2} X_2(W)^\top X_1(W), \quad P(W) := \text{softmax}(S(W)) \quad (\text{columnwise}),$$

and the value aggregation

$$H(W) := X_3(W) P(W).$$

The output projection preactivation is

$$X_4(W) = W_4 H(W) = W_O H(W),$$

and the attention residual is

$$X^{\text{att}}(W) := X^{(0)}(W) + X_4(W).$$

We then RMS-normalize X^{att} as

$$A_4(W) := A_{\text{mlp}}^{\text{rms}}(W) := \text{RMSNorm}(X^{\text{att}}(W)),$$

and form the MLP preactivations

$$X_5(W) = W_5 A_4(W) = W_1 A_{\text{mlp}}^{\text{rms}}, \quad X_6(W) = W_6 B(W) = W_2 B(W),$$

where

$$B(W) := \sigma(X_5(W))$$

is the pointwise MLP activation. Finally, the block output is

$$X^{(+)}(W) := X^{\text{att}}(W) + X_6(W).$$

In this notation, the preactivations are $X_\ell(W) = W_\ell A_{\ell-1}(W)$ for $\ell = 1, \dots, 6$, with $A_{-1}(W) = X^{(0)}(W)$ and $A_0(W), A_4(W), B(W)$ as above. The corresponding activation maps

$$A_\ell(W) = \Phi_\ell(X_1(W), \dots, X_\ell(W)), \quad \ell = 0, \dots, 6,$$

collect the nonlinear operations that produce the data matrices feeding each linear map; for example

$$\Phi_0(X^{(0)}) = \text{RMSNorm}(X^{(0)}),$$

$$\Phi_3(X_1, X_2, X_3) = A^{\text{rms}}(W) \quad (\text{the attention inputs, reused for } W_Q, W_K, W_V),$$

$$\Phi_4(X_1, \dots, X_4) = \text{RMSNorm}(X^{(0)} + X_4) = A^{\text{rms}}(W),$$

$$\Phi_5(X_1, \dots, X_5) = \sigma(X_5), \quad \Phi_6(X_1, \dots, X_6) = X^{(+)} = X^{\text{att}} + X_6.$$

Derivative bounds. With this structure in hand, the derivative constants $J_{\Phi, \ell}$ and $H_{\Phi, \ell}$ for the transformer block can be bounded by combining the primitive bounds for RMSNorm, softmax, and the MLP nonlinearity. As before, we assume that the MLP activation σ satisfies

$$\sup_{t \in \mathbf{R}} |\sigma'(t)| \leq L_1, \quad \sup_{t \in \mathbf{R}} |\sigma''(t)| \leq L_2.$$

For the RMS normalization, a direct computation of the Jacobian and Hessian shows that, as long as the rescaled squared norms $d_{\text{model}}^{-1} \|X^{(0)}\|_F^2$ and $d_{\text{model}}^{-1} \|X^{\text{att}}\|_F^2$ remain in a fixed compact interval, there exist constants $C_{\text{rms},1}, C_{\text{rms},2}$ (depending only on the RMSNorm hyperparameters) such that

$$\|D(\text{RMSNorm})(\cdot)[U]\|_F \leq C_{\text{rms},1} \|U\|_F, \quad \|D^2(\text{RMSNorm})(\cdot)[U, U]\|_F \leq C_{\text{rms},2} \|U\|_F^2.$$

For the softmax, viewed columnwise on $S \in \mathbf{R}^{T \times T}$, there exist constants $C_{\text{sm},1}, C_{\text{sm},2}$ such that

$$\|D(\text{softmax})(S)[U]\|_F \leq C_{\text{sm},1} \|U\|_F, \quad \|D^2(\text{softmax})(S)[U, U]\|_F \leq C_{\text{sm},2} \|U\|_F^2$$

for all S, U . The linear projections $W_\ell A_{\ell-1}$ always contribute their spectral norms:

$$\|D(W_\ell A_{\ell-1})[U]\|_F \leq \|W_\ell\|_{\text{op}} \|U\|_F, \quad D^2(W_\ell A_{\ell-1})[\cdot, \cdot] \equiv 0.$$

Combining these primitive estimates through the chain rule, one finds that the constants $J_{\Phi, \ell}, H_{\Phi, \ell}$ are bounded above by expressions of the form

$$J_{\Phi, \ell} \leq C_1 \prod_{\ell' \in \mathcal{N}(\ell)} \|W_{\ell'}\|_{\text{op}}, \quad H_{\Phi, \ell} \leq C_2 \left(1 + \sum_{\ell' \in \mathcal{N}(\ell)} \|W_{\ell'}\|_{\text{op}}^2 \right),$$

where $\mathcal{N}(\ell)$ denotes the (finite) collection of projection matrices whose outputs feed into the nonlinearities affecting $A_{\ell-1}$, and C_1, C_2 depend only on the scalar nonlinearities (RMSNorm, softmax, σ) and not on d_{model} or T . In particular, these bounds show that J_Φ and H_Φ remain bounded as the width and sequence length vary.

4.3 From feature metric to blockwise Lipschitz constants

The mixed Hessian bound of Proposition 4.3 controls the curvature of \mathcal{L} in terms of the feature perturbations $\Delta W_\ell A_{\ell-1}(W)$ and the operator norms $\|\Delta W_\ell\|_{\text{op}}$:

$$\langle \Delta W, \nabla^2 \mathcal{L}(W) \Delta W \rangle \leq C_F(W) \sum_{\ell=1}^L \|\Delta W_\ell A_{\ell-1}(W)\|_F^2 + C_{\text{op}}(W) \sum_{\ell=1}^L \|\Delta W_\ell\|_{\text{op}}^2.$$

The feature term in this inequality plays exactly the same role as in the random-feature model: it yields blockwise curvature constants that are determined by the activations $A_{\ell-1}(W)$. The parameter-only term $C_{\text{op}}(W) \sum_{\ell} \|\Delta W_\ell\|_{\text{op}}^2$ contributes an extra, geometry-independent correction which we will account for in the descent comparison, but it does not affect which activation matrices are relevant for each block or the stable-rank ratio.

In many architectures of interest, and in particular in the multilayer and transformer examples discussed in Section 1.2.1, each activation $A_{\ell-1}(W)$ admits a natural factorization

$$A_{\ell-1}(W) = M_{\ell, \text{left}}(W) \tilde{A}_{\ell-1}(W) M_{\ell, \text{right}}(W), \quad (4.7)$$

where:

- $\tilde{A}_{\ell-1}(W)$ is the *core activation* feeding block ℓ (for example, the post-activation $A_{\ell-1}$ in an MLP, or an RMS-normalized activation or MLP post-activation in a transformer block as in Section 1.2.1); and
- $M_{\ell,\text{left}}(W)$ and $M_{\ell,\text{right}}(W)$ are fixed linear operators (at the current W) capturing the surrounding linear structure: projections, attention kernels, residual maps, etc.

The dependence on W is smooth but, crucially, these matrices are independent of ΔW . Using submultiplicativity of the operator norm, we obtain the Frobenius and operator bounds, for each block ℓ , given by

$$\begin{aligned}\|\Delta W_\ell A_{\ell-1}(W)\|_F &\leq \|\Delta W_\ell\|_F \|A_{\ell-1}(W)\|_{\text{op}}, \\ \|\Delta W_\ell A_{\ell-1}(W)\|_F &\leq \|\Delta W_\ell\|_{\text{op}} \|A_{\ell-1}(W)\|_F.\end{aligned}$$

Using the factorization (4.7) once more, we obtain

$$\begin{aligned}\|A_{\ell-1}(W)\|_{\text{op}} &\leq \|M_{\ell,\text{left}}(W)\|_{\text{op}} \|\tilde{A}_{\ell-1}(W)\|_{\text{op}} \|M_{\ell,\text{right}}(W)\|_{\text{op}}, \\ \|A_{\ell-1}(W)\|_F &\leq \|M_{\ell,\text{left}}(W)\|_{\text{op}} \|\tilde{A}_{\ell-1}(W)\|_F \|M_{\ell,\text{right}}(W)\|_{\text{op}}.\end{aligned}$$

Combining these inequalities with the feature part of the Hessian bound, we obtain feature-based blockwise curvature constants

$$\begin{aligned}L_\ell^F(W) &:= C_F(W) \|M_{\ell,\text{left}}(W)\|_{\text{op}}^2 \|\tilde{A}_{\ell-1}(W)\|_{\text{op}}^2 \|M_{\ell,\text{right}}(W)\|_{\text{op}}^2, \\ L_\ell^{\text{op}}(W) &:= C_F(W) \|M_{\ell,\text{left}}(W)\|_{\text{op}}^2 \|\tilde{A}_{\ell-1}(W)\|_F^2 \|M_{\ell,\text{right}}(W)\|_{\text{op}}^2,\end{aligned}\tag{4.8}$$

for which the feature term in the Hessian satisfies

$$\langle \Delta W, \nabla^2 \mathcal{L}(W) \Delta W \rangle_{\text{feature}} \leq \sum_{\ell=1}^L L_\ell^F(W) \|\Delta W_\ell\|_F^2,\tag{4.9}$$

$$\langle \Delta W, \nabla^2 \mathcal{L}(W) \Delta W \rangle_{\text{feature}} \leq \sum_{\ell=1}^L L_\ell^{\text{op}}(W) \|\Delta W_\ell\|_{\text{op}}^2.\tag{4.10}$$

By construction, the ratio of these two constants depends only on the stable rank of the *core activation* $\tilde{A}_{\ell-1}(W)$, while the surrounding linear maps cancel:

$$\frac{L_\ell^{\text{op}}(W)}{L_\ell^F(W)} = \frac{\|\tilde{A}_{\ell-1}(W)\|_F^2}{\|\tilde{A}_{\ell-1}(W)\|_{\text{op}}^2} = \text{st}(\tilde{A}_{\ell-1}(W)).\tag{4.11}$$

In words, the feature-based curvature in the spectral geometry is larger than that in the Frobenius geometry by a factor equal to the stable rank of the core activation.

Two special cases are worth highlighting.

- **Fully-connected networks.** For standard MLPs, we may take $M_{\ell,\text{left}}(W) = I$ and $M_{\ell,\text{right}}(W) = I$, so that $\tilde{A}_{\ell-1}(W) = A_{\ell-1}(W)$ is exactly the layerwise post-activation introduced in (1.2). In this case, L_ℓ^F and L_ℓ^{op} are proportional to $\|A_{\ell-1}\|_{\text{op}}^2$ and $\|A_{\ell-1}\|_F^2$, and their ratio is the stable rank $\text{st}(A_{\ell-1})$.

- **Transformer blocks.** In transformer architectures, the effective feature matrices $A_{\ell-1}(W)$ entering each block factor as in Section 1.2.1: the core activation $\tilde{A}_{\ell-1}$ is one of the RMS-normalized hidden states or MLP post-activations, while $M_{\ell,\text{left}}$ and $M_{\ell,\text{right}}$ collect attention kernels, projection matrices, and residual maps. The expressions (4.8)–(4.11) then show that the feature-based curvature is governed, up to fixed operator–norm factors, by the stable rank of the corresponding RMS or MLP activations.

The full Hessian bound of Proposition 4.3 adds the parameter-only term $C_{\text{op}}(W) \sum_{\ell} \|\Delta W_{\ell}\|_{\text{op}}^2$ to the right-hand side of (4.9)–(4.10). This term does not depend on the activations and therefore does not change which feature matrices are relevant for a given block or the stable-rank ratio (4.11); it will appear only as a small, blockwise correction in the one-step descent analysis below.

4.4 Descent bounds and spectral-vs.-Euclidean comparison

We now use the blockwise constants from (4.8)–(4.11) together with the full Hessian bound of Proposition 4.3 to compare one-step decreases under Euclidean (Frobenius) and spectral updates acting on all matrix blocks. We write $G_{\ell}(W) := \nabla_{W_{\ell}} \mathcal{L}(W)$ for the block gradients, and let $\mathcal{S} \subseteq \{1, \dots, L\}$ denote the subset of matrix-valued blocks on which we intend to apply spectral updates (for example, the internal MLP and attention weights in a transformer stack, as in Section 1.2.1). For notational brevity, we fix W and write G_{ℓ} , L_{ℓ}^F , L_{ℓ}^{op} , C_F , and C_{op} .

Taylor model. Expanding \mathcal{L} around W in the direction $\Delta W = (\Delta W_1, \dots, \Delta W_L)$ yields

$$\mathcal{L}(W + \Delta W) = \mathcal{L}(W) + \sum_{\ell=1}^L \langle G_{\ell}, \Delta W_{\ell} \rangle + \frac{1}{2} \langle \Delta W, \nabla^2 \mathcal{L}(W) \Delta W \rangle + R(\Delta W), \quad (4.12)$$

where $R(\Delta W)$ collects third and higher order terms. Combining the feature-based bounds (4.9)–(4.10) with the additional parameter term in Proposition 4.3, we obtain the Frobenius-geometry bound

$$\langle \Delta W, \nabla^2 \mathcal{L}(W) \Delta W \rangle \leq \sum_{\ell} L_{\ell}^F \|\Delta W_{\ell}\|_F^2 + C_{\text{op}}(W) \sum_{\ell} \|\Delta W_{\ell}\|_{\text{op}}^2, \quad (4.13)$$

valid for all ΔW . For mixed Euclidean/spectral updates that use spectral geometry only on the subset \mathcal{S} , we will also use the corresponding mixed bound

$$\langle \Delta W, \nabla^2 \mathcal{L}(W) \Delta W \rangle \leq \sum_{\ell \in \mathcal{S}} L_{\ell}^{\text{op}} \|\Delta W_{\ell}\|_{\text{op}}^2 + \sum_{\ell \notin \mathcal{S}} L_{\ell}^F \|\Delta W_{\ell}\|_F^2 + C_{\text{op}}(W) \sum_{\ell} \|\Delta W_{\ell}\|_{\text{op}}^2,$$

which is obtained by applying the spectral feature bound on blocks in \mathcal{S} , the Frobenius feature bound on blocks not in \mathcal{S} , and the same parameter-only term on all blocks.

Definition of the GD and spectral updates. We now define a full Euclidean (Frobenius) gradient step and a mixed spectral step by choosing blockwise step sizes that are natural for the quadratic model (4.12) under the mixed Hessian bounds above.

For the Euclidean step we set, for each block ℓ ,

$$a_{\text{GD},\ell} := L_{\ell}^F + \frac{C_{\text{op}}(W)}{\text{st}(G_{\ell})}, \quad \text{st}(G_{\ell}) := \frac{\|G_{\ell}\|_F^2}{\|G_{\ell}\|_{\text{op}}^2},$$

and define

$$W_{\ell}^{\text{GD}} := W_{\ell} - \frac{1}{a_{\text{GD},\ell}} G_{\ell}, \quad \Delta W_{\ell}^{\text{GD}} := W_{\ell}^{\text{GD}} - W_{\ell} = -\frac{1}{a_{\text{GD},\ell}} G_{\ell},$$

so that $W^{\text{GD}} := (W_1^{\text{GD}}, \dots, W_L^{\text{GD}})$ is the full GD update.

For the spectral step we set, for each $\ell \in \mathcal{S}$,

$$a_{\text{Spec},\ell} := L_\ell^{\text{op}} + C_{\text{op}}(W),$$

and define

$$W_\ell^{\text{Spec}} := W_\ell - \frac{\|G_\ell\|_*}{a_{\text{Spec},\ell}} \text{polar}(G_\ell), \quad \Delta W_\ell^{\text{Spec}} := W_\ell^{\text{Spec}} - W_\ell = -\frac{\|G_\ell\|_*}{a_{\text{Spec},\ell}} \text{polar}(G_\ell),$$

where $\text{polar}(G_\ell)$ is the orthogonal factor in the polar decomposition of G_ℓ . For blocks $\ell \notin \mathcal{S}$ we simply set $W_\ell^{\text{Spec}} := W_\ell^{\text{GD}}$. In this way $W^{\text{Spec}} := (W_1^{\text{Spec}}, \dots, W_L^{\text{Spec}})$ is the full mixed update which uses spectral geometry on blocks in \mathcal{S} and Euclidean geometry on the others.

One-step bound for the Euclidean step. For the Euclidean update, the linear term in (4.12) is

$$\langle G_\ell, \Delta W_\ell^{\text{GD}} \rangle = -\frac{1}{a_{\text{GD},\ell}} \|G_\ell\|_F^2.$$

For the quadratic term we use (4.13) together with

$$\|\Delta W_\ell^{\text{GD}}\|_F^2 = \frac{1}{a_{\text{GD},\ell}^2} \|G_\ell\|_F^2, \quad \|\Delta W_\ell^{\text{GD}}\|_{\text{op}}^2 = \frac{1}{a_{\text{GD},\ell}^2} \|G_\ell\|_{\text{op}}^2 = \frac{1}{a_{\text{GD},\ell}^2} \frac{\|G_\ell\|_F^2}{\text{st}(G_\ell)}.$$

Thus the contribution of block ℓ to the quadratic term is bounded by

$$\frac{1}{2} \left(L_\ell^{\text{F}} \frac{\|G_\ell\|_F^2}{a_{\text{GD},\ell}^2} + C_{\text{op}}(W) \frac{\|G_\ell\|_F^2}{a_{\text{GD},\ell}^2 \text{st}(G_\ell)} \right) = \frac{a_{\text{GD},\ell}}{2} \frac{\|G_\ell\|_F^2}{a_{\text{GD},\ell}^2} = \frac{1}{2a_{\text{GD},\ell}} \|G_\ell\|_F^2.$$

Plugging ΔW^{GD} into (4.12) and summing over ℓ gives

$$\mathcal{L}(W^{\text{GD}}) \leq \mathcal{L}(W) - \sum_{\ell=1}^L \frac{1}{a_{\text{GD},\ell}} \|G_\ell\|_F^2 + \frac{1}{2} \sum_{\ell=1}^L \frac{1}{a_{\text{GD},\ell}} \|G_\ell\|_F^2 + R(\Delta W^{\text{GD}}),$$

so the quadratic model predicts the total decrease

$$\Delta_{\text{GD}} := \mathcal{L}(W) - \mathcal{L}(W^{\text{GD}}) \geq \frac{1}{2} \sum_{\ell=1}^L \frac{\|G_\ell\|_F^2}{a_{\text{GD},\ell}} = \frac{1}{2} \sum_{\ell=1}^L \frac{\|G_\ell\|_F^2}{L_\ell^{\text{F}} + C_{\text{op}}(W)/\text{st}(G_\ell)}. \quad (4.14)$$

One-step bound for the spectral step. For the spectral update on $\ell \in \mathcal{S}$ we have

$$\langle G_\ell, \Delta W_\ell^{\text{Spec}} \rangle = -\frac{\|G_\ell\|_*^2}{a_{\text{Spec},\ell}}, \quad \|\Delta W_\ell^{\text{Spec}}\|_{\text{op}}^2 = \frac{\|G_\ell\|_*^2}{a_{\text{Spec},\ell}^2},$$

and for $\ell \notin \mathcal{S}$ the update coincides with the Euclidean one, so the contribution to the linear and quadratic terms on those blocks is exactly the same as in the GD case. Using the mixed Hessian bound (spectral geometry on \mathcal{S} , Frobenius geometry on its complement), the contribution of block $\ell \in \mathcal{S}$ to the quadratic term is bounded by

$$\frac{1}{2} \left(L_\ell^{\text{op}} \frac{\|G_\ell\|_*^2}{a_{\text{Spec},\ell}^2} + C_{\text{op}}(W) \frac{\|G_\ell\|_*^2}{a_{\text{Spec},\ell}^2} \right) = \frac{a_{\text{Spec},\ell}}{2} \frac{\|G_\ell\|_*^2}{a_{\text{Spec},\ell}^2} = \frac{1}{2a_{\text{Spec},\ell}} \|G_\ell\|_*^2.$$

Proceeding as above and summing over all blocks, we obtain the total decrease guarantee

$$\begin{aligned}\Delta_{\text{Spec}} := \mathcal{L}(W) - \mathcal{L}(W^{\text{Spec}}) &\geq \frac{1}{2} \sum_{\ell \in \mathcal{S}} \frac{\|G_\ell\|_*^2}{a_{\text{Spec},\ell}} + \frac{1}{2} \sum_{\ell \notin \mathcal{S}} \frac{\|G_\ell\|_F^2}{a_{\text{GD},\ell}} \\ &= \frac{1}{2} \sum_{\ell \in \mathcal{S}} \frac{\|G_\ell\|_*^2}{L_\ell^{\text{op}} + C_{\text{op}}(W)} + \frac{1}{2} \sum_{\ell \notin \mathcal{S}} \frac{\|G_\ell\|_F^2}{L_\ell^{\text{F}} + C_{\text{op}}(W)/\text{st}(G_\ell)}.\end{aligned}\quad (4.15)$$

Nuclear-rank vs. stable-rank condition. Comparing the global guarantees (4.14) and (4.15), we see that whenever we keep the GD update on blocks $\ell \notin \mathcal{S}$, the total spectral decrease is guaranteed to be at least as large as the Euclidean decrease provided that, for every $\ell \in \mathcal{S}$,

$$\frac{\|G_\ell\|_*^2}{L_\ell^{\text{op}} + C_{\text{op}}(W)} \geq \frac{\|G_\ell\|_F^2}{L_\ell^{\text{F}} + C_{\text{op}}(W)/\text{st}(G_\ell)} \iff \frac{\|G_\ell\|_*^2}{\|G_\ell\|_F^2} \geq \frac{L_\ell^{\text{op}} + C_{\text{op}}(W)}{L_\ell^{\text{F}} + C_{\text{op}}(W)/\text{st}(G_\ell)}.$$

Using the feature-based ratio (4.11), we may rewrite the right-hand side in terms of the stable rank of the core activation feeding block ℓ . Setting

$$s_\ell := \text{st}(\tilde{A}_{\ell-1}(W)) = \frac{L_\ell^{\text{op}}}{L_\ell^{\text{F}}}, \quad \alpha_\ell := \frac{C_{\text{op}}(W)}{L_\ell^{\text{F}}},$$

we have

$$\frac{L_\ell^{\text{op}} + C_{\text{op}}(W)}{L_\ell^{\text{F}} + C_{\text{op}}(W)/\text{st}(G_\ell)} = \frac{s_\ell + \alpha_\ell}{1 + \alpha_\ell/\text{st}(G_\ell)}.$$

Thus the per-block condition for the spectral update on block $\ell \in \mathcal{S}$ to improve upon the Euclidean update on that block is

$$\text{nr}(G_\ell) := \frac{\|G_\ell\|_*^2}{\|G_\ell\|_F^2} \geq \frac{\text{st}(\tilde{A}_{\ell-1}(W)) + \alpha_\ell}{1 + \alpha_\ell/\text{st}(G_\ell)}.\quad (4.16)$$

The right-hand side of (4.16) is increasing in the denominator parameter $\text{st}(G_\ell)$. Since $\text{st}(G_\ell) \leq \text{nr}(G_\ell)$ by definition, we may therefore replace $\text{st}(G_\ell)$ by $\text{nr}(G_\ell)$ in the denominator, which only *increases* the right-hand side and yields a stronger (more conservative) but still sufficient condition for the spectral update to dominate GD. With this replacement, (4.16) is implied by

$$\text{nr}(G_\ell) \geq \frac{\text{st}(\tilde{A}_{\ell-1}(W)) + \alpha_\ell}{1 + \alpha_\ell/\text{nr}(G_\ell)}.\quad (4.17)$$

A simple algebraic rearrangement shows that the stronger inequality (4.17) is in fact *equivalent* to the bare inequality

$$\text{nr}(G_\ell) \geq \text{st}(\tilde{A}_{\ell-1}(W)).\quad (4.18)$$

Indeed, writing $r := \text{nr}(G_\ell)$, $s := \text{st}(\tilde{A}_{\ell-1}(W))$ and $\alpha := \alpha_\ell$, the inequality $r \geq (s + \alpha)/(1 + \alpha/r)$ is equivalent to $r(1 + \alpha/r) \geq s + \alpha$, i.e. $r + \alpha \geq s + \alpha$, hence $r \geq s$.

Summing over all blocks, it follows that whenever the sufficient condition (4.18) holds for every $\ell \in \mathcal{S}$, the quadratic model guarantees that the full mixed spectral update $W \mapsto W^{\text{Spec}}$ (spectral on \mathcal{S} , Euclidean elsewhere) achieves at least as much decrease as the full Euclidean update $W \mapsto W^{\text{GD}}$ (up to the common remainder term $R(\Delta W)$). This is precisely the same rule that emerged in our random-feature analysis: spectral updates are most advantageous on those blocks whose incoming core activations $\tilde{A}_{\ell-1}(W)$ have low stable rank while the corresponding gradients G_ℓ have large nuclear rank.

4.5 Extension: diagonal RMS-normalization weights

In the layered model, the blocks W_ℓ were arbitrary matrices, and the spectral step used the full polar factor of $\nabla_{W_\ell} \mathcal{L}(W)$. The RMS-normalization layers are more structured: their weights are diagonal, and in this case the spectral steepest-descent step reduces to a “signSGD”-type update on the RMSNorm weights, with a corresponding ℓ_1/ℓ_2 analogue of the nuclear-rank condition. We record this diagonal case here.

Each RMSNorm layer carries weights $\gamma \in \mathbf{R}^d$ and acts on a hidden state $X \in \mathbf{R}^{d \times n}$ as

$$\text{RMSNorm}_\gamma(X) = \text{Diag}(\gamma) \tilde{A}^{\text{rms}}(X), \quad A := \tilde{A}^{\text{rms}}(X) \in \mathbf{R}^{d \times n},$$

where $\tilde{A}^{\text{rms}}(X)$ is the parameter-free RMS-normalized activation. In our notation we write $\Gamma := \text{Diag}(\gamma)$ and regard it as a diagonal block with incoming activations A . A perturbation of the RMSNorm weights has the form $\Delta\Gamma = \text{Diag}(\delta\gamma)$ and appears in the same feature term $\|\Delta\Gamma A\|_F^2$ as any other block in the Hessian bound.

For diagonal $\Delta\Gamma$ we have

$$\|\Delta\Gamma A\|_F \leq \|\Delta\Gamma\|_F \|A\|_{\text{op}} = \|\delta\gamma\|_2 \|A\|_{\text{op}}, \quad \|\Delta\Gamma A\|_F \leq \|\Delta\Gamma\|_{\text{op}} \|A\|_F = \|\delta\gamma\|_\infty \|A\|_F.$$

Thus, at the level of the feature term, the RMSNorm block has the same two curvature constants as any matrix block,

$$L_{\text{rms}}^F(W) = C_F(W) \|A\|_{\text{op}}^2, \quad L_{\text{rms}}^{\text{op}}(W) = C_F(W) \|A\|_F^2,$$

and their ratio is

$$\frac{L_{\text{rms}}^{\text{op}}(W)}{L_{\text{rms}}^F(W)} = \frac{\|A\|_F^2}{\|A\|_{\text{op}}^2} = \text{st}(A).$$

Let $g := \nabla_\gamma \mathcal{L}(W) \in \mathbf{R}^d$ be the gradient with respect to the RMSNorm weights. At the level of matrix blocks, this corresponds to the diagonal matrix $G_{\text{diag}} := \text{Diag}(g)$, whose Frobenius and operator norms are

$$\|G_{\text{diag}}\|_F^2 = \|g\|_2^2, \quad \|G_{\text{diag}}\|_{\text{op}}^2 = \|g\|_\infty^2.$$

The analogue of the stable rank of the gradient in this diagonal setting is therefore

$$\text{st}_{\text{diag}}(g) := \frac{\|G_{\text{diag}}\|_F^2}{\|G_{\text{diag}}\|_{\text{op}}^2} = \frac{\|g\|_2^2}{\|g\|_\infty^2}.$$

For this diagonal block we can repeat exactly the one-step analysis from Section 4.4, now with the gradient represented by G_{diag} and curvature constants $L_{\text{rms}}^F(W)$ and $L_{\text{rms}}^{\text{op}}(W)$. In particular, in analogy with (4.14)–(4.15), we define blockwise step sizes

$$a_{\text{GD,rms}} := L_{\text{rms}}^F(W) + \frac{C_{\text{op}}(W)}{\text{st}_{\text{diag}}(g)}, \quad a_{\text{Spec,rms}} := L_{\text{rms}}^{\text{op}}(W) + C_{\text{op}}(W),$$

and consider the two updates

$$\gamma_{\text{GD}}^+ := \gamma - \frac{1}{a_{\text{GD,rms}}} g, \quad \gamma_{\text{Spec}}^+ := \gamma - \frac{\|g\|_1}{a_{\text{Spec,rms}}} \text{sign}(g).$$

For the Euclidean update, the same quadratic-model calculation as in (4.14) (with G_ℓ replaced by G_{diag} and L_ℓ^F by L_{rms}^F) gives the one-step bound

$$\Delta_{\text{GD,rms}} \geq \frac{\|g\|_2^2}{2(L_{\text{rms}}^F(W) + C_{\text{op}}(W)/\text{st}_{\text{diag}}(g))}.$$

For the spectral update, the same argument as in (4.15) (using that $\|\text{Diag}(\text{sign}(g))\|_{\text{op}} = 1$ and $\|\text{Diag}(\text{sign}(g))A\|_F \leq \|A\|_F$) yields

$$\Delta_{\text{Spec,rms}} \geq \frac{\|g\|_1^2}{2(L_{\text{rms}}^{\text{op}}(W) + C_{\text{op}}(W))}.$$

Thus, at the level of the quadratic model, the spectral update dominates the Euclidean update on this diagonal block whenever

$$\frac{\|g\|_1^2}{L_{\text{rms}}^{\text{op}}(W) + C_{\text{op}}(W)} \geq \frac{\|g\|_2^2}{L_{\text{rms}}^{\text{F}}(W) + C_{\text{op}}(W)/\text{st}_{\text{diag}}(g)}.$$

Using $L_{\text{rms}}^{\text{op}}/L_{\text{rms}}^{\text{F}} = \text{st}(A)$ and defining

$$s_A := \text{st}(A) = \frac{\|A\|_F^2}{\|A\|_{\text{op}}^2}, \quad \alpha_{\text{rms}} := \frac{C_{\text{op}}(W)}{L_{\text{rms}}^{\text{F}}(W)},$$

we can rewrite this condition exactly as in (4.16):

$$\frac{\|g\|_1^2}{\|g\|_2^2} \geq \frac{s_A + \alpha_{\text{rms}}}{1 + \alpha_{\text{rms}}/\text{st}_{\text{diag}}(g)}.$$

The right-hand side is increasing in $\text{st}_{\text{diag}}(g)$. On the other hand, for any nonzero g we have the scalar inequality

$$\frac{\|g\|_1^2}{\|g\|_2^2} \geq \frac{\|g\|_2^2}{\|g\|_{\infty}^2} = \text{st}_{\text{diag}}(g),$$

so it is sufficient to impose the stronger condition obtained by replacing $\text{st}_{\text{diag}}(g)$ in the denominator by $\|g\|_1^2/\|g\|_2^2$. This gives

$$\frac{\|g\|_1^2}{\|g\|_2^2} \geq \frac{s_A + \alpha_{\text{rms}}}{1 + \alpha_{\text{rms}}\|g\|_2^2/\|g\|_1^2}.$$

A short algebraic manipulation shows that this is equivalent to

$$\frac{\|g\|_1^2}{\|g\|_2^2} \geq s_A.$$

In other words, the ℓ_1/ℓ_2 ‘‘nuclear rank’’ of the RMSNorm gradient must exceed the (low) stable rank of the incoming RMS-normalized activation matrix A . This is the exact diagonal analogue of the matrix-level condition $\text{nr}(G_{\ell}) \geq \text{st}(\tilde{A}_{\ell-1}(W))$ from (4.18), with the role of $\text{nr}(G_{\ell})$ played by the scalar $\|g\|_1^2/\|g\|_2^2$ and the role of $\text{st}(A_{\ell-1})$ played by $\text{st}(A)$.

References

- [1] Jinho Baik, Gérard Ben Arous, and Sandrine Péché. Phase transition of the largest eigenvalue for nonnull complex sample covariance matrices. 2005.
- [2] Lucas Benigni and Sandrine Péché. Largest eigenvalues of the conjugate kernel of single-layered neural networks. *arXiv preprint arXiv:2201.04753*, 2022.
- [3] Jeremy Bernstein and Laker Newhouse. Old optimizer, new norm: An anthology. *arXiv preprint arXiv:2409.20325*, 2024.

- [4] Jeremy Bernstein and Laker Newhouse. Modular duality in deep learning. In *Proceedings of the 42nd International Conference on Machine Learning*, volume 267, pages 3920–3930. PMLR, 2025.
- [5] Rajendra Bhatia. *Positive Definite Matrices*. Princeton University Press, Princeton, NJ, 2007. Thm. 1.4.1 (“Norm of the Schur product”) gives $\|S_A\| = \max_i a_{ii}$ when $A \succeq 0$; Sec. 1.2 states the Schur product theorem.
- [6] Åke Björck and Gene H. Golub. Numerical methods for computing angles between linear subspaces. *Mathematics of Computation*, 27(123):579–594, 1973.
- [7] David Carlson, Volkan Cevher, and Lawrence Carin. Stochastic spectral descent for restricted boltzmann machines. In *International Conference on Artificial Intelligence and Statistics*, pages 111–119, 2015.
- [8] David E Carlson, Edo Collins, Ya-Ping Hsieh, Lawrence Carin, and Volkan Cevher. Preconditioned spectral descent for deep learning. *Advances in neural information processing systems*, 28, 2015.
- [9] David E. Carlson, Edward Collins, Cho-Jui Hsieh, Lawrence Carin, and Volkan Cevher. Preconditioned spectral descent for deep learning. In *Advances in Neural Information Processing Systems*, volume 28, 2015.
- [10] Xiuyuan Cheng and Amit Singer. The spectrum of random inner-product kernel matrices. *Random Matrices: Theory and Applications*, 2(04):1350010, 2013.
- [11] Youngmin Cho and Lawrence K. Saul. Kernel methods for deep learning. In *Advances in Neural Information Processing Systems 22 (NIPS 2009)*, 2009.
- [12] Hadi Daneshmand, Jonas Kohler, Francis Bach, Thomas Hofmann, and Aurelien Lucchi. Batch normalization provably avoids ranks collapse for randomly initialised deep networks. *Advances in Neural Information Processing Systems*, 33:18387–18398, 2020.
- [13] Amit Daniely, Roy Frostig, and Yoram Singer. Toward deeper understanding of neural networks: The power of initialization and a dual view on expressivity. In *Advances in Neural Information Processing Systems 29 (NIPS 2016)*, 2016.
- [14] Chandler Davis and William Morton Kahan. The rotation of eigenvectors by a perturbation. iii. *SIAM Journal on Numerical Analysis*, 7(1):1–46, 1970.
- [15] John Duchi, Elad Hazan, and Yoram Singer. Adaptive subgradient methods for online learning and stochastic optimization. *Journal of Machine Learning Research*, 12(61):2121–2159, 2011.
- [16] Behrooz Ghorbani, Shankar Krishnan, and Ying Xiao. An investigation into neural net optimization via hessian eigenvalue density. In *Proceedings of the 36th International Conference on Machine Learning*, volume 97 of *Proceedings of Machine Learning Research*, pages 2232–2241. PMLR, 2019.
- [17] Vineet Gupta, Tomer Koren, and Yoram Singer. Shampoo: Preconditioned stochastic tensor optimization. In *Proceedings of the 35th International Conference on Machine Learning (ICML)*, volume 80 of *Proceedings of Machine Learning Research*, pages 1842–1850, Stockholm, Sweden, 2018. PMLR.

[18] Guy Gur-Ari, Daniel A. Roberts, and Ethan Dyer. Gradient descent happens in a tiny subspace. *arXiv preprint arXiv:1812.04754*, 2018.

[19] Roger A. Horn and Charles R. Johnson. *Matrix Analysis*. Cambridge University Press, Cambridge, 2nd edition, 2013. See Sec. 5.6; in particular eq. (5.6.0.2) for $\|A\|_F^2 = \sum_i \sigma_i(A)^2$ and $\|A\|_{\text{op}} = \sigma_1(A)$.

[20] Daniel Hsu, Sham Kakade, and Tong Zhang. A tail inequality for quadratic forms of subgaussian random vectors. 2012.

[21] Daniel Hsu, Sham M. Kakade, and Tong Zhang. A tail inequality for quadratic forms of subgaussian random vectors. *Electronic Communications in Probability*, 17(52):1–6, 2012.

[22] Minyoung Huh, Hossein Mobahi, Richard Zhang, Brian Cheung, Pulkit Agrawal, and Phillip Isola. The low-rank simplicity bias in deep networks. *Transactions on Machine Learning Research*, 2023.

[23] Sergey Ioffe and Christian Szegedy. Batch normalization: Accelerating deep network training by reducing internal covariate shift. In *International conference on machine learning*, pages 448–456. pmlr, 2015.

[24] Iain M Johnstone. On the distribution of the largest eigenvalue in principal components analysis. *The Annals of statistics*, 29(2):295–327, 2001.

[25] Keller Jordan and collaborators. Modded-nanogpt (july 18 2025 snapshot). <https://github.com/KellerJordan/modded-nanogpt/tree/0d20074260664590e2a1686b9371936944a3ddff>, 2025. Commit 0d20074260664590e2a1686b9371936944a3ddff.

[26] Keller Jordan, Yuchen Jin, Vlado Boža, Jiacheng You, Franz Cesista, Laker Newhouse, and Jeremy Bernstein. Muon: An optimizer for hidden layers in neural networks. <https://kellerjordan.github.io/posts/muon/>, 2024.

[27] Noureddine El Karoui. The spectrum of kernel random matrices. *The Annals of Statistics*, pages 1–50, 2010.

[28] Jordan Keller, Larry Dial, and contributors. modded-nanogpt. <https://github.com/KellerJordan/modded-nanogpt>, 2025. GitHub repository, accessed 31 Oct 2025.

[29] Diederik P. Kingma and Jimmy Ba. Adam: A method for stochastic optimization. In *International Conference on Learning Representations (ICLR)*, 2015.

[30] Vladimir Koltchinskii and Karim Lounici. Concentration inequalities and moment bounds for sample covariance operators. *Bernoulli*, 23(1):110–133, 2017.

[31] Vladimir Koltchinskii and Shahar Mendelson. Bounding the smallest singular value of a random matrix without concentration. *International Mathematics Research Notices*, (23):12991–13008, 2015.

[32] Tim Large, Yang Liu, Minyoung Huh, Hyojin Bahng, Phillip Isola, and Jeremy Bernstein. Scalable optimization in the modular norm. In *Advances in Neural Information Processing Systems*, 2024. arXiv:2405.14813.

[33] Béatrice Laurent and Pascal Massart. Adaptive estimation of a quadratic functional by model selection. *Annals of Statistics*, 28(5):1302–1338, 2000.

[34] Guillaume Lecué and Shahar Mendelson. Performance of empirical risk minimization in linear aggregation. *Bernoulli*, 22(3):1520–1534, 2016.

[35] Guillaume Lecué and Shahar Mendelson. Regularization and the small-ball method ii: Complexity dependent error rates. *Journal of Machine Learning Research*, 18(146):1–48, 2017.

[36] Guillaume Lecué and Shahar Mendelson. Sparse recovery under weak moment assumptions. *Journal of the European Mathematical Society*, 19(3):881–904, 2017.

[37] Guillaume Lecué and Shahar Mendelson. Regularization and the small-ball method i: Sparse recovery. *Annals of Statistics*, 46(2):611–641, 2018.

[38] Michel Ledoux and Michel Talagrand. *Probability in Banach Spaces: isoperimetry and processes*. Springer Science & Business Media, 2013.

[39] James Martens and Roger Grosse. Optimizing neural networks with kronecker-factored approximate curvature. In *Proceedings of the 32nd International Conference on Machine Learning (ICML)*, volume 37 of *Proceedings of Machine Learning Research*, pages 2408–2417, Lille, France, Jul 2015. PMLR.

[40] Shahar Mendelson. Learning without concentration. In *Proceedings of the 27th Conference on Learning Theory*, volume 35 of *Proceedings of Machine Learning Research*, pages 25–39. PMLR, 2014.

[41] Shahar Mendelson. Extending the scope of the small-ball method. *arXiv preprint arXiv:1709.00843*, 2017.

[42] Vardan Papyan. The full spectrum of deepnet Hessians at scale: Dynamics with sgd training and sample size. *arXiv preprint arXiv:1811.07062*, 2018.

[43] Jeffrey Pennington and Pratik Worah. Nonlinear random matrix theory for deep learning. *Advances in neural information processing systems*, 30, 2017.

[44] Thomas Pethick, Weijia Xie, Konstantinos Antonakopoulos, Zhenyu Zhu, Alberto Silveti-Falls, and Volkan Cevher. Training deep learning models with norm-constrained LMOs. *arXiv preprint arXiv:2502.07529*, 2025.

[45] Ali Rahimi and Benjamin Recht. Random features for large-scale kernel machines. In *Advances in Neural Information Processing Systems 20 (NIPS 2007)*, 2007.

[46] Ali Rahimi and Benjamin Recht. Weighted sums of random kitchen sinks: Replacing minimization with randomization in learning. In *Advances in Neural Information Processing Systems 21 (NIPS 2008)*, 2008.

[47] Alessandro Rudi and Lorenzo Rosasco. Generalization properties of learning with random features. In *Advances in Neural Information Processing Systems 30 (NIPS 2017)*, 2017.

[48] Levent Sagun, Léon Bottou, and Yann LeCun. Eigenvalues of the hessian in deep learning: Singularity and beyond. *arXiv preprint arXiv:1611.07476*, 2016.

[49] Wei Shen, Ruichuan Huang, Minhui Huang, Cong Shen, and Jiawei Zhang. On the convergence analysis of muon. *CoRR*, abs/2505.23737, 2025.

[50] Rishi Sonthalia, Michael Murray, and Guido Montúfar. Low rank gradients and where to find them. *arXiv preprint arXiv:2510.01303*, 2025.

[51] Nikhil Srivastava and Roman Vershynin. Covariance estimation for distributions with $2 + \varepsilon$ moments. *Annals of Probability*, 41(5):3081–3111, 2013.

[52] Robert C Thompson. The behavior of eigenvalues and singular values under perturbations of restricted rank. *Linear Algebra and its Applications*, 13(1-2):69–78, 1976.

[53] Tijmen Tieleman and Geoffrey Hinton. Lecture 6.5—rmsprop: Divide the gradient by a running average of its recent magnitude. Coursera: Neural Networks for Machine Learning, 2012. Lecture slides.

[54] Joel A. Tropp. User-friendly tail bounds for sums of random matrices. *Foundations of Computational Mathematics*, 12(4):389–434, 2012.

[55] Roman Vershynin. Introduction to the non-asymptotic analysis of random matrices. *arXiv preprint arXiv:1011.3027*, 2010.

[56] Roman Vershynin. How close is the sample covariance matrix to the actual covariance matrix? *Journal of Theoretical Probability*, 25(3):655–686, 2012.

[57] Roman Vershynin. *High-dimensional probability: An introduction with applications in data science*, volume 47. Cambridge university press, 2018.

[58] Shuche Wang, Fengzhuo Zhang, Jiaxiang Li, Cunxiao Du, Chao Du, Tianyu Pang, Zhuoran Yang, Mingyi Hong, and Vincent YF Tan. Muon outperforms adam in tail-end associative memory learning. *arXiv preprint arXiv:2509.26030*, 2025.

[59] Zhichao Wang, Denny Wu, and Zhou Fan. Nonlinear spiked covariance matrices and signal propagation in deep neural networks. In *The Thirty Seventh Annual Conference on Learning Theory*, pages 4891–4957. PMLR, 2024.

[60] Per-Åke Wedin. Perturbation bounds in connection with singular value decomposition. *BIT Numerical Mathematics*, 12(1):99–111, 1972.

[61] Yi Yu, Tengyao Wang, and Richard J. Samworth. A useful variant of the davis–kahan theorem for statisticians. *Biometrika*, 102(2):315–323, 2015.

[62] Jiawei Zhao, Zhenyu Zhang, Beidi Chen, Zhangyang Wang, Anima Anandkumar, and Yuan-dong Tian. GaLore: Memory-efficient LLM training by gradient low-rank projection. In *International Conference on Learning Representations*, 2024.

A Sparse Regression and SwiGLU activations

We now return to the sparse regression setup of Figure 1 and replace the squared-ReLU activation by SwiGLU. The architecture and target remain unchanged: we train a four-layer feedforward network on the cubic $f(x) = x_1 x_2 x_3$ from Gaussian inputs using full-batch GD and SpecGD, applying spectral updates only to the hidden layers as in Section 1.2.1. Our aim is to examine how the change in activation affects the stable rank of the post-activations and, in turn, the relative behavior of Euclidean and spectral updates.

Figure 17 reports the stable rank of the post-activation matrices at initialization as a function of batch size. In contrast with the ReLU and squared-ReLU experiments, the stable ranks now grow noticeably with the batch size, reflecting the fact that SwiGLU is approximately centered and therefore does not induce a large mean spike in the hidden-layer Gram matrices.

To see how this change in stable rank interacts with training dynamics, Figure 18 compares the training loss of GD and SpecGD for two batch sizes. For the smaller batch ($n = 512$, left panel), the network is still in a mildly low-stable-rank regime and SpecGD enjoys a visible early advantage, much as in the ReLU case. For the larger batch ($n = 8196$, right panel), the initialization stable ranks of the hidden layers are substantially higher, and the performance of GD and SpecGD becomes similar. As the batch size grows, the inequality $\text{nr}(\nabla \mathcal{L}(W_\ell)) \gtrsim \text{st}(A_{\ell-1})$ is no longer strongly activated, and the structural advantage of spectral updates predicted in Section 1.2 is correspondingly reduced.

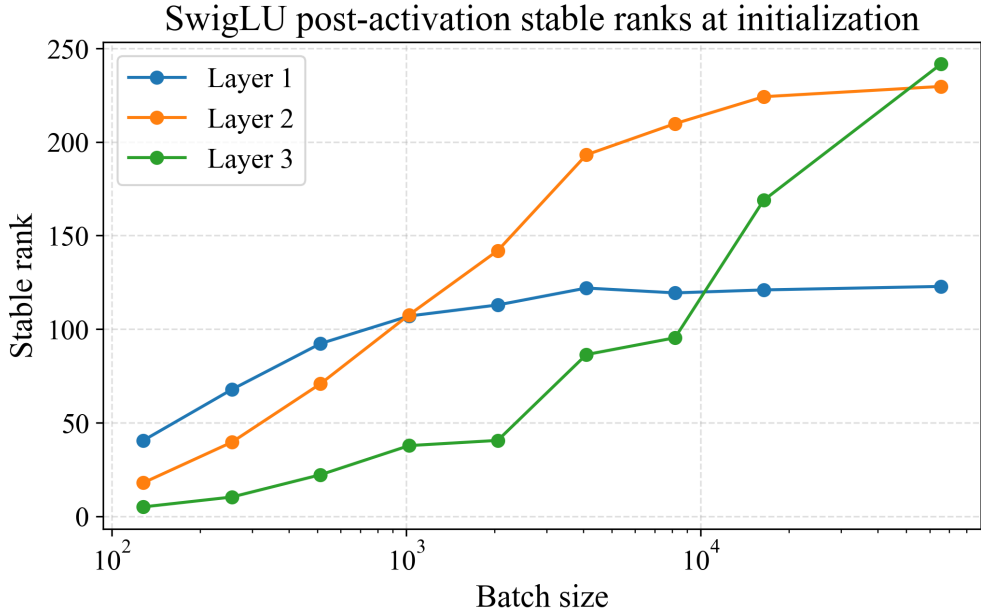


Figure 17: Stable rank at initialization of the post-activation matrices in the sparse regression network with SwiGLU activations, as a function of batch size. For small batches the hidden layers remain only moderately high-stable-rank, but as the batch size increases the stable ranks grow toward their ambient dimension, in contrast with the ReLU and squared-ReLU experiments where the mean-induced spike keeps $\text{st}(A_\ell)$ essentially constant.

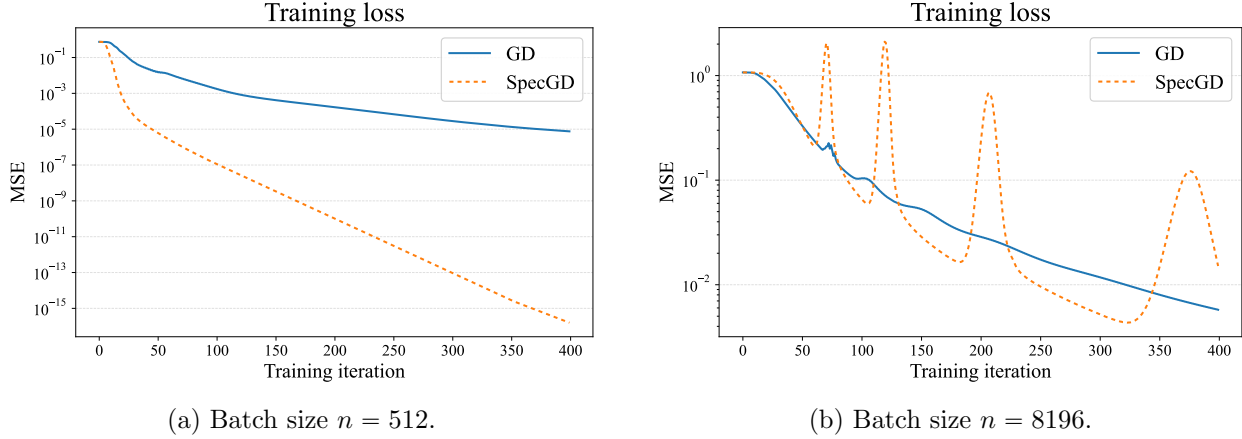


Figure 18: Sparse regression with SwiGLU activations: training loss for gradient descent (GD) and spectral gradient descent (SpecGD) at two batch sizes. For $n = 512$ (left) the methods behave similarly to the ReLU experiment, with SpecGD exhibiting a faster initial decrease in loss. For $n = 8196$ (right), where the initialization stable ranks of the hidden layers are much larger (Figure 17), the trajectories of GD and SpecGD essentially coincide. In both runs, the stable ranks of the first two hidden layers remain close to their initialization values, while the third layer drops rapidly to stable rank ≈ 3 ; this drop occurs in the final scalar-output layer, where the weights form a vector and no spectral update is applied in SpecGD.

B Trace and operator-norm bounds for the sample second moment under sub-Gaussian tails

In this section, we recall basic deviations inequalities between the sample and population second-moment matrices, closely following the text [57]. Throughout, we will use the following notation. Let $z \in \mathbb{R}^d$ be a random vector with mean $\mu := \mathbb{E}z$, let $\tilde{z} := z - \mu$ be its centering, and define the covariance

$$\Sigma := \mathbb{E}[\tilde{z} \tilde{z}^\top] \succeq 0.$$

The (uncentered) second-moment matrix is

$$M := \mathbb{E}[zz^\top] = \Sigma + \mu\mu^\top.$$

Given i.i.d. samples z_1, \dots, z_n of z , define the sample second moment

$$M_n := \frac{1}{n} \sum_{i=1}^n z_i z_i^\top.$$

As usual, we write $\text{er}(M) := \text{tr}(M)/\|M\|_{\text{op}} \in [1, d]$ for the effective rank. Throughout, we impose the sub-Gaussian assumption: there exists a constant $K \geq 1$ such that the estimate holds:

$$\|\langle \tilde{z}, u \rangle\|_{\psi_2} \leq K \langle Mu, u \rangle^{1/2} \quad \forall u \in \mathbb{R}^d \quad (\text{B.1})$$

Here $\|\cdot\|_{\psi_2}$ is the sub-Gaussian norm. The sub-exponential norm will be denoted by $\|\cdot\|_{\psi_1}$. Notice that the right-side of (B.1) is governed by the second-moment matrix M and not by the covariance Σ , and is therefore a looser condition. Condition (B.1) can be equivalently restated as requiring $\|\langle M^{-1/2} \tilde{z}, u \rangle\|_{\psi_2} \leq K \|u\|$ for all vectors $u \in \mathbb{R}^d$.

The following two theorems bound the deviations, $\text{tr}(M_n) - \text{tr}(M)$ and $\|M_n - M\|_{\text{op}}$, respectively. Similar bounds for covariance matrices have appeared for example in [21, 30, 33, 51, 54, 56]. The only difference with existing literature is that the bounds below apply for the second moment matrix.

Theorem B.1 (Trace bound). *Under (B.1), there exist constants $c, C < \infty$ such that for every $u \geq 1$, with probability at least $1 - 4e^{-cu}$, it holds:*

$$|\text{tr}(M_n) - \text{tr}(M)| \leq CK^2 \text{tr}(M) \left(\sqrt{\frac{u}{n}} + \frac{u}{n} \right). \quad (\text{B.2})$$

Proof. Write $z_i = \mu + \tilde{z}_i$ with \tilde{z}_i i.i.d., mean zero, satisfying (B.1). Then we can write:

$$\text{tr}(M_n) - \text{tr}(M) = \frac{1}{n} \sum_{i=1}^n (\|z_i\|^2 - \mathbb{E}\|z\|^2) = \underbrace{\frac{2}{n} \sum_{i=1}^n \langle \tilde{z}_i, \mu \rangle}_{=:A_n} + \underbrace{\frac{1}{n} \sum_{i=1}^n (\|\tilde{z}_i\|^2 - \text{tr}(\Sigma))}_{=:B_n}.$$

We bound A_n and B_n in order. First, by (B.1), $\langle \tilde{z}_i, \mu \rangle$ is sub-Gaussian with $\|\langle \tilde{z}_i, \mu \rangle\|_{\psi_2} \leq K\sqrt{\mu^\top \Sigma \mu}$. Therefore Hoeffding inequality [57, Theorem 2.2.1], implies that for all $t > 0$, the estimate

$$A_n \leq C_1 K \sqrt{\frac{t}{n}} \sqrt{\langle M\mu, \mu \rangle},$$

holds with probability at least $1 - 2e^{-t}$. Note moreover the bound $\langle M\mu, \mu \rangle \leq \|M\|_{\text{op}}\|\mu\|_2^2 \leq \|M\|_{\text{op}}^2$.

Next applying (B.1) with $u = e_j$ we deduce that the j 'th coordinate of \tilde{z} is $KM_{jj}^{1/2}$ sub-Gaussian, and therefore its square is $K^2 M_{jj}$ sub-exponential [57, Lemma 2.8.5]. Therefore by the triangle inequality, $\|\tilde{z}\|_2^2$ is sub-exponential with parameter $K^2 \text{tr}(M)$. Applying Bernstein's inequality [57, Theorem 2.9.1], we deduce $\|B_n\|_{\text{op}} \leq CK^2 \text{tr}(M)(\sqrt{\frac{u}{n}} + \frac{u}{n})$ with probability at least $1 - 2e^{-cu}$. Combining the two bounds on A_n and B_n completes the proof. \square

Theorem B.2 (Operator-norm bound). *There exist a constant $C < \infty$ such that for all $u \geq 1$, the estimate*

$$\|M_n - M\|_{\text{op}} \leq CK^4 \left(\sqrt{\frac{\text{er}(M) + u}{n}} + \frac{\text{er}(M) + u}{n} \right) \|M\|_{\text{op}},$$

holds with probability at least $1 - 4e^{-u}$.

Proof. Setting $\bar{z}_n = \frac{1}{n} \sum_{i=1}^n \tilde{z}_i$, we may write

$$M_n - \Sigma = \underbrace{\bar{z}_n \mu^\top + \mu \bar{z}_n^\top}_{=:A_n} + \underbrace{\Sigma_n - \Sigma}_{=:B_n}.$$

Note that \bar{z}_n satisfies

$$\|\langle \bar{z}_n, u \rangle\|_{\psi_2}^2 = \frac{\|\langle \tilde{z}, u \rangle\|_{\psi_2}^2}{n} \leq \frac{K^2}{n} \langle M\mu, u \rangle.$$

Therefore the vector $M^{-1/2}\bar{z}_n$ is sub-Gaussian with parameter K/\sqrt{n} . An application of the one-sided Hanson-Wright inequality [57, Exercise 6.10] therefore implies

$$\|\bar{z}_n\|_2 \leq \frac{CK}{\sqrt{n}} \left(\sqrt{\text{tr}(M)} + t \sqrt{\|M\|_{\text{op}}} \right),$$

with probability at least $1 - e^{-t^2}$. Taking into account $\|\mu\|_2^2 \leq \|M\|_{\text{op}}$, we deduce the bound

$$\|A_n\|_{\text{op}} \leq CK\|M\|_{\text{op}}\sqrt{\frac{\text{er}(M) + t}{n}}.$$

The same proof as [57, Theorem 9.2.2 and Remark 9.2.3] but using the anisotropic matrix deviation inequality [57, Exercise 9.4] yields the estimate

$$\|B_n\|_{\text{op}} \leq CK^4 \left(\sqrt{\frac{\text{tr}(M)\|M\|_{\text{op}} + u\|M\|_{\text{op}}^2}{n}} + \frac{\text{tr}(M) + u\|M\|_{\text{op}}}{n} \right),$$

with probability at least $1 - 2e^{-u}$. Combining the estimates on A_n and B_n completes the proof. \square

C Proofs from Section 2.2

C.1 Proof of Lemma 2.11

We prove the result for $\sigma = 1$; the general case follows by scaling. We also assume $\|x\| \neq 0$, otherwise the result is trivial. Let $g \sim \mathcal{N}(0, I_d)$ and set

$$A := \|x\|_2^2, \quad B := \|g\|_2^2, \quad C := 2\langle x, g \rangle.$$

Then

$$\|x + g\|_2^2 = A + B + C.$$

The desired pair of inequalities

$$(1 - \varepsilon)(A + B) \leq A + B + C \leq (1 + \varepsilon)(A + B)$$

is equivalent to

$$|C| \leq \varepsilon(A + B).$$

Define the event

$$F := \left\{ |B - d| \leq \frac{\varepsilon}{4}d \right\}.$$

The standard Chernoff's method yields

$$\mathbb{P}(F^c) = \mathbb{P}\left(|B - d| > \frac{\varepsilon}{4}d\right) \leq 2\exp\left(-\frac{\varepsilon^2 d}{64}\right). \quad (\text{C.1})$$

Next, observe that $C = 2\langle x, g \rangle$ is Gaussian with mean zero and variance

$$\text{Var}(C) = 4\|x\|_2^2 = 4A.$$

Hence, for any $t > 0$, we have

$$\mathbb{P}(|C| > t) \leq 2\exp\left(-\frac{t^2}{8A}\right). \quad (\text{C.2})$$

We distinguish two cases.

Case 1: $A \geq d$. We may estimate

$$\mathbb{P}(|C| > \varepsilon(A + B)) \leq \mathbb{P}(|C| > \varepsilon A) \leq 2\exp\left(-\frac{\varepsilon^2 A}{8}\right) \leq 2\exp\left(-\frac{\varepsilon^2 d}{8}\right),$$

thereby completing the proof in this case.

Case 2: $A < d$. On event F we have $B \geq (1 - \varepsilon/4)d$ and hence $\varepsilon(A + B) \geq \varepsilon\left(1 - \frac{\varepsilon}{4}\right)d := t$. Consequently, within the event $F \cap \{|C| \leq t\}$ the conclusion $|C| \leq \varepsilon(A + B)$ holds. Taking a union bound, this event occurs with probability $1 - 2\exp\left(-\frac{t^2}{8A}\right) - 2\exp\left(-\frac{\varepsilon^2 d}{64}\right)$. Since $A < d$, we have

$$\frac{t^2}{8A} \geq \frac{\varepsilon^2(1 - \varepsilon/4)^2 d^2}{8d} = \frac{\varepsilon^2(1 - \varepsilon/4)^2 d}{8} \geq \frac{\varepsilon^2 d}{16},$$

and the result follows immediately.

D Proof of Lemma 2.10

Let C be the diagonal matrix with entries $c_t := \sqrt{d}/\|x_t\|_2$, so that $A^{\text{rms}} = XC$. The bounds on column norms imply

$$\sqrt{\frac{d}{U}} \leq c_t \leq \sqrt{\frac{d}{L}} \quad \text{for all } t,$$

and hence

$$s_{\min} := \sqrt{\frac{d}{U}} \leq \sigma_{\min}(C) \leq \sigma_{\max}(C) \leq \sqrt{\frac{d}{L}} =: s_{\max},$$

where σ_{\min} and σ_{\max} denote the smallest and largest singular values. Since C is invertible, we have

$$s_{\min} \|X\|_{\text{op}} \leq \|A^{\text{rms}}\|_{\text{op}} \leq s_{\max} \|X\|_{\text{op}}.$$

On the other hand,

$$\|A^{\text{rms}}\|_F^2 = \sum_{t=1}^n \|a_t\|_2^2 = nd.$$

Combining these facts yields

$$\text{st}(A^{\text{rms}}) = \frac{\|A^{\text{rms}}\|_F^2}{\|A^{\text{rms}}\|_{\text{op}}^2} \leq \frac{nd}{s_{\min}^2 \|X\|_{\text{op}}^2} = \frac{U}{d} \frac{nd}{\|X\|_{\text{op}}^2} = \frac{U}{L} \frac{\|X\|_F^2}{\|X\|_{\text{op}}^2} = \frac{U}{L} \text{st}(X),$$

since $\|X\|_F^2 \geq nL$.

D.1 Proof of Lemma 2.12

Write $A = [a_1, \dots, a_n]$ and let w_i^\top be the i -th row of W . Fix a column $a \in \mathbf{R}^d$ with $\|a\|_2^2 = d$. Then

$$z_i := \langle w_i, a \rangle \sim \mathcal{N}(0, 1), \quad i = 1, \dots, k,$$

independently, and

$$\|\sigma(Wa)\|_2^2 = \sum_{i=1}^k \sigma(z_i)^2.$$

Define indicators

$$I_i := \mathbf{1}\{|\sigma(z_i)| \geq \tau_\sigma\}, \quad S_k := \sum_{i=1}^k I_i.$$

By the small-ball assumption, $\mathbb{E}[I_i] \geq p_\sigma$, so S_k is a sum of i.i.d. Bernoulli variables with mean at least p_σ . A standard Chernoff bound yields constants $c_2 > 0$ (depending only on p_σ) such that, for all $\varepsilon \in (0, 1)$, we have

$$\mathbb{P}(S_k \leq (1 - \varepsilon)p_\sigma k) \leq \exp(-c_2 \varepsilon^2 k).$$

On the complementary event we have $S_k \geq (1 - \varepsilon)p_\sigma k$, and each index with $I_i = 1$ contributes at least τ_σ^2 to the sum of squares, so

$$\|\sigma(Wa)\|_2^2 = \sum_{i=1}^k \sigma(z_i)^2 \geq \tau_\sigma^2 S_k \geq (1 - \varepsilon) \tau_\sigma^2 p_\sigma k.$$

Applying this bound to each column a_t and taking a union bound over $t = 1, \dots, n$ gives

$$\mathbb{P}\left(\forall t, \|\sigma(Wa_t)\|_2^2 \geq (1 - \varepsilon) \tau_\sigma^2 p_\sigma k\right) \geq 1 - 2n \exp(-c_2 \varepsilon^2 k).$$

On this event, we have

$$\|\sigma(WA)\|_F^2 = \sum_{t=1}^n \|\sigma(Wa_t)\|_2^2 \geq (1 - \varepsilon) \tau_\sigma^2 p_\sigma k n.$$

Since each column of A has squared norm d , we have $\|A\|_F^2 = nd$, and therefore

$$\|\sigma(WA)\|_F^2 \geq (1 - \varepsilon) \tau_\sigma^2 p_\sigma \frac{k}{d} \|A\|_F^2.$$

This is (2.16) with $c_1 = \frac{1}{2} \tau_\sigma^2 p_\sigma$ (after possibly absorbing the extra factor $\frac{1}{2}$ into ε), and taking square roots yields the stated Frobenius lower bound.

D.2 Proof of Lemma 2.13

Write the columns of X and H as

$$X = [x_1, \dots, x_n] \in \mathbf{R}^{d \times n}, \quad H = [h_1, \dots, h_n] \in \mathbf{R}^{k \times n},$$

and set

$$G := WH = [g_1, \dots, g_n] \in \mathbf{R}^{d \times n}, \quad g_j := Wh_j.$$

We bound the Frobenius and operator norms of $X + G$ separately.

Columnwise Gaussian perturbation (Frobenius upper bound). Fix $\delta \in (0, 1)$ and set

$$\varepsilon := \frac{\delta}{8}.$$

For each $j \in \{1, \dots, n\}$, the vector g_j is clearly Gaussian $g_j \sim \mathcal{N}(0, \sigma_j^2 I_d)$ with $\sigma_j^2 := \frac{\|h_j\|_2^2}{k}$.

By Lemma 2.11, applied to the pair (x_j, g_j) with parameter ε , we obtain for each fixed j :

$$(1 - \varepsilon)(\|x_j\|_2^2 + \|g_j\|_2^2) \leq \|x_j + g_j\|_2^2 \leq (1 + \varepsilon)(\|x_j\|_2^2 + \|g_j\|_2^2)$$

with probability at least $1 - 4 \exp(-c_0 \varepsilon^2 d)$ for some absolute constant $c_0 > 0$.

A union bound over $j = 1, \dots, n$ yields an event \mathcal{E}_1 with

$$\mathbb{P}(\mathcal{E}_1) \geq 1 - 4n \exp(-c_0 \varepsilon^2 d),$$

on which

$$(1 - \varepsilon)(\|x_j\|_2^2 + \|g_j\|_2^2) \leq \|x_j + g_j\|_2^2 \leq (1 + \varepsilon)(\|x_j\|_2^2 + \|g_j\|_2^2) \quad \forall j. \quad (\text{D.1})$$

Summing (D.1) over j and using only the upper bound, we obtain on \mathcal{E}_1 :

$$\|X + G\|_F^2 = \sum_{j=1}^n \|x_j + g_j\|_2^2 \leq (1 + \varepsilon) \sum_{j=1}^n (\|x_j\|_2^2 + \|g_j\|_2^2) = (1 + \varepsilon)(\|X\|_F^2 + \|G\|_F^2). \quad (\text{D.2})$$

Frobenius norm of $G = WH$. Fix j and assume $h_j \neq 0$ (the case $h_j = 0$ is trivial). By the standard χ^2 concentration inequality (see, e.g., [57, Theorem 3.1.1]), there exists $c_1 > 0$ such that for any $\eta \in (0, 1)$, we have

$$\mathbb{P}\left(\|g_j\|_2^2 \leq (1 + \eta) \frac{d}{k} \|h_j\|_2^2\right) \geq 1 - 2 \exp(-c_1 \eta^2 d).$$

Setting $\eta := \frac{\delta}{8}$ and using a union bound over $j = 1, \dots, n$ yields an event \mathcal{E}_2 with

$$\mathbb{P}(\mathcal{E}_2) \geq 1 - 2n \exp(-c_1 \eta^2 d),$$

on which

$$\|g_j\|_2^2 \leq (1 + \eta) \frac{d}{k} \|h_j\|_2^2 \quad \forall j.$$

Summing over j gives, on \mathcal{E}_2 ,

$$\|G\|_F^2 = \sum_{j=1}^n \|g_j\|_2^2 \leq (1 + \eta) \frac{d}{k} \sum_{j=1}^n \|h_j\|_2^2 = (1 + \eta) \frac{d}{k} \|H\|_F^2. \quad (\text{D.3})$$

Combining (D.2) and (D.3), we obtain on $\mathcal{E}_1 \cap \mathcal{E}_2$:

$$\|X + G\|_F^2 \leq (1 + \varepsilon) \left(\|X\|_F^2 + (1 + \eta) \frac{d}{k} \|H\|_F^2 \right). \quad (\text{D.4})$$

Operator norm lower bounds in the X - and H -directions. We now lower bound $\|X + G\|_{\text{op}}$ in terms of both $\|X\|_{\text{op}}$ and $\frac{d}{k} \|H\|_{\text{op}}$.

(3a) *Lower bound in terms of $\|X\|_{\text{op}}$.* Let $v_X \in \mathbf{R}^n$ be a unit right singular vector of X :

$$\|v_X\|_2 = 1, \quad \|Xv_X\|_2 = \|X\|_{\text{op}}.$$

Define

$$x := Xv_X, \quad h := Hv_X, \quad g := Wh.$$

Then $(X + G)v_X = x + g$. By Lemma 2.11 applied to (x, g) with parameter ε , there is an event \mathcal{E}_{3X} with

$$\mathbb{P}(\mathcal{E}_{3X}) \geq 1 - 4 \exp(-c_0 \varepsilon^2 d)$$

such that

$$\|x + g\|_2^2 \geq (1 - \varepsilon)(\|x\|_2^2 + \|g\|_2^2) \geq (1 - \varepsilon)\|x\|_2^2 = (1 - \varepsilon)\|X\|_{\text{op}}^2.$$

Hence, on \mathcal{E}_{3X} ,

$$\|X + G\|_{\text{op}}^2 \geq \|(X + G)v_X\|_2^2 = \|x + g\|_2^2 \geq (1 - \varepsilon)\|X\|_{\text{op}}^2. \quad (\text{D.5})$$

(3b) *Lower bound in terms of $\|H\|_{\text{op}}$.* Let $v_H \in \mathbf{R}^n$ be a unit right singular vector of H :

$$\|v_H\|_2 = 1, \quad \|Hv_H\|_2 = \|H\|_{\text{op}}.$$

Set

$$x' := Xv_H, \quad h' := Hv_H, \quad g' := Wh'.$$

Then g' is Gaussian with

$$g' = Wh' \sim \mathcal{N}\left(0, \frac{\|h'\|_2^2}{k} I_d\right) = \mathcal{N}\left(0, \frac{\|H\|_{\text{op}}^2}{k} I_d\right).$$

The lower-tail χ^2 concentration inequality shows that there exists $c_2 > 0$ such that for all $\eta \in (0, 1)$, we have

$$\mathbb{P}\left(\|g'\|_2^2 \geq (1 - \eta) \frac{d}{k} \|H\|_{\text{op}}^2\right) \geq 1 - 2 \exp(-c_2 \eta^2 d).$$

With our choice $\eta = \delta/8$, this yields an event \mathcal{E}_{2H} with

$$\mathbb{P}(\mathcal{E}_{2H}) \geq 1 - 2 \exp(-c_2 \eta^2 d), \quad \|g'\|_2^2 \geq (1 - \eta) \frac{d}{k} \|H\|_{\text{op}}^2 \quad \text{on } \mathcal{E}_{2H}. \quad (\text{D.6})$$

Now apply Lemma 2.11 again to the pair (x', g') with parameter ε . This gives an event \mathcal{E}_{3H} with

$$\mathbb{P}(\mathcal{E}_{3H}) \geq 1 - 4 \exp(-c_0 \varepsilon^2 d)$$

such that

$$\|x' + g'\|_2^2 \geq (1 - \varepsilon)(\|x'\|_2^2 + \|g'\|_2^2) \geq (1 - \varepsilon)\|g'\|_2^2.$$

Combining with (D.6), on $\mathcal{E}_{2H} \cap \mathcal{E}_{3H}$ we obtain

$$\|x' + g'\|_2^2 \geq (1 - \varepsilon)(1 - \eta) \frac{d}{k} \|H\|_{\text{op}}^2.$$

Since $(X + G)v_H = x' + g'$, it follows that on $\mathcal{E}_{2H} \cap \mathcal{E}_{3H}$,

$$\|X + G\|_{\text{op}}^2 \geq \| (X + G)v_H \|_2^2 = \|x' + g'\|_2^2 \geq (1 - \varepsilon)(1 - \eta) \frac{d}{k} \|H\|_{\text{op}}^2. \quad (\text{D.7})$$

Define

$$\mathcal{E}_3 := \mathcal{E}_{3X} \cap \mathcal{E}_{2H} \cap \mathcal{E}_{3H}.$$

Combining (D.5) and (D.7), we conclude that on \mathcal{E}_3 ,

$$\|X + G\|_{\text{op}}^2 \geq \max \left\{ (1 - \varepsilon)\|X\|_{\text{op}}^2, (1 - \varepsilon)(1 - \eta) \frac{d}{k} \|H\|_{\text{op}}^2 \right\}. \quad (\text{D.8})$$

Combining Frobenius and operator bounds. Set

$$\mathcal{E} := \mathcal{E}_1 \cap \mathcal{E}_2 \cap \mathcal{E}_3.$$

On \mathcal{E} we have (D.4) and (D.8), so

$$\text{st}(X + G) = \frac{\|X + G\|_F^2}{\|X + G\|_{\text{op}}^2} \leq \frac{(1 + \varepsilon) \left(\|X\|_F^2 + (1 + \eta) \frac{d}{k} \|H\|_F^2 \right)}{\max \left\{ (1 - \varepsilon)\|X\|_{\text{op}}^2, (1 - \varepsilon)(1 - \eta) \frac{d}{k} \|H\|_{\text{op}}^2 \right\}}.$$

Recall that $\varepsilon = \eta = \delta/8$. For $\delta \in (0, 1)$ we have

$$1 + \varepsilon \leq 1 + \delta, \quad 1 + \eta \leq 1 + \delta, \quad (1 - \varepsilon)(1 - \eta) \geq 1 - \delta.$$

Thus, on \mathcal{E} , we have

$$\text{st}(X + G) \leq \frac{1 + \delta}{1 - \delta} \cdot \frac{\|X\|_F^2 + \frac{d}{k} \|H\|_F^2}{\max \left\{ \|X\|_{\text{op}}^2, \frac{d}{k} \|H\|_{\text{op}}^2 \right\}},$$

which is exactly (2.17).

Probability of the good event. Finally we bound $\mathbb{P}(\mathcal{E})$. By construction,

$$\mathcal{E}^c \subseteq \mathcal{E}_1^c \cup \mathcal{E}_2^c \cup \mathcal{E}_{3X}^c \cup \mathcal{E}_{2H}^c \cup \mathcal{E}_{3H}^c,$$

so

$$\begin{aligned} \mathbb{P}(\mathcal{E}^c) &\leq \mathbb{P}(\mathcal{E}_1^c) + \mathbb{P}(\mathcal{E}_2^c) + \mathbb{P}(\mathcal{E}_{3X}^c) + \mathbb{P}(\mathcal{E}_{2H}^c) + \mathbb{P}(\mathcal{E}_{3H}^c) \\ &\leq 4n \exp(-c_0 \varepsilon^2 d) + 2n \exp(-c_1 \eta^2 d) + 4 \exp(-c_0 \varepsilon^2 d) + 2 \exp(-c_2 \eta^2 d) + 4 \exp(-c_0 \varepsilon^2 d). \end{aligned}$$

Using $\varepsilon^2 = \eta^2 = \delta^2/64$ and absorbing constants, there exist absolute constants $C', c' > 0$ such that

$$\mathbb{P}(\mathcal{E}^c) \leq C'(n+2) \exp(-c' \delta^2 d).$$

If $d \geq C\delta^{-2} \log(n+2)$ for a sufficiently large absolute C , then

$$C'(n+2) \exp(-c' \delta^2 d) \leq C \exp(-c \delta^2 d)$$

for suitable absolute constants $C, c > 0$, and hence

$$\mathbb{P}(\mathcal{E}) \geq 1 - C \exp(-c \delta^2 d).$$

Together with (2.17) on \mathcal{E} , this completes the proof.

E Proof of Proposition 2.14

Throughout, $c, C > 0$ denote absolute constants that may change from line to line and depend only on c_{\pm}, δ , and the law of $\sigma(G)$ for $G \sim \mathcal{N}(0, 1)$, but never on d or n .

RMS normalization of the input. By Assumption C, each column of X satisfies $c_- d \leq \|x_t\|_2^2 \leq c_+ d$, so Lemma 2.10 with $L = c_- d, U = c_+ d$ yields

$$\text{st}(A^{\text{rms}}) \leq \frac{U}{L} \text{st}(X) = \frac{c_+}{c_-} \text{st}(X), \tag{E.1}$$

which is the first bound in (ii). Recall also that every column of A^{rms} has norm \sqrt{d} , so

$$\|A^{\text{rms}}\|_F^2 = nd. \tag{E.2}$$

Bounding $H = W_V A^{\text{rms}} P$ and X^{att} . Let us write $Y := A^{\text{rms}} P$ and denote its columns by y_t . Since each column p_t of P is a probability vector, Jensen's inequality gives

$$\|y_t\|_2^2 = \left\| \sum_i p_t(i) a_i \right\|_2^2 \leq \sum_i p_t(i) \|a_i\|_2^2 \leq d, \quad \forall t.$$

Therefore we obtain

$$\|Y\|_F^2 = \sum_t \|y_t\|_2^2 \leq nd = \|A^{\text{rms}}\|_F^2. \quad (\text{E.3})$$

Let W_V have i.i.d. entries $\mathcal{N}(0, 1/d)$ and define $H := W_V Y$, with columns h_t . Conditional on Y we have

$$h_t | Y \sim \mathcal{N}\left(0, \frac{\|y_t\|_2^2}{d} I_d\right).$$

Fix $\varepsilon := \delta/16$. By the χ^2 concentration inequality and a union bound over t , we obtain an event \mathcal{E}_V with $\mathbb{P}(\mathcal{E}_V) \geq 1 - e^{-c\delta^2 d}$ on which

$$\|h_t\|_2^2 \leq (1 + \varepsilon)\|y_t\|_2^2 \leq (1 + \varepsilon)d, \quad \forall t, \quad \|H\|_F^2 \leq (1 + \varepsilon)\|Y\|_F^2 \leq (1 + \varepsilon)nd. \quad (\text{E.4})$$

Now set $R := W_O H$, where recall W_V has i.i.d. entries $\mathcal{N}(0, 1/d)$, and denote its columns by r_t . Conditional on H , each r_t is Gaussian:

$$r_t | H \sim \mathcal{N}\left(0, \frac{\|h_t\|_2^2}{d} I_d\right).$$

Applying the same χ^2 argument and union bound (possibly shrinking c and enlarging C) yields an event $\mathcal{E}_O^{(1)}$ with

$$\mathbb{P}(\mathcal{E}_O^{(1)}) \geq 1 - Ce^{-c\delta^2 d}$$

such that

$$\|r_t\|_2^2 \leq (1 + \varepsilon)\|h_t\|_2^2 \leq (1 + \varepsilon)^2 d \leq (1 + \delta)d, \quad \forall t, \quad (\text{E.5})$$

where we used $(1 + \varepsilon)^2 \leq 1 + \delta$ for $\varepsilon = \delta/16$ and $\delta \leq \frac{1}{4}$.

We now set

$$X^{\text{att}} := X + R, \quad x_t^{\text{att}} := x_t + r_t.$$

Applying Lemma 2.11 with parameter ε to each pair (x_t, r_t) and taking a union bound gives an event $\mathcal{E}_O^{(2)}$ with

$$\mathbb{P}(\mathcal{E}_O^{(2)}) \geq 1 - e^{-c\delta^2 d}$$

such that

$$(1 - \varepsilon)(\|x_t\|_2^2 + \|r_t\|_2^2) \leq \|x_t^{\text{att}}\|_2^2 \leq (1 + \varepsilon)(\|x_t\|_2^2 + \|r_t\|_2^2), \quad \forall t. \quad (\text{E.6})$$

Combining Assumption C, (E.5), and (E.6), and using $\varepsilon \leq \delta$, we obtain on $\mathcal{E}_V \cap \mathcal{E}_O^{(1)} \cap \mathcal{E}_O^{(2)}$:

$$\|x_t^{\text{att}}\|_2^2 \geq (1 - \varepsilon)\|x_t\|_2^2 \geq (1 - \delta)c_- d,$$

and

$$\|x_t^{\text{att}}\|_2^2 \leq (1 + \varepsilon)(c_+ d + (1 + \delta)d) \leq (1 + \delta)(c_+ + 1)d.$$

Thus the column norms of X^{att} satisfy

$$c_-^{\text{att}} d \leq \|x_t^{\text{att}}\|_2^2 \leq c_+^{\text{att}} d, \quad t = 1, \dots, n, \quad (\text{E.7})$$

with

$$c_-^{\text{att}} := (1 - \delta)c_-, \quad c_+^{\text{att}} := (1 + \delta)(c_+ + 1).$$

Summing (E.6) over t and using (E.5) and $\|X\|_F^2 \geq nc_- d$ gives

$$\|X^{\text{att}}\|_F^2 \leq (1 + \varepsilon)(\|X\|_F^2 + \|R\|_F^2) \leq (1 + \delta)(\|X\|_F^2 + n(1 + \delta)d) \leq (1 + 2/c_-)(1 + \delta)\|X\|_F^2.$$

Therefore on $\mathcal{E}_V \cap \mathcal{E}_O^{(1)} \cap \mathcal{E}_O^{(2)}$ we have

$$\|X^{\text{att}}\|_F^2 \leq (1 + \delta) \left(1 + \frac{2}{c_-}\right) \|X\|_F^2. \quad (\text{E.8})$$

Finally, Lemma 2.13 applied with X and H (and $W = W_O$) and the same δ shows that, on another event $\mathcal{E}_O^{(3)}$ with $\mathbb{P}(\mathcal{E}_O^{(3)}) \geq 1 - e^{-c\delta^2 d}$,

$$\text{st}(X^{\text{att}}) \leq \frac{1 + \delta}{1 - \delta} \cdot \frac{\|X\|_F^2 + \|H\|_F^2}{\|X\|_{\text{op}}^2} = \frac{1 + \delta}{1 - \delta} \left(1 + \frac{\|H\|_F^2}{\|X\|_F^2}\right) \text{st}(X).$$

Using (E.4) and $\|X\|_F^2 \geq nc_- d$, we deduce

$$\frac{\|H\|_F^2}{\|X\|_F^2} \leq \frac{1 + \varepsilon}{c_-} \leq \frac{2}{c_-},$$

so on $\mathcal{E}_V \cap \mathcal{E}_O^{(3)}$, we have

$$\text{st}(X^{\text{att}}) \leq \frac{1 + \delta}{1 - \delta} \left(1 + \frac{2}{c_-}\right) \text{st}(X), \quad (\text{E.9})$$

which is the second inequality in (ii).

RMS normalization after attention. By Lemma 2.10 applied to X^{att} , using the column bounds (E.7), we have

$$\text{st}(A_{\text{mlp}}^{\text{rms}}) \leq \frac{c_+^{\text{att}}}{c_-^{\text{att}}} \text{st}(X^{\text{att}}).$$

Combining with (E.9) yields

$$\text{st}(A_{\text{mlp}}^{\text{rms}}) \leq \frac{c_+^{\text{att}}}{c_-^{\text{att}}} \frac{1 + \delta}{1 - \delta} \left(1 + \frac{2}{c_-}\right) \text{st}(X). \quad (\text{E.10})$$

Since

$$\frac{c_+^{\text{att}}}{c_-^{\text{att}}} = \frac{(1 + \delta)(c_+ + 1)}{(1 - \delta)c_-},$$

we obtain

$$\text{st}(A_{\text{mlp}}^{\text{rms}}) \leq \frac{(1 + \delta)^2}{(1 - \delta)^2} \frac{c_+ + 1}{c_-} \left(1 + \frac{2}{c_-}\right) \text{st}(X),$$

which is the third inequality in (ii).

The MLP block: $B = \sigma(W_1 A_{\text{mlp}}^{\text{rms}})$. Condition on $A_{\text{mlp}}^{\text{rms}}$ and let W_1 have i.i.d. entries $\mathcal{N}(0, 1/d)$. Theorem 2.7 together implies that with $K_B = 2\pi$, we have with probability $1 - e^{-c\delta^2 d}$ that

$$\text{st}(B) \leq K_B. \quad (\text{E.11})$$

This gives the fourth inequality in (ii).

For the Frobenius norm, Lemma 2.12 applied with $W = W_1$, $A = A_{\text{mlp}}^{\text{rms}}$ and $\sigma = \sigma$ yields constants $c_\sigma = (1/2)(1 - \Phi(1))$ and $c > 0$ such that, for $\varepsilon' := \delta/16$ and all large d ,

$$\mathbb{P}\left(\|B\|_F^2 \geq (1 - \varepsilon')c_\sigma \frac{k}{d} \|A_{\text{mlp}}^{\text{rms}}\|_F^2 \mid A_{\text{mlp}}^{\text{rms}}\right) \geq 1 - e^{-c\delta^2 d}.$$

Using $\|A_{\text{mlp}}^{\text{rms}}\|_F^2 = nd$ and the upper bound $\|X^{\text{att}}\|_F^2 \leq c_+^{\text{att}}nd$ from (E.7), we have on another event $\mathcal{E}_B^{(1)}$ of probability at least $1 - e^{-c\delta^2d}$:

$$\|B\|_F^2 \geq (1 - \varepsilon')c_\sigma \frac{k}{d} \|A_{\text{mlp}}^{\text{rms}}\|_F^2 \geq \frac{(1 - \varepsilon')c_\sigma}{c_+^{\text{att}}} \frac{k}{d} d \|X^{\text{att}}\|_F^2. \quad (\text{E.12})$$

Since $\text{st}(B) \leq K_B$, we have $\|B\|_{\text{op}}^2 \geq \|B\|_F^2/K_B$, and thus

$$\frac{k}{d} \frac{\|X^{\text{att}}\|_F^2}{\|B\|_{\text{op}}^2} \leq \frac{k}{d} \frac{\|X^{\text{att}}\|_F^2 K_B}{\|B\|_F^2} \leq \frac{c_+^{\text{att}} K_B}{(1 - \varepsilon')c_\sigma} \leq \frac{2c_+^{\text{att}} K_B}{c_\sigma}, \quad (\text{E.13})$$

where we used $\varepsilon' = \delta/16 \leq \frac{1}{4}$.

Stable rank and column norms of $X^+ = X^{\text{att}} + W_2 B$.

Stable rank. Condition on X^{att} and B , and let W_2 have i.i.d. entries $\mathcal{N}(0, 1/k)$. Lemma 2.13 with $X \leftarrow X^{\text{att}}$ and $H \leftarrow B$ (and the same δ) yields an event $\mathcal{E}_2^{\text{sr}}$ with $\mathbb{P}(\mathcal{E}_2^{\text{sr}}) \geq 1 - e^{-c\delta^2d}$ such that

$$\text{st}(X^+) \leq \frac{1 + \delta}{1 - \delta} \cdot \frac{\|X^{\text{att}}\|_F^2 + \frac{d}{k} \|B\|_F^2}{\max \left\{ \|X^{\text{att}}\|_{\text{op}}^2, \frac{d}{k} \|B\|_{\text{op}}^2 \right\}}.$$

Using $\max\{a, b\} \geq b$ and rearranging, we get

$$\text{st}(X^+) \leq \frac{1 + \delta}{1 - \delta} \left(\frac{k}{d} \frac{\|X^{\text{att}}\|_F^2}{\|B\|_{\text{op}}^2} + \frac{\|B\|_F^2}{\|B\|_{\text{op}}^2} \right) = \frac{1 + \delta}{1 - \delta} \left(\frac{k}{d} \frac{\|X^{\text{att}}\|_F^2}{\|B\|_{\text{op}}^2} + \text{st}(B) \right).$$

Combining with (E.13) and (E.11), we obtain on $\mathcal{E}_B^{(1)} \cap \mathcal{E}_2^{\text{sr}}$:

$$\text{st}(X^+) \leq \frac{1 + \delta}{1 - \delta} \left(\frac{2c_+^{\text{att}} K_B}{c_\sigma} + K_B \right) \leq \frac{1 + \delta}{1 - \delta} K_B \cdot \left(1 + \frac{c_+^{\text{att}}}{c_\sigma(1 - \delta)} \right), \quad (\text{E.14})$$

after enlarging constants once more if needed. This is the last inequality in (ii).

Column norms. Write $R' := W_2 B$ and let r'_t denote its t -th column. Conditional on B ,

$$r'_t \mid B \sim \mathcal{N}\left(0, \frac{\|b_t\|_2^2}{k} I_d\right).$$

We first bound $\|b_t\|_2^2$. For each t ,

$$u_t := (W_1 A_{\text{mlp}}^{\text{rms}})_t \sim \mathcal{N}(0, I_k)$$

coordinatewise, so since $|\sigma(u)| \leq |u|$, we have

$$\mathbb{E}\|b_t\|_2^2 = \mathbb{E}\|\sigma(u_t)\|_2^2 \leq \mathbb{E}\|u_t\|_2^2 = k.$$

Standard sub-Gaussian concentration then yields an event $\mathcal{E}_2^{(1)}$ with $\mathbb{P}(\mathcal{E}_2^{(1)}) \geq 1 - e^{-c\delta^2d}$ on which

$$\|b_t\|_2^2 \leq (1 + \varepsilon)k, \quad \forall t. \quad (\text{E.15})$$

Conditional on B , another χ^2 argument gives an event $\mathcal{E}_2^{(2)}$ with $\mathbb{P}(\mathcal{E}_2^{(2)}) \geq 1 - e^{-c\delta^2d}$ such that

$$\|r'_t\|_2^2 \leq (1 + \varepsilon)^2 \frac{d}{k} \|b_t\|_2^2 \leq (1 + \varepsilon)^2 d \leq (1 + \delta) d, \quad \forall t. \quad (\text{E.16})$$

We now apply Lemma 2.11 with parameter ε to (x_t^{att}, r'_t) . A union bound produces an event $\mathcal{E}_2^{(3)}$ with $\mathbb{P}(\mathcal{E}_2^{(3)}) \geq 1 - e^{-c\delta^2 d}$ such that

$$(1 - \varepsilon)(\|x_t^{\text{att}}\|_2^2 + \|r'_t\|_2^2) \leq \|x_t^+\|_2^2 \leq (1 + \varepsilon)(\|x_t^{\text{att}}\|_2^2 + \|r'_t\|_2^2), \quad \forall t. \quad (\text{E.17})$$

Combining (E.7), (E.16) and (E.17), and using $\varepsilon \leq \delta$, we obtain on $\mathcal{E}^+ := \mathcal{E}^{\text{att}} \cap \mathcal{E}_2^{(1)} \cap \mathcal{E}_2^{(2)} \cap \mathcal{E}_2^{(3)}$:

$$\|x_t^+\|_2^2 \geq (1 - \varepsilon)\|x_t^{\text{att}}\|_2^2 \geq (1 - \delta)c_-^{\text{att}}d = (1 - \delta)^2c_-d = c_-^+d,$$

and

$$\|x_t^+\|_2^2 \leq (1 + \varepsilon)(c_+^{\text{att}}d + (1 + \delta)d) \leq (1 + \delta)((1 + \delta)(c_+ + 1) + (1 + \delta))d \leq (1 + \delta)^2(c_+ + 2)d.$$

This yields

$$c_-^+d \leq \|x_t^+\|_2^2 \leq c_+^+d, \quad \forall t,$$

with

$$c_-^+ := (1 - \delta)^2c_-, \quad c_+^+ := (1 + \delta)^2(c_+ + 2),$$

as stated.

Probability of the good event. All events introduced have the form E_1, \dots, E_q with $\mathbb{P}(E_{i+1} \mid \bigcap_{j \leq i} E_j) \geq 1 - c_i \exp(-C_i \delta^2 d)$, and where q, c_i, C_i are some numerical constants. Clearly, by increasing c_i and C_i if necessary, we can assume that they are uniform across all $i = 1, \dots, q$. Therefore, we can estimate the intersection as

$$\mathbb{P}\left(\bigcap_{i=1}^q E_i\right) = \mathbb{P}\left(E_q \mid \bigcap_{j \leq q-1} E_j\right) \mathbb{P}\left(\bigcap_{j \leq q-1} E_j\right) \geq (1 - c \exp(-C \delta^2 d)) \cdot \mathbb{P}\left(\bigcap_{j \leq q-1} E_j\right).$$

Unrolling the recursion and using the elementary inequality $(1 - q)^q \geq 1 - kq$ for any $q \in [0, 1]$, we deduce

$$\mathbb{P}\left(\bigcap_{i=1}^q E_i\right) \geq (1 - c \exp(-C \delta^2 d))^q \geq 1 - cq \exp(-C \delta^2 d).$$

This completes the proof.

F Proof of Corollary 2.15

Throughout the proof, c, C, c', C', \dots denote positive numerical constants whose value may change from line to line and may depend on the choice of activation (here ReLU) but never on d, n, p_{\max} or the specific token sequence. We write $\text{st}(\cdot)$ for the stable rank as usual.

Fix the depth $L \geq 1$ and set

$$\delta := \frac{1}{8L} \in \left(0, \frac{1}{8}\right).$$

We also fix a small numerical constant $\varepsilon \in (0, 1/4)$ in Lemma 2.9; for concreteness we may take $\varepsilon = 1/4$. All blockwise applications of Proposition 2.14 will use this δ .

Each of Lemma 2.9 and Proposition 2.14 holds with probability at least $1 - Ce^{-c\varepsilon^2 d}$ or $1 - Ce^{-c\delta^2 d}$ respectively, after possibly enlarging C and shrinking c . Since there are $O(L)$ blocks and $O(1)$ activation types per block, a union bound shows that there exists a (events) $\Omega_{L,d}$ with

$$\mathbb{P}(\Omega_{L,d}) \geq 1 - e^{-cd}$$

for some $c > 0$ (depending only on L and the fixed activation) on which *all* the conclusions of Lemma 2.9 and Proposition 2.14 hold for every layer $\ell = 0, \dots, L-1$. The lower bound on d of the form $d \geq CL^2 \log n$ is chosen large enough so that the concentration estimates behind these results and the union bound are valid. From now on we work throughout on $\Omega_{L,d}$.

The embedding layer ($\ell = 0$). Let $X^{(0)} \in \mathbf{R}^{d \times n}$ be the embedding matrix associated with the fixed token sequence, constructed as in Assumption D. Lemma 2.9 applied with our choice of ε yields, on $\Omega_{L,d}$,

$$(1 - \varepsilon)d \leq \|x_t^{(0)}\|_2^2 \leq (1 + \varepsilon)d, \quad t = 1, \dots, n, \quad (\text{F.1})$$

and

$$\text{st}(X^{(0)}) \leq \frac{1 + \varepsilon}{1 - \varepsilon} \frac{1}{p_{\max}}. \quad (\text{F.2})$$

Moreover, writing $A^{\text{rms},(0)} := \text{RMSNorm}(X^{(0)})$, Lemma 2.10 gives

$$\text{st}(A^{\text{rms},(0)}) \leq \frac{1 + \varepsilon}{1 - \varepsilon} \text{st}(X^{(0)}) \lesssim \frac{1}{p_{\max}}. \quad (\text{F.3})$$

We now view the first transformer block (with index $\ell = 0$) as in Proposition 2.14, with input $X = X^{(0)}$. In the notation of that proposition we may take

$$c_-^{(0)} := 1 - \varepsilon, \quad c_+^{(0)} := 1 + \varepsilon,$$

so that (F.1) reads $c_-^{(0)}d \leq \|x_t^{(0)}\|_2^2 \leq c_+^{(0)}d$.

Applying Proposition 2.14 with this input, and recalling that we use the ReLU activation, we obtain on $\Omega_{L,d}$:

$$\text{st}(A^{\text{rms},(0)}) \leq \frac{c_+^{(0)}}{c_-^{(0)}} \text{st}(X^{(0)}), \quad (\text{F.4})$$

$$\text{st}(A_{\text{mlp}}^{\text{rms},(0)}) \leq \frac{(1 + \delta)^2}{(1 - \delta)^2} \frac{c_+^{(0)} + 1}{c_-^{(0)}} \left(1 + \frac{2}{c_-^{(0)}}\right) \text{st}(X^{(0)}), \quad (\text{F.5})$$

$$\text{st}(B^{(0)}) \leq 2\pi, \quad (\text{F.6})$$

$$\text{st}(X^{(1)}) \leq 2\pi \frac{1 + \delta}{1 - \delta} \left(1 + \frac{(1 + \delta)(c_+^{(0)} + 1)}{\frac{1}{2}(1 - \Phi(1))(1 - \delta)}\right), \quad (\text{F.7})$$

where Φ is the standard Gaussian CDF. The last inequality shows that $\text{st}(X^{(1)})$ is bounded by a numerical constant depending only on $c_{\pm}^{(0)}$ and δ , hence independent of p_{\max} .

Combining (F.2) with (F.4) and (F.5), and absorbing the numerical factors coming from $c_{\pm}^{(0)}$ and δ into a single constant, we obtain

$$\text{st}(X^{(0)}), \text{st}(A^{\text{rms},(0)}), \text{st}(A_{\text{mlp}}^{\text{rms},(0)}) \leq \frac{C_{\text{in}}}{p_{\max}}$$

for some numerical $C_{\text{in}} > 0$. In addition, (F.6) ensures that $\text{st}(B^{(0)}) \leq 2\pi$. This establishes the first set of bounds appearing in the statement of the corollary.

Evolution of column norms through the layers. For each $\ell \geq 0$ we write

$$X^{(\ell)} = [x_t^{(\ell)}]_{t=1}^n, \quad c_-^{(\ell)}d \leq \|x_t^{(\ell)}\|_2^2 \leq c_+^{(\ell)}d \quad (t = 1, \dots, n),$$

for some constants $0 < c_-^{(\ell)} \leq c_+^{(\ell)} < \infty$. We have already identified $c_{\pm}^{(0)}$ above. Applying Proposition 2.14 at layer ℓ with input $X = X^{(\ell)}$ shows that, on $\Omega_{L,d}$, the block output $X^{(\ell+1)}$ has squared column norms between $c_-^{(\ell+1)}d$ and $c_+^{(\ell+1)}d$ with

$$c_-^{(\ell+1)} = (1 - \delta)^2 c_-^{(\ell)}, \quad c_+^{(\ell+1)} = (1 + \delta)^2 (c_+^{(\ell)} + 2).$$

Iterating the lower recurrence gives

$$c_-^{(\ell)} = (1 - \delta)^{2\ell} c_-^{(0)}.$$

Using the elementary inequality $(1 - x)^k \geq 1 - kx$ for $x \in (0, 1)$ and $k \in \mathbb{N}$, together with $\delta = 1/(8L)$ and $\ell \leq L$, we obtain

$$c_-^{(\ell)} = (1 - \delta)^{2\ell} c_-^{(0)} \geq (1 - 2\ell\delta) c_-^{(0)} \geq \left(1 - \frac{1}{4}\right) c_-^{(0)} = \frac{3}{4} c_-^{(0)}.$$

Since $c_-^{(0)} = 1 - \varepsilon \geq 3/4$, we may fix once and for all a numerical constant $c_* > 0$ (for instance $c_* := \frac{1}{2}$) such that

$$c_-^{(\ell)} \geq c_* \quad \text{for all } 0 \leq \ell \leq L. \quad (\text{F.8})$$

For the upper recurrence, write $r := (1 + \delta)^2$ and note that $r \in (1, 2)$ for our choice of δ . We have

$$c_+^{(\ell+1)} \leq r c_+^{(\ell)} + 2r.$$

Unfolding this inequality gives

$$c_+^{(\ell)} \leq r^\ell c_+^{(0)} + 2r \sum_{j=0}^{\ell-1} r^j \leq r^\ell c_+^{(0)} + 2r\ell \max\{1, r^{\ell-1}\}.$$

Using the bound $r^\ell \leq \exp(2\delta\ell) \leq \exp(2\delta L) = \exp(1/4)$, we conclude that

$$c_+^{(\ell)} \leq C(1 + \ell), \quad 0 \leq \ell \leq L, \quad (\text{F.9})$$

for some numerical constant $C > 0$. Combining (F.8) and (F.9), we obtain

$$\frac{c_+^{(\ell)}}{c_-^{(\ell)}} \leq C_1(1 + \ell), \quad 0 \leq \ell \leq L, \quad (\text{F.10})$$

for another numerical constant $C_1 > 0$.

Stable ranks of the hidden states $X^{(\ell)}$ for $\ell \geq 1$. Let $s_\ell := \text{st}(X^{(\ell)})$ for $\ell \geq 0$. The bound (F.7) shows that $s_1 \leq C$ for some numerical constant C depending only on δ and $c_{\pm}^{(0)}$, hence only on L and our choice of ε .

For a general layer $\ell \geq 0$, applying Proposition 2.14 at that layer yields

$$s_{\ell+1} = \text{st}(X^{(\ell+1)}) \leq 2\pi \frac{1 + \delta}{1 - \delta} \left(1 + \frac{(1 + \delta)(c_+^{(\ell)} + 1)}{\frac{1}{2}(1 - \Phi(1))(1 - \delta)}\right).$$

Since $\delta \leq 1/8$ and $c_+^{(\ell)} \leq C(1 + \ell)$ by (F.9), the right-hand side is bounded by a numerical constant times $(1 + c_+^{(\ell)})$, and hence by a numerical constant times $(1 + \ell)$. We may therefore write, for all $0 \leq \ell \leq L - 1$,

$$s_{\ell+1} \leq C_2(1 + \ell) \quad (\text{F.11})$$

for some numerical $C_2 > 0$. In particular, for every $\ell \geq 1$ we have $s_\ell \leq C_2 \ell$.

Intermediate activations inside each block for $\ell \geq 1$. Fix a layer index $1 \leq \ell \leq L-1$, and consider the corresponding block input $X^{(\ell)}$. Proposition 2.14 yields, on $\Omega_{L,d}$,

$$\text{st}(A^{\text{rms},(\ell)}) \leq \frac{c_+^{(\ell)}}{c_-^{(\ell)}} s_\ell, \quad (\text{F.12})$$

$$\text{st}(A_{\text{mlp}}^{\text{rms},(\ell)}) \leq \frac{(1+\delta)^2}{(1-\delta)^2} \frac{c_+^{(\ell)} + 1}{c_-^{(\ell)}} \left(1 + \frac{2}{c_-^{(\ell)}}\right) s_\ell, \quad (\text{F.13})$$

$$\text{st}(B^{(\ell)}) \leq 2\pi. \quad (\text{F.14})$$

Using the uniform lower bound (F.8) and the linear bound (F.10) on $c_+^{(\ell)}/c_-^{(\ell)}$, together with the linear growth (F.11) of s_ℓ , we obtain

$$\begin{aligned} \text{st}(A^{\text{rms},(\ell)}) &\leq C_1(1+\ell) s_\ell \lesssim 1 + \ell^2, \\ \text{st}(A_{\text{mlp}}^{\text{rms},(\ell)}) &\leq C_3(1+\ell) s_\ell \lesssim (1+\ell)^2 \end{aligned}$$

for suitable numerical constants.

The final RMS layer. At the top of the network we have the final hidden state $X^{(L)}$ and $A_{\text{final}}^{\text{rms}} = \text{RMSNorm}(X^{(L)})$. By the same argument as in Lemma 2.10, applied with $L = c_-^{(L)}d$ and $U = c_+^{(L)}d$ where $c_\pm^{(L)}$ satisfy (F.8) and (F.9), we obtain

$$\text{st}(A_{\text{final}}^{\text{rms}}) \leq \frac{c_+^{(L)}}{c_-^{(L)}} \text{st}(X^{(L)}) \lesssim (1+L)^2,$$

as desired.

G Auxiliary linear algebraic results.

Lemma G.1 (Minimal singular value of blocked matrices). *Let $a \in \mathbf{R}$, let $z \in \mathbf{R}^p$, and let $D \in \mathbf{R}^{(q-1) \times p}$ with $q-1 \leq p$. Define*

$$M := \begin{bmatrix} a & z^\top \\ 0 & D \end{bmatrix} \in \mathbf{R}^{q \times (p+1)}.$$

Then assuming $a \neq 0$, we have $\sigma_q(M) \geq \frac{\min\{|a|, \sigma_{q-1}(D)\}}{1 + \|z\|_2/|a|}$.

Proof. We may write $M = AN$, where

$$A = \begin{bmatrix} a & 0 \\ 0 & D \end{bmatrix}, \quad N = \begin{bmatrix} 1 & a^{-1}z^\top \\ 0 & I_p \end{bmatrix}.$$

Clearly we have

$$\sigma_q(M) \geq \sigma_q(A) \sigma_q(N). \quad (\text{G.1})$$

Because A is block diagonal, we have

$$\sigma_q(A) = \min\{|a|, \sigma_{q-1}(D)\}. \quad (\text{G.2})$$

The matrix N is invertible with

$$N^{-1} = \begin{bmatrix} 1 & -a^{-1}z^\top \\ 0 & I_p \end{bmatrix} = I_{p+1} + E, \quad \text{where we set} \quad E := \begin{bmatrix} 0 & -a^{-1}z^\top \\ 0 & 0 \end{bmatrix}.$$

Hence $\|N^{-1}\|_{\text{op}} \leq 1 + \frac{\|z\|_2}{|a|}$ and therefore $\sigma_q(N) = \|N^{-1}\|_{\text{op}}^{-1} \geq \frac{1}{1 + \|z\|_2/|a|}$. Substituting (G.2) and this bound for $\sigma_q(N)$ into (G.1) yields the claimed result. \square

Lemma G.2 (Lower bound on the nuclear rank). *Consider a matrix $M \in \mathbf{R}^{m \times d}$ and a vector $v \in \mathbf{R}^d$. Then for any subset $P \subset [d]$ the estimate holds:*

$$\|M \text{Diag}(v)\|_* \geq \left(\min_{i \in P} |v_i| \right) \cdot \|M_P\|_*,$$

where $M_P \in \mathbf{R}^{m \times |P|}$ is the submatrix of M formed by columns indexed by P .

Proof. Let $e_P \in \mathbf{R}^d$ denote the vector with ones in all coordinates indexed by P and zeros elsewhere and set $q := \min_{i \in P} |v_i|$. Then observe

$$M \text{Diag}(v) \text{Diag}(v)^\top M^\top \geq q^2 \cdot M e_P e_P^\top M^\top = q^2 \cdot M_P M_P^\top.$$

Taking matrix square roots of both sides and taking the trace completes the proof. \square

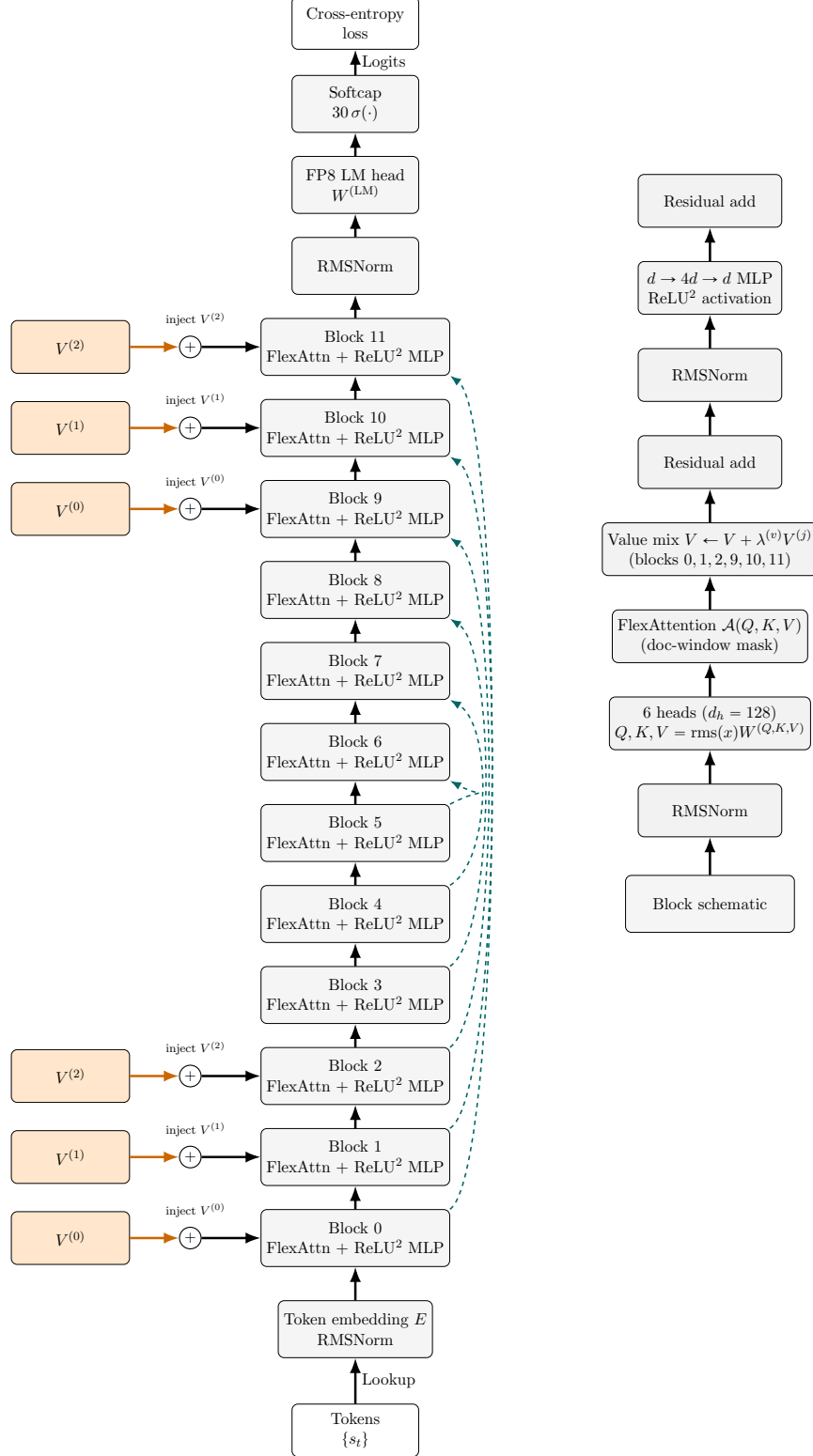


Figure 19: The `train_gpt.py` architecture of snapshot [28]. Value embeddings $V^{(0)}, V^{(1)}, V^{(2)}$ enter through explicit addition nodes in blocks 0, 1, 2 and 9, 10, 11, while the block schematic (right) shows the RMS normalisations, six-head FlexAttention, and two-layer ReLU-squared MLP shared across the stack. Teal skip arcs connect block k to block $11 - k$, indicating the pop step $x^{(i+1)} = \tilde{x}^{(i+1)} + \kappa_i s^{(i)}$.